University of Alberta

Characterization of Oil Sands Process-affected Water Using Fluorescence Technology

by

Andrea Marie Ewanchuk

A thesis submitted to the Faculty of Graduate Studies and Research
in partial fulfillment of the requirements for the degree of

Master of Science
in
Geoenvironmental Engineering

Department of Civil and Environmental Engineering

Fall 2011
Edmonton, Alberta

ABSTRACT

Fluorescence technology was examined as an analytical tool for identifying naphthenic acids in process-affected water. The fluorescence signal from process-affected water was narrowed down to the extractable organic acid fraction, known to contain naphthenic acids. A characteristic intensity peak was observed in a consistent location in the emission spectrum when scanned at 280nm excitation wavelength for water obtained from three oil sands operations. The signals obtained for each water source exhibited similar shapes but varied by intensity. The intensity observed was compared to naphthenic acid concentration determined by the industry standard analytical method. When examined individually there was a strong linear correlation between fluorescence intensity and concentration for the water sources. Models developed using the parallel factor analysis method found that process-affected water from each oil sand operation had five fluorescent species which contributed to the overall signal, and that the species were similar between process-affected water from each company.

Acknowledgements

There are so many people that I want to thank for their support and contributions during my time at the UofA. My parents, Teri and Garry Ewanchuk, thank you so much for your endless support and making it financially possible for me to follow my dreams of academia. I love you two so much. My sister, Sheila Ewanchuk, thank you for being there all these years, despite it being somewhat mandatory. I'm proud to call you my sister, and my best friend. And thanks to my baby brother, John Ewanchuk, I'm so lucky to have you in my life. Without the support of all of you I wouldn't be where I am today and I love you all.

Thanks to my supervisors, Dr. Ania Ulrich and Dr. Dave Sego, for your endless patience and understanding. I've learned so much over these years and I am forever grateful. Thank you to NSERC and Syncrude for their financial support, without which this research could not be completed.

And to all the friends I've made from the lab group, thank you for an awesome time, it's been a blast working with everyone. Thanks to Christina Small for being an awesome , for her friendship in and out of the lab.

To all the friends that have been by my side for the whole ride, and all the friends I've made along the way.

A special thanks to Darryl Vogler as my editor, motorcycle mechanic, snake specialist, and all around go to guy no matter what hour of the night it is. If there's any grammatical errors in this section; I apologize.

And I can't forget my furheads, Echo, Raz and Lola, as well as my slithery friend Toki; who have been forced to listen to countless practice presentations.

Table of Contents

List of Appendices

List of Tables

List of Figures

List of Abbreviations and Symbols

a.u.	arbitrary units
^{o}C	degrees centigrade
DCM	dichloromethane
DOC	dissolved organic carbon
EEM	excitation-emission matrix
FTIR	Fourier Transform Infrared Spectroscopy
GC-MS	Gas chromatography mass spectrometry
HPLC	High performance liquid chromatography
HRMS	High resolution mass spectrometry
mg/L	milligrams per litre
NaOH	Sodium Hydroxide
Nm	nanometer
PAH	polycyclic aromatic hydrocarbons
PARAFAC	parallel factor analysis
Π	pi
σ	sigma
SFS	synchronous fluorescence spectrometry
UV	ultraviolet

1. Introduction

1.1 Background

The oil sands deposits in Northern Alberta, Canada, represent one of the largest in the world with reserves of 171 billion barrels of proven recoverable oil (Alberta Government 2011). Approximately three barrels of water are used in the extraction process for every one barrel of oil produced, with up to 85% of the used water being recycled water (Allen 2008). Water that is not able to be recycled within the system is transferred to tailings pond impoundments. This process-affected tailings contains sands and clays which settle within the ponds (Allen 2008; Headley and McMartin 2004). During the extraction process, naturally occurring organic acids are released from the bitumen and carried throughout the plants in the process water (Janfada et al. 2006). Within the organic acid fraction are naphthenic acids, which have been shown to be toxic to various organisms (Allen 2008). A zero-discharge policy is in place for the water used in the oil sands industry in order to minimize impacts to the surrounding environment; however, at the end of the mine life there is a requirement to remediate and return the land back to its original state with the intent to facilitate sustainable ecosystems (Allen 2008).

Process-affected water from the tailings ponds produces a characteristic fluorescence signal when exposed to ultraviolet (UV) light in the wavelength range of 260 to 450 nm. Compounds exhibit fluorescence due to their electron structure and chemical bonds within aromatic components (Alostaz et al. 2008). Naphthenic acids falling within the general formula $C_nH_{2n+Z}O_2$ do not indicate that fluorescence will occur due to the absence of a double bond. However, naphthenic acids in tailings ponds have been found to deviate from the general formula $C_nH_{2n+Z}O_2$. The presence of pyrolles, thiophenes, and phenols has been detected in the naphthenic acid portion of a Californian crude oil using UV and Infrared analysis (Seifert et al. 1969). Similarly thin layer chromatography has identified the presence of phenol, nitrogen, and sulphur within the naphthenic acid

fraction of a Californian crude oil (Seifert and Teether 1969). In addition, mass spectrometry methods were able to determine compositions containing oxygen, ozone, tetraoxygen (O_4), O_2S, O_3S, and O_4S within a heavy crude from South America (Headley et al. 2009). Recently, Grewer et al. (2010) used ultrahigh resolution electrospray ionization fourier transform ion cyclotron resonance mass spectrometry (ESI-FT-ICR MS) and found that less than 50% of what is extracted out of oil sands water and is categorized as naphthenic acids fits the classical definition. The organic acid fraction containing the naphthenic acids has been shown to exhibit fluorescence. The fluorescence signals obtained are unique to each particular compound, and thus can be used in identification for analytical purposes (Lackowitz 2006).

Concentrations of naphthenic acids within the tailings ponds have been found in the range of 40-120 mg/L (Holowenko et al. 2001). Oil sands operators currently quantify naphthenic acids using Fourier Transform Infrared (FTIR) spectroscopy (Jivraj et al. 1995). This method requires extraction with dichloromethane (DCM), and quantification is based on comparing the petroleum based naphthenic acids to commercially produced naphthenic acids. There is currently no procedure that is able to separate naphthenic acid compounds individually (Scott et al. 2008). Other analytical methods include various types of mass spectrometry such as gas chromatography, negative ion electrospray ionization, and fast atom bombardment (Clemente and Fedorak 2004; Fan 2001; Hao et al. 2005). High-performance liquid chromatography (HPLC) can be used in conjunction with mass spectrometry methods, such as high-resolution mass spectrometry (HRMS), and is an enhanced technique relative to FTIR analysis (Bataineh et al. 2006; Han et al. 2009). HPLC/HRMS has been shown to be more selective as FTIR will respond to any carboxylic acid present, not just naphthenic acids (Han et al. 2009). As previously mentioned, recently ultrahigh resolution electrospray ionization Fourier transform ion cyclotron resonance mass spectrometry (ESI-FT-ICR MS) has been used to further characterize naphthenic acids (Grewer et al. 2010).

The fluorescence signals obtained from process-affected water are complex and can be difficult to resolve when there are multiple fluorescent components. Light scatter is an unavoidable product that occurs during fluorescence scanning. Stray light is transmitted by the sample and picked up by the detection system; it must be manually removed for data analysis. Additionally inner filter effects can become prominent at lower wavelengths for process-affected water. In the case of overlapping signals, a decompostional statistical method, such as parallel factor analysis (PARAFAC), can be used. PARAFAC is a multivariable statistical procedure that can be used to decompose fluorescence data and aid in differentiating the number of fluorescent species within a mixture (Alostaz et al. 2008).

1.2 Objectives

The main objective of this research was to demonstrate fluorescence technology as an analytical tool to characterize process-affected water and specifically naphthenic acids within the water from the oil sands industry. Process-affected water was extracted down to the basic, neutral and acidic fractions to determine where the fluorescence species originated. The aim of the research was to understand how fluorescence signals represent process-affected water from various oil sands operations and to determine distinctive characteristics to identify the effects of changing concentration of process-affected water. These fluorescence results were compared to techniques established for process-affected water and the organic acid fraction containing the naphthenic acids. The fluorescence signals were further analyzed using the statistical technique PARAFAC to determine how many fluorescent species are contributing to the overall fluorescence signal. The number of fluorescent species was determined for process-affected water from various sources, in addition to commercial naphthenic acids.

1.3 Methodology

Fluorescence signals were created using a Varian Cary Eclipse Spectrometer for process-affected water from three oil sands operations. Basic, neutral and acidic fractions were extracted from each source and fluoresced for comparison to the undiluted process-affected water samples. The waters from each source were then diluted to various levels for comparative analysis. The procedure was repeated for commercial naphthenic acids. The signatures were decomposed into their underlying fluorescent species using the statistical model PARAFAC.

1.4 Organization of Thesis

This thesis has been written in paper format and is organized as follows. Chapter 1 provides an overview of the background, objectives, and methodology of this research. Chapter 2 reviews current literature on organic acids in oil sands process-affected water, analytical techniques and PARAFAC. Chapter 3 examines fluorescence signals and the characteristics associated with process-affected water and naphthenic acids. Chapter 4 discusses how the statistical program PARAFAC can be applied to fluorescence signals to further analyze the fluorescent species. Chapter 5 summarizes the major findings and details suggestions for future work.

1.5 References

Alberta Government. 2011. Alberta's Oil Sands. [online] Available from http://www.oilsands.alberta.ca/resource.html [accessed Jan 2011]

Allen, E.W. 2008. Water treatment in Canada's oil sands industry I: Target pollutants and treatment objectives. Journal of Environmental Engineering and Science, 7: 123-128.

Alostaz, M., Biggar, K., Donahue, R., and Hall, G. 2008. Petroleum contamination characterization and quantification using fluorescence emission excitation matrices (EEMs) and parallel factor analysis (PARAFAC). Journal of Environmental Engineering and Science. 7: 183–197.

Bataineh, M., Scott, A.C., Fedorak, P.M., and Martin, J.W. 2006. Capillary HPLC/QTOF-MS for Characterizing Complex Naphthenic Acid Mixtures and Their Microbial Transformation. Analytical Chemistry, 78: 8354-8361.

Clemente, J.S. and Fedorak, P.M. 2004. Evaluation of the analyses of tert-butyldimethysilyl derivatives of naphthenic acids by gas chromatography – electron impact mass spectrometry. Journal of Chromatography, 1047(2004): 117-128.

Fan, T.P. 1991. Characterization of Naphthenic Acids in Petroleum by Fast Atom Bombardment Mass Spectrometry. Energy & Fuels, 5: 371-375.

Grewer, D.M., Young, R.F., Whittal, R.M., and Fedorak, P.M. 2010. Naphthenic Acids and other acid-extractables in water samples from Alberta: What is being measured? Science of the Total Environment. 408(23): 5997-6010.

Han, X., MacKinnon, M.D., Martin, J.W. 2009. Estimating the in situ biodegradation of naphthenic acids in oil sands process waters by HPLC/HRMS. Chemosphere. 76: 63-70.

Hao, C. et. al. 2005. Characterization and pattern recognition of oil sand naphthenic acids using comprehensive two dimensional gas chromatography/time of flight mass spectrometry. Journal of Chromatography, 1067: 277-284.

Headley, J.V. and McMartin, D.W. 2004. A Review of the Occurrence and Fate of Naphthenic Acids in Aquatic Environments. Journal of Environmental Science and Health, A39(8): 1989-2010.

Headley, J.V., Peru, K.M., and Barrow, M.P. 2009. Mass Spectrometric Characterization of Naphthenic Acids in Environmental Samples: A Review. Mass Spectrometry Reviews, 2009, 28, 121– 134.

Holowenko F, MacKinnon M and Fedorak P. 2001. Naphthenic acids and surrogate naphthenic acids in methanogenic microcosms. Water Resources, 35: 2596–2606.

Janfada, A. et al. 2006. A Laboratory Evaluation of the Sorption of Oil Sands Naphthenic Acids on Organic Rich Soils. Journal of Environmental Science and Health, A41: 985-997.

Jivraj, M., M. Mackinnon, B. Fung (1995). Naphthenic Acid Extraction and Quantitative Analysis With FT- IR Spectroscopy. In Syncrude Analytical Manuals, 4th Edition, Research Department, Syncrude Canada Ltd., Edmonton, AB

Lakowicz, J.R. 2006. Principles of Fluorescence Spectroscopy, 3rd Ed. Springer Science+Business Media, LLC, New York, NY.

Seifert, W., and Teeter, R. 1969. Preparative Thin-Layer Chromatography and High Resolution Mass Spectrometry of Crude Oil Carboxylic Acids. Analytical Chemistry, 41(6): 786-795.

Seifert, W., Teeter, R., Howells, W.G., and Cantow, M. 1969. Analysis of Crude Oil Carboxylic Acids after Conversion to Their Corresponding Hydrocarbons. Analytical Chemistry, 41(12): 1639-1647.

Scott, A.C., Young, R.F., and Fedorak, P.M. 2008. Comparison of GC-MS and FTIR methods for quantifying naphthenic acids in water samples. Chemosphere **73**: 1258-1264.

2. Literature Review

The following reviews available literature and data published related to the previously discussed research objectives. Naphthenic acids and their chemical properties that make them a compound of interest to the oil sands are reviewed. The available analytical techniques previously used to evaluate naphthenic acids are then reviewed. A discussion on fluorescence as an analytical technique and how it can be applied to process-affected water is then presented. In addition, the use of the statistical method parallel factor analysis (PARAFAC) in conjunction with fluorescence is then addressed.

2.1 Organic Acids in the Oil Sands

Bitumen extraction in the oil sands is currently carried out via modified versions of the Clark Hot Water Extraction method (Allen 2008). The raw ore is digested using warm water (50-80^{o}C) and sodium hydroxide (NaOH) that acts as a conditioning agent (Holowenko et al. 2002; Yen et al. 2004). During the extraction process naturally occurring organic acids are released from the bitumen and carried throughout the extraction plant in the process water (Janfada et al. 2006). When the water used in extraction is not able to be recycled, it is transferred to an impoundment with the tailings. This process affected water contains sands and clays and other particulate matter, including the organic acids, which are contained within the tailings pond impoundments (Allen 2008, Headley & McMartin 2004).

The organic acid fraction of process-affected water is of interest to the oil sands industry; it has been shown to have detrimental toxic properties, as well as corrosive properties. Earlier research identified naphthenic acids as the compound of interest (Allen 2008). Naphthenic acids are carboxylic acids of the form $C_nH_{2n+z}O_2$, where n is the number of carbons and Z indicates the hydrogen deficiency resulting from the ring formation. Ring structures typically contain

five or six carbons; with the Z value ranging from 0 to -12 and each multiple of -2 signifying another ring (Brient et al. 1995). Figure 2.1 shows some of the typical structures of naphthenic acids, where R represents an alkyl group, and m represents the length of the alkyl chain.

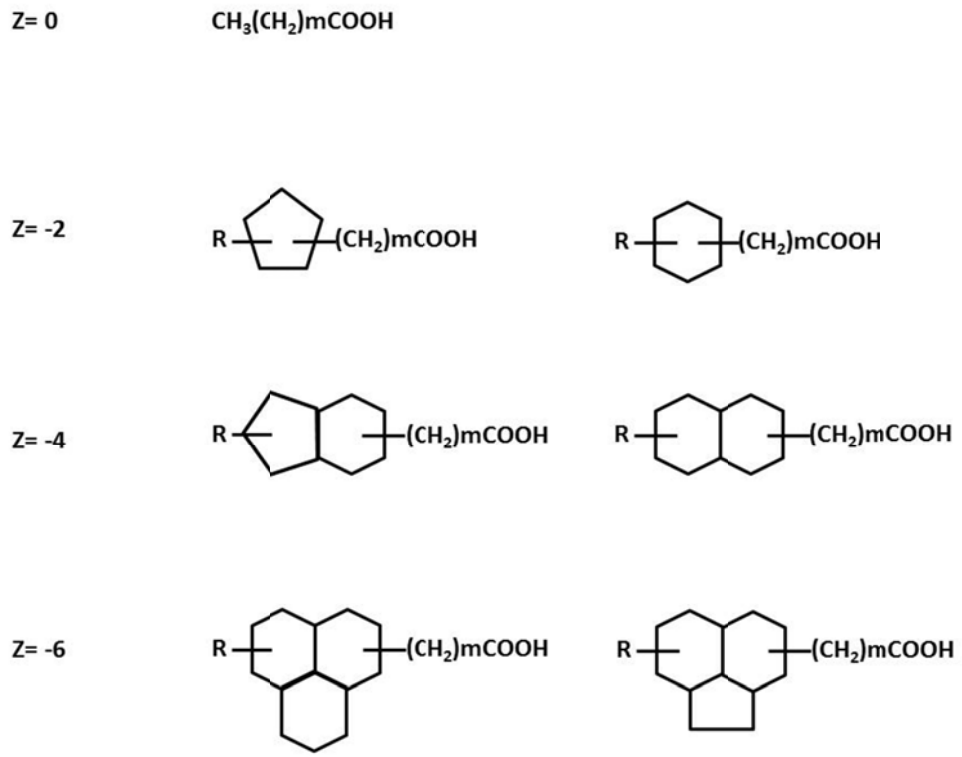

Figure 2.1: Naphthenic acid structures (Adapted from Hao et al. 2005). R represents an alkyl group, m represents the length of the alkyl chain, and Z corresponds to the number of rings in the acids.

2.2.1 Toxicity

The toxicity in the process affected water is generally associated with the surfactant properties of naphthenic acids (Headley and McMartin 2004). Higher levels of toxicity were reported in samples that were dominated by lower molecular weights, though a specific compound has yet to be established (Allen 2008; Janfada et al. 2006; McMartin 2004). Freshly deposited tailings water has

been found to contain the highest levels of toxicity, and predominately contains lower molecular weight naphthenic acids. As the ponds are allowed to age, the naphthenic acid mixture shifts towards larger molecules of higher molecular weight and toxicity levels are shown to decrease (Allen 2008).

One of the issues when determining toxic effects to organisms was the type of naphthenic acid the organism was exposed to. The complex nature implies that much of the research on toxicity is not comparable, as different naphthenic structures were used in the testing. For example, in review done by Clemente and Fedorak (2005) they indicate testing was completed using commercially available naphthenic acids, whereas others were obtained from the oil sands tailings ponds. Noted in the review was that the commercially available compounds contained lower molecular weights, whereas the tailings ponds tended to contain the higher end of the molecular weight spectrum. This makes it difficult to determine which naphthenic acids are of the most concern with respect to toxicity.

2.2.2 Corrosion

A second issue associated with naphthenic acids is corrosion. The corrosion reactions are not fully established due to the complex nature of naphthenic acid composition and structure (Slavcheva 1999). The amount of corrosion experienced by the system depends on the composition of the naphthenic acids, and is generally associated with the total acid number, or acidity present, as well as the layout of the system (Babaian-Kibala, 1994; Slavecheva 1999).

2.3 Analytical Techniques

The current industry standard for quantification of naphthenic acids is through Fourier Transform Infrared (FTIR) spectroscopy (Jivraj et al. 1995). The acid fraction of the water samples is extracted and then scanned in the spectrometer, where the absorbance of the monomeric and dimeric forms of the carbonyl groups

at their respective wavelengths of 1743 and 1706 cm^{-1} are measured. The results are then quantified by calibration curves derived from commercially available naphthenic acids. This method is unable to determine individual naphthenic acid species or give insight into which compounds are predominant.

Table 2.1 summarizes several of the published results where concentrations of naphthenic acids determined by research test methods are compared to the industry FTIR method for various sources. Other publications have detailed methodology for characterizing the naphthenic acid fraction by molecular weight but do not quantify a total naphthenic acid concentration (Bataineh et al. 2006;; Clemente and Fedorak, 2004; Fan 1991; Han et al. 2009; Hao et al. 2005; Zhenbo et al. 2006). Grewer et al. (2010) and Scott et al. (2008) compared gas chromatography mass spectrometry (GC-MS) to FTIR analysis, and found that FTIR consistently reported higher concentrations of naphthenic acids. Yen et al. (2004) compared FTIR analysis to high performance liquid chromatography (HPLC), and reported HPLC concentrations that were generally higher than the FTIR analysis.

Table 2.1: Reported naphthenic acid concentrations in various process affected water samples.

Source of naphthenic acids	Concentration (mg/L)	Test Method	Reference
Syncrude – Mildred Lake Settling Basin	44	FTIR	Grewer et al. 2010
	28	GC-MS	
Syncrude – West In-Pit	60	FTIR	
	36	GC-MS	
Syncrude – Pond 9	20	FTIR	
	7.1	GC-MS	
Syncrude – Demo Pond	14	FTIR	
	5.9	GC-MS	
Suncor – Pond 2/3	63	FTIR	
	47	GC-MS	
Suncor – Pond 5	38	FTIR	
	26	GC-MS	
Suncor – Steam Assisted Gravity Drainage	130	FTIR	
	38	GC-MS	
Albian – Tailings Pond	35	FTIR	
	18	GC-MS	

Source of naphthenic acids	Concentration (mg/L)	Test Method	Reference
Company A – Tailings Pond 1	45	FTIR	Scott et al. 2008
	17	GC-MS	
Company A – Tailings Pond 2	25	FTIR	
	6.4	GC-MS	
Company A – Aged Sample	11	FTIR	
	2.9	GC-MS	
Company B – Tailings Pond sampled in 2004	17	FTIR	
	4.0	GC-MS	
Company B – Tailings Pond sampled in 2007	34	FTIR	
	12	GC-MS	
Company C – Consolidated Tailings	18	FTIR	
	4.9	GC-MS	
Company C – Tailings Pond	78±1.5	FTIR	
	53±15	GC-MS	
Company C – Steam Assisted Gravity Drainage	120	FTIR	
	21	GC-MS	
Syncrude naphthenic acid extract – 0 mg/L	0.5	FTIR	Yen et al. 2004
	4±2.5	HPLC	
Syncrude naphthenic acid extract – 10 mg/L	8	FTIR	
	13±1.8	HPLC	
Syncrude naphthenic acid extract – 30 mg/L	24	FTIR	
	22±2.1	HPLC	
Syncrude naphthenic acid extract – 60 mg/L	51	FTIR	
	64±2.6	HPLC	
Syncrude naphthenic acid extract – 80 mg/L	75	FTIR	
	78±0.5	HPLC	

Clemente and Fedorak (2004) suggested that gas chromatography was the most accessible method available for mass spectrometry of naphthenic acids. In gas chromatography, an inert gas is passed through an inert column, where various parts of the naphthenic acid components would emerge after different retention times. As the number of carbons and rings in the structure are increased, their retention time in the chromatography column is increased (Hao et. al., 2005). The analysis gives a nominal mass that could then be used to predict the carbon number and subsequent empirical formula for the naphthenic acids. This method

1. Introduction

1.1 Background

The oil sands deposits in Northern Alberta, Canada, represent one of the largest in the world with reserves of 171 billion barrels of proven recoverable oil (Alberta Government 2011). Approximately three barrels of water are used in the extraction process for every one barrel of oil produced, with up to 85% of the used water being recycled water (Allen 2008). Water that is not able to be recycled within the system is transferred to tailings pond impoundments. These process-affected tailings contain sands and clays which settle within the ponds (Allen 2008; Headley and McMartin 2004). During the extraction process, naturally occurring organic acids are released from the bitumen and carried throughout the plants in the process water (Janfada et al. 2006). Within the organic acid fraction are naphthenic acids, which have been shown to be toxic to various organisms (Allen 2008). A zero-discharge policy is in place for the water used in the oil sands industry in order to minimize impacts to the surrounding environment; however, at the end of the mine life there is a requirement to remediate and return the land back to its original state with the intent to facilitate sustainable ecosystems (Allen 2008).

Process-affected water from the tailings ponds produces a characteristic fluorescence signal when exposed to ultraviolet (UV) light in the wavelength range of 260 to 450 nm. Compounds exhibit fluorescence due to their electron structure and chemical bonds within aromatic components (Alostaz et al. 2008). Naphthenic acids falling within the general formula $C_nH_{2n+Z}O_2$ do not indicate that fluorescence will occur due to the absence of a double bond. However, naphthenic acids in tailings ponds have been found to deviate from the general formula $C_nH_{2n+Z}O_2$. The presence of pyrolles, thiophenes, and phenols has been detected in the naphthenic acid portion of a Californian crude oil using UV and Infrared analysis (Seifert et al. 1969). Similarly thin layer chromatography has

identified the presence of phenol, nitrogen, and sulphur within the naphthenic acid fraction of a Californian crude oil (Seifert and Teether 1969). In addition, mass spectrometry methods were able to determine compositions containing oxygen, ozone, tetraoxygen (O_4), O_2S, O_3S, and O_4S within a heavy crude from South America (Headley et al. 2009). Recently, Grewer et al. (2010) used ultrahigh resolution electrospray ionization fourier transform ion cyclotron resonance mass spectrometry (ESI-FT-ICR MS) and found that less than 50% of what is extracted out of oil sands water and is categorized as naphthenic acids fits the classical definition. The organic acid fraction containing the naphthenic acids has been shown to exhibit fluorescence. The fluorescence signals obtained are unique to each particular compound, and thus can be used in identification for analytical purposes (Lackowitz 2006).

Concentrations of naphthenic acids within the tailings ponds have been found in the range of 40-120 mg/L (Holowenko et al. 2001). Oil sands operators currently quantify naphthenic acids using Fourier Transform Infrared (FTIR) spectroscopy (Jivraj et al. 1995). This method requires extraction with dichloromethane (DCM), and quantification is based on comparing the petroleum based naphthenic acids to commercially produced naphthenic acids. There is currently no procedure that is able to separate naphthenic acid compounds individually (Scott et al. 2008). Other analytical methods include various types of mass spectrometry such as gas chromatography, negative ion electrospray ionization, and fast atom bombardment (Clemente and Fedorak 2004; Fan 2001; Hao et al. 2005). High-performance liquid chromatography (HPLC) can be used in conjunction with mass spectrometry methods, such as high-resolution mass spectrometry (HRMS), and is an enhanced technique relative to FTIR analysis (Bataineh et al. 2006; Han et al. 2009). HPLC/HRMS has been shown to be more selective as FTIR will respond to any carboxylic acid present, not just naphthenic acids (Han et al. 2009). As previously mentioned, recently ultrahigh resolution electrospray ionization Fourier transform ion cyclotron resonance mass spectrometry (ESI-FT-

ICR MS) has been used to further characterize naphthenic acids (Grewer et al. 2010).

The fluorescence signals obtained from process-affected water are complex and can be difficult to resolve when there are multiple fluorescent components. Light scatter is an unavoidable product that occurs during fluorescence scanning. Stray light is transmitted by the sample and picked up by the detection system; it must be manually removed for data analysis. Additionally inner filter effects can become prominent at lower wavelengths for process-affected water. In the case of overlapping signals, a decompostional statistical method, such as parallel factor analysis (PARAFAC), can be used. PARAFAC is a multivariable statistical procedure that can be used to decompose fluorescence data and aid in differentiating the number of fluorescent species within a mixture (Alostaz et al. 2008).

1.2 Objectives

The main objective of this research was to demonstrate fluorescence technology as an analytical tool to characterize process-affected water and specifically naphthenic acids within the water from the oil sands industry. Process-affected water was extracted down to the basic, neutral and acidic fractions to determine where the fluorescence species originated. The aim of the research was to understand how fluorescence signals represent process-affected water from various oil sands operations and to determine distinctive characteristics to identify the effects of changing concentration of process-affected water. These fluorescence results were compared to techniques established for process-affected water and the organic acid fraction containing the naphthenic acids. The fluorescence signals were further analyzed using the statistical technique PARAFAC to determine how many fluorescent species are contributing to the overall fluorescence signal. The number of fluorescent species was determined

for process-affected water from various sources, in addition to commercial naphthenic acids.

1.3 Methodology

Fluorescence signals were created using a Varian Cary Eclipse Spectrometer for process-affected water from three oil sands operations. Basic, neutral and acidic fractions were extracted from each source and fluoresced for comparison to the undiluted process-affected water samples. The waters from each source were then diluted to various levels for comparative analysis. The procedure was repeated for commercial naphthenic acids. The signatures were decomposed into their underlying fluorescent species using the statistical model PARAFAC.

1.4 Organization of Thesis

This thesis has been written in paper format and is organized as follows. Chapter 1 provides an overview of the background, objectives, and methodology of this research. Chapter 2 reviews current literature on organic acids in oil sands process-affected water, analytical techniques and PARAFAC. Chapter 3 examines fluorescence signals and the characteristics associated with process-affected water and naphthenic acids. Chapter 4 discusses how the statistical program PARAFAC can be applied to fluorescence signals to further analyze the fluorescent species. Chapter 5 summarizes the major findings and details suggestions for future work.

1.5 References

Alberta Government. 2011. Alberta's Oil Sands. [online] Available from http://www.oilsands.alberta.ca/resource.html [accessed Jan 2011].

Allen, E.W. 2008. Water treatment in Canada's oil sands industry I: Target pollutants and treatment objectives. Journal of Environmental Engineering and Science, 7: 123-128.

Alostaz, M., Biggar, K., Donahue, R., and Hall, G. 2008. Petroleum contamination characterization and quantification using fluorescence emission excitation matrices (EEMs) and parallel factor analysis (PARAFAC). Journal of Environmental Engineering and Science, 7: 183–197.

Bataineh, M., Scott, A.C., Fedorak, P.M., and Martin, J.W. 2006. Capillary HPLC/QTOF-MS for characterizing complex naphthenic acid mixtures and their microbial transformation. Analytical Chemistry, 78: 8354-8361.

Clemente, J.S. and Fedorak, P.M. 2004. Evaluation of the analyses of tert-butyldimethysilyl derivatives of naphthenic acids by gas chromatography – electron impact mass spectrometry. Journal of Chromatography, 1047(2004): 117-128.

Fan, T.P. 1991. Characterization of naphthenic acids in petroleum by Fast Atom Bombardment Mass Spectrometry. Energy & Fuels, 5: 371-375.

Grewer, D.M., Young, R.F., Whittal, R.M., and Fedorak, P.M. 2010. Naphthenic Acids and other acid-extractables in water samples from Alberta: What is being measured? Science of the Total Environment, 408(23): 5997-6010.

Han, X., MacKinnon, M.D., and Martin, J.W. 2009. Estimating the in situ biodegradation of naphthenic acids in oil sands process waters by HPLC/HRMS. Chemosphere, 76: 63-70.

Hao, C., Headley, J.V., Peru, K.M., Frank, R., Yang, P., and Solomon, K.R. 2005. Characterization and pattern recognition of oil sand naphthenic acids using

comprehensive two dimensional gas chromatography/time of flight mass spectrometry. Journal of Chromatography, 1067: 277-284.

Headley, J.V. and McMartin, D.W. 2004. A Review of the occurrence and fate of naphthenic acids in aquatic environments. Journal of Environmental Science and Health, A39(8): 1989-2010.

Headley, J.V., Peru, K.M., and Barrow, M.P. 2009. Mass Spectrometric characterization of naphthenic acids in environmental samples: A Review. Mass Spectrometry Reviews, 28: 121– 134.

Holowenko F, MacKinnon M and Fedorak P. 2001. Naphthenic acids and surrogate naphthenic acids in methanogenic microcosms. Water Resources, 35: 2596–2606.

Janfada, A., Headley, J.V., Peru, K.M., and Barbour, S.L. 2006. A laboratory evaluation of the sorption of oil sands naphthenic acids on organic rich soils. Journal of Environmental Science and Health, A41: 985-997.

Jivraj, M., M. Mackinnon, and B. Fung. 1995. Naphthenic Acid Extraction and Quantitative Analysis With FT- IR Spectroscopy. In Syncrude Analytical Manuals, 4th Edition, Research Department, Syncrude Canada Ltd., Edmonton, AB.

Lakowicz, J.R. 2006. Principles of Fluorescence Spectroscopy, 3rd Ed. Springer Science+Business Media, LLC, New York, NY.

Seifert, W., and Teeter, R. 1969. Preparative thin-layer chromatography and High Resolution Mass Spectrometry of crude oil carboxylic acids. Analytical Chemistry, 41(6): 786-795.

Seifert, W., Teeter, R., Howells, W.G., and Cantow, M. 1969. Analysis of crude oil carboxylic acids after conversion to their corresponding hydrocarbons. Analytical Chemistry, 41(12): 1639-1647.

Scott, A.C., Young, R.F., and Fedorak, P.M. 2008. Comparison of GC-MS and FTIR methods for quantifying naphthenic acids in water samples. Chemosphere, **73**: 1258-1264.

2. Literature Review

The following reviews available literature and data published related to the previously discussed research objectives. Naphthenic acids and their chemical properties that make them a compound of interest to the oil sands are reviewed. The available analytical techniques previously used to evaluate naphthenic acids are then reviewed. A discussion on fluorescence as an analytical technique and how it can be applied to process-affected water is then presented. In addition, the use of the statistical method parallel factor analysis (PARAFAC) in conjunction with fluorescence is then addressed.

2.1 Organic Acids in the Oil Sands

Bitumen extraction in the oil sands is currently carried out via modified versions of the Clark Hot Water Extraction method (Allen 2008). The raw ore is digested using warm water (50-80^{o}C) and sodium hydroxide (NaOH) that acts as a conditioning agent (Holowenko et al. 2002; Yen et al. 2004). During the extraction process naturally occurring organic acids are released from the bitumen and carried throughout the extraction plant in the process water (Janfada et al. 2006). When the water used in extraction is not able to be recycled, it is transferred to an impoundment with the tailings. This process affected water contains sands and clays and other particulate matter, including the organic acids, which are contained within the tailings pond impoundments (Allen 2008, Headley & McMartin 2004).

The organic acid fraction of process-affected water is of interest to the oil sands industry; it has been shown to have detrimental toxic properties, as well as corrosive properties. Earlier research identified naphthenic acids as the compound of interest (Allen 2008). Naphthenic acids are carboxylic acids of the form $C_nH_{2n+z}O_2$, where n is the number of carbons and Z indicates the hydrogen deficiency resulting from the ring formation. Ring structures typically contain

five or six carbons; with the Z value ranging from 0 to -12 and each multiple of -2 signifying another ring (Brient et al. 1995). Figure 1 shows some of the typical structures of naphthenic acids, where R represents an alkyl group, and m represents the length of the alkyl chain.

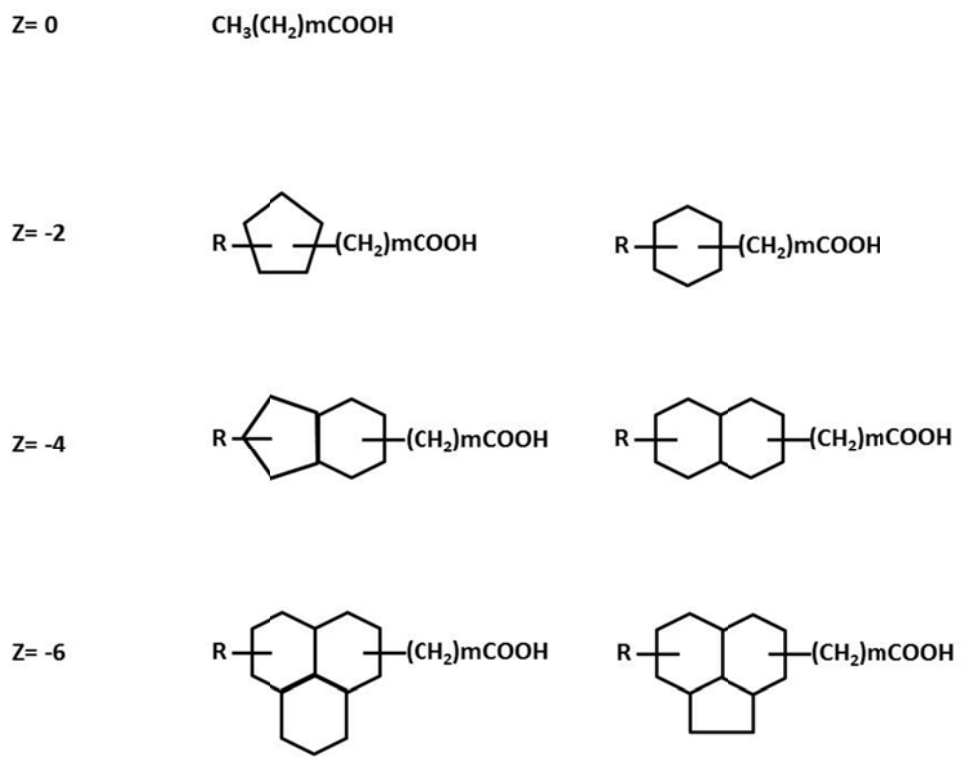

Figure 1: Naphthenic acid structures (Adapted from Hao et al. 2005). R represents an alkyl group, m represents the length of the alkyl chain, and Z corresponds to the number of rings in the acids.

2.2.1 Toxicity

The toxicity in the process affected water is generally associated with the surfactant properties of naphthenic acids (Headley and McMartin 2004). Higher levels of toxicity were reported in samples that were dominated by lower molecular weights, though a specific compound has yet to be established (Allen 2008; Janfada et al. 2006; McMartin 2004). Freshly deposited tailings water has been found to contain the highest levels of toxicity, and predominately contains

lower molecular weight naphthenic acids. As the ponds are allowed to age, the naphthenic acid mixture shifts towards larger molecules of higher molecular weight and toxicity levels are shown to decrease (Allen 2008).

One of the issues when determining toxic effects to organisms was the type of naphthenic acid the organism was exposed to. The complex nature implies that much of the research on toxicity is not comparable, as different naphthenic structures were used in the testing. For example, in review done by Clemente and Fedorak (2005) they indicate testing was completed using commercially available naphthenic acids, whereas others were obtained from the oil sands tailings ponds. Noted in the review was that the commercially available compounds contained lower molecular weights, whereas the tailings ponds tended to contain the higher end of the molecular weight spectrum. This makes it difficult to determine which naphthenic acids are of the most concern with respect to toxicity.

2.2.2 Corrosion

A second issue associated with naphthenic acids is corrosion. The corrosion reactions are not fully established due to the complex nature of naphthenic acid composition and structure (Slavcheva 1999). The amount of corrosion experienced by the system depends on the composition of the naphthenic acids, and is generally associated with the total acid number, or acidity present, as well as the layout of the system (Babaian-Kibala, 1994; Slavecheva 1999).

2.3 Analytical Techniques

The current industry standard for quantification of naphthenic acids is through Fourier Transform Infrared (FTIR) spectroscopy (Jivraj et al. 1995). The acid fraction of the water samples is extracted and then scanned in the spectrometer, where the absorbance of the monomeric and dimeric forms of the carbonyl groups at their respective wavelengths of 1743 and 1706 cm^{-1} are measured. The results

are then quantified by calibration curves derived from commercially available naphthenic acids. This method is unable to determine individual naphthenic acid species or give insight into which compounds are predominant.

Table 1 summarizes several of the published results where concentrations of naphthenic acids determined by research test methods are compared to the industry FTIR method for various sources. Other publications have detailed methodology for characterizing the naphthenic acid fraction by molecular weight but do not quantify a total naphthenic acid concentration (Bataineh et al. 2006;; Clemente and Fedorak, 2004; Fan 1991; Han et al. 2009; Hao et al. 2005; Zhenbo et al. 2006). Grewer et al. (2010) and Scott et al. (2008) compared gas chromatography mass spectrometry (GC-MS) to FTIR analysis, and found that FTIR consistently reported higher concentrations of naphthenic acids. Yen et al. (2004) compared FTIR analysis to high performance liquid chromatography (HPLC), and reported HPLC concentrations that were generally higher than the FTIR analysis.

Table 1: Reported naphthenic acid concentrations in various process affected water samples.

Source of naphthenic acids	Concentration (mg/L)	Test Method	Reference
Syncrude – Mildred Lake Settling Basin	44	FTIR	Grewer et al. 2010
	28	GC-MS	
Syncrude – West In-Pit	60	FTIR	
	36	GC-MS	
Syncrude – Pond 9	20	FTIR	
	7.1	GC-MS	
Syncrude – Demo Pond	14	FTIR	
	5.9	GC-MS	
Suncor – Pond 2/3	63	FTIR	
	47	GC-MS	
Suncor – Pond 5	38	FTIR	
	26	GC-MS	
Suncor –	130	FTIR	

Steam Assisted Gravity Drainage	38	GC-MS	
Albian –	35	FTIR	
Tailings Pond	18	GC-MS	
Company A –	45	FTIR	Scott et al. 2008
Tailings Pond 1	17	GC-MS	
Company A –	25	FTIR	
Tailings Pond 2	6.4	GC-MS	
Company A –	11	FTIR	
Aged Sample	2.9	GC-MS	
Company B –	17	FTIR	
Tailings Pond sampled in 2004	4.0	GC-MS	
Company B –	34	FTIR	
Tailings Pond sampled in 2007	12	GC-MS	
Company C –	18	FTIR	
Consolidated Tailings	4.9	GC-MS	
Company C –	78±1.5	FTIR	
Tailings Pond	53±15	GC-MS	
Company C –	120	FTIR	
Steam Assisted Gravity Drainage	21	GC-MS	
Syncrude naphthenic acid extract –	0.5	FTIR	Yen et al. 2004
0 mg/L	4±2.5	HPLC	
Syncrude naphthenic acid extract –	8	FTIR	
10 mg/L	13±1.8	HPLC	
Syncrude naphthenic acid extract –	24	FTIR	
30 mg/L	22±2.1	HPLC	
Syncrude naphthenic acid extract –	51	FTIR	
60 mg/L	64±2.6	HPLC	
Syncrude naphthenic acid extract –	75	FTIR	
80 mg/L	78±0.5	HPLC	

Clemente and Fedorak (2004) suggested that gas chromatography was the most accessible method available for mass spectrometry of naphthenic acids. In gas chromatography, an inert gas is passed through an inert column, where various parts of the naphthenic acid components would emerge after different retention times. As the number of carbons and rings in the structure are increased, their retention time in the chromatography column is increased (Hao et. al., 2005). The analysis gives a nominal mass that could then be used to predict the carbon number and subsequent empirical formula for the naphthenic acids. This method provides deeper insight to the isotopes present in the naphthenic acid fraction, however it is unable to separate individual compounds. This method produces higher resolution data that is presumably more accurate. High performance liquid chromatography (HPLC) requires the derivatization of the carboxyl group. The

derivatized compounds are eluted from a column at retention times related to their mass. In both GC-MS and HPLC methods, the total naphthenic acid concentration was determined using calibration curves derived from commercial naphthenic acids.

As analytical methods have progressed so has the knowledge of the organic acid fraction, including of naphthenic acids. What has been classified as the naphthenic acid fraction does not always fall within the general formula $C_nH_{2n+Z}O_2$. The presence of pyrolles, thiophenes, phenols, nitrogen and sulphur has been detected in the naphthenic acid portion in crude oil (Seifert et al. 1969; Seifert and Teether 1969). Using high resolution mass spectrometry (HRMS) in conjunction with HPLC, naphthenic acids with three to five oxygens, instead of two commonly associated with naphthenic acids, were found: these are known as oxy naphthenic acids, were found (Bataineh et al 2006; Han et al. 2009). Clemente and Fedorak (2004) acknowledged that a disadvantage of GC-MS was misclassification by mass, as these oxy naphthenic acids were incorrectly classified as higher molecular weight compounds. Recently, a study used ultra-high resolution electrospray ionization fourier transform ion cyclotron resonance mass spectrometry (ESI-FT-ICR MS) and found that less than 50% of what is extracted from oil sands water, and is categorized as naphthenic acids fits the classical definition (Grewer et al. 2010).

2.4 Fluorescence

Compounds will exhibit a florescence due to their electron structure and chemical bonds within aromatic components (Alostaz et al. 2008). Aromatic compounds are comprised of single and double bonds. The single bonds contain a shared electron pair, which forms a σ bond containing low energy levels. In a double bond, the first shared electron pair forms a σ bond and the second electron pair forms a π bond (Alostaz et al. 2008). The π bond exhibits weak binding forces that, when subjected to ultraviolet light, allow electrons to absorb the energy and are subsequently promoted to a higher energy level.

The fluorescence spectra can be obtained using two different scanning techniques, emission and excitation fluorescence spectra. In the emission spectrum the excitation wavelength is held constant and the emission fluorescence radiation is measured. Conversely, in the excitation spectrum the observation wavelength is held constant and intensity is measured as a function of excitation wavelength (Alostaz et al. 2008). Combining the information obtained from the two spectra enables the construction of a three dimensional plot known as an excitation-emission matrix (EEM) (Rho and Stewart 1978). The EEM is a three way array of fluorescence intensity, the emission spectrum, and the excitation spectrum.

In cases where multiple components are present, the fluorescence signals obtained can overlap and become difficult to resolve. Alternative techniques such as synchronous fluorescence spectrometry (SFS) and time resolved fluorescence spectrometry may be used. In SFS both the excitation and emission wavelengths are scanned simultaneously while keeping a constant wavelength interval between them (Vo-Dinh 1978). Time resolved fluorescence spectrometry utilizes the varying fluorescent times of each of the multiple components. The intensity contributions of each compound can then be resolved using time or frequency (Alostaz et al. 2008).

Fluorescence spectrometry has been used as an analytical technique in several different areas of application including biochemistry, medicine and molecular biology to determine biomolecules, metal ions and organic compounds (Díaz-García and Badía-Líaño 2005). Fluorescence has been used to determine trace levels of species in clinical, biological and environmental samples. Petroleum products such as gasoline, diesel, and heavy crude oil that contain polycyclic aromatic hydrocarbons (PAHs) have been shown to produce unique EEMs which can be used to track and determine contamination (Alostaz et al. 2008). Synchronous fluorescence spectrometry has been used for detecting natural

organic matter, as well as PAHs and petroleum contaminants (Kavanagh et al. 2009).

Fluorescence spectrometry as an analytical technique has many benefits; it is highly sensitive and can be used to identify trace components in small sample sizes (Díaz-García and Badía-Líaño 2005). Samples do not require preparation and are not affected or destroyed during measurement, nor are hazardous by-products generated (Alostaz et al. 2008). In addition fluorescence methods are readily reproducible, simple and cost effective (Brown et al. 2009). The signatures generated are unique and offer the ability to identify individual compounds, making fluorescence techniques a powerful characterization tool.

2.4.1 Applications to Naphthenic Acids and Process Affected Water

Recently fluorescence technology has been applied to naphthenic acid measurements in process affected waters. The general formula used to describe traditional naphthenic acids, $C_nH_{2n+Z}O_2$, does not indicate that fluorescence will occur. However the naphthenic acids extracted from oil sands have been shown to contain various levels of aromaticity (Headley et al. 2009). Mohammed et al. (2008) demonstrated this ability and determined a linear response in UV light absorbed and naphthenic acid concentrations from 1-100 mg/L.

Brown et al. (2009) used fluorescence EEM for process affected water samples from various oil sand companies and groundwater samples in the Athabaskan area. The EEMs obtained demonstrated that fluorescent signatures differed between each of the companies sampled and groundwater samples exhibited less intensity. The deviations among the process affected water samples were attributed to the proprietary refining methods used by each company, and the age and storage of the samples (Brown et al. 2009). It is suggested that lower molecular weight naphthenic acids will fluoresce at shorter emission wavelengths than the higher molecular weight. Previous characterization methods have

confirmed that the naphthenic acid concentrations in the ground water are lower than those found in the process affected water (Allen 2008). In order to confirm that the intensity observed in the EEMs was correlated to concentration, Brown et al. (2009) performed a series of dilutions. The resulting emission spectrum showed that as the sample was diluted to lower concentrations, the observed intensity was also lowered without shifting of the peak to other wavelengths.

Similar excitation peaks were observed at approximately 290nm for process affected water in both studies performed by Brown et al. (2009) and Mohammed et al. (2008). The excitation peak for groundwater samples was found to be lower at an excitation wavelength of approximately 260nm (Brown et al. 2009). Emission peaks were observed at 305nm and 340nm for fresh process affected water samples in the study completed by Brown et al. (2009) and a similar peak was observed at 346nm in the study completed by Mohammed et al. (2008). In an aged sample, the first observed peak was observed at a lower emission wavelength of 290nm and the second peak was again at 340nm, though not as prominent (Brown et al. 2009). Similar results have been determined using synchronous fluorescence spectrometry by Kavanagh et al. (2009). Samples were scanned at an offset wavelength interval of 18nm and fluorescence peaks were established at wavelengths of 282.5nm and a broad peak in the range of 320 to 340nm (Kavanagh et al. 2009).

2.5 Parallel Factor Analysis (PARAFAC)

Where multiple fluorescent components are present the signals obtained can become complex due to light scatter, interferences and overlapping signals (Anderson and Bro 2003). In the case of overlapping signals a decomposition algorithm can be used, such as parallel factor analysis (PARAFAC). PARAFAC is a multivariable statistical procedure that can be used to decompose EEM data and differentiate the components of the mixture (Alostaz et al. 2008). The data

collected from an EEM can be classified as multi-way data, where several sets of data variables are measured in a crossed fashion.

PARAFAC can be used to break down the EEM signal to determine the number of significant fluorescent components, or fluorophores, when it is unknown in the sample (Goncalves et al. 2008). When EEMs of the sample are obtained at different concentrations a three way array is created with elements f_{ijk} (fluorescence intensity of sample i, at excitation wavelength j, and emission wavelength k) that are given by Equation 1.

$$f_{ijk} = \sum_{n=1}^{F1} c_{in} ex_{jn} em_{kn} + res_{ijk} \quad (1)$$

In Equation 1 the number of different fluorophores is represented by F1, c_{in} is the concentration of the nth fluorophore in sample i, ex_{jn} and em_{kn} are the excitation and emission spectra vectors of the nth fluorophore, and res_{ijk} is the residual error.

PARAFAC creates a model matrix **X** based on the above equation by breaking it down into three loading matrices and a matrix of error. **A** is the estimated concentration (or fluorescence intensity), **B** is the matrix of excitation wavelengths and **D** is the emission wavelengths. Each element of matrix **X** can be calculated according to Equation 2, where $a_{in}, b_{jn},$ and d_{kn} are the respective elements from the loading matrices.

$$x_{ijk} = \sum_{n=1}^{F1} a_{in} b_{jn} d_{kn} + Error_{ijk} \quad (2)$$

The method uses an alternating least squares approach, which approximates a solution when there are more equations than unknowns. The loadings in two of the modes are known and the last set of unknown parameters is estimated. This is

done successively until the stop criterion is reached. The most common criterion is to stop the iterations when the relative change between two iterations is below a certain value (Bro 1997). The program utilizes a random initialization starting point, so the algorithm should be run twice to ensure the convergence to the same solution.

The optimal number of fluorescent components (F1 in both equations 1 and 2) that can be determined is decided using three different criteria. The first is by looking at the residuals between the data and the function provided by PARAFAC. The residuals should be random and described noise instead of systematic variation in the data. The second criterion is the deviation of the data and the model known as the internal parameter core consistency. The core consistency plot depicts the core elements and shows which elements are ideally either zero or non-zero (Bro 1997). Lastly the number of fluorescent components that can be determined can be determined by the amount of distinct component peaks visible within the excitation and emission matrix plots.

PARAFAC is similar to other decompositional methods such as Tucker3 and Principle Component Analysis (PCA). These methods transform possibly correlated variables into smaller uncorrelated variables (Bro 1997). The advantage of PARAFAC over these other methods is that it uses fewer degrees of freedom, and offers a unique solution.

2.6 References

Allen, E.W. 2008. Water treatment in Canada's oil sands industry I: Target pollutants and treatment objectives. Journal of Environmental Engineering and Science, 7: 123-128.

Alostaz, M., Biggar, K., Donahue, R., and Hall, G. 2008. Petroleum contamination characterization and quantification using fluorescence emission

excitation matrices (EEMs) and parallel factor analysis (PARAFAC). Journal of Environmental Engineering and Science, 7: 183–197.

Anderson C.M., and Bro. R. 2003. Practical aspects of PARAFAC modeling of fluorescence excitation-emission data. Journal of Chemometrics, 17:200-215.

Babaian-Kibala, E. 1994. Phosphate ester inhibitors solve naphthenic acid corrosion problems. Oil and Gas Journal, 92: 31-35.

Bataineh, M., Scott, A.C., Fedorak, P.M., and Martin, J.W. 2006. Capillary HPLC/QTOF-MS for characterizing complex naphthenic acid mixtures and their microbial transformation. Analytical Chemistry, 78: 8354-8361.

Brient, J.A.; Wessner, P.J.; Doyler, M.N. Naphthenic acids. In Kirk-Othmer Encyclopedia of Chemical Technology, 4th ed.; Kroschwitz, J.I., Ed.; John Wiley and Sons: New York, 1995; 1017–1029.

Brown, L.D., Alostaz, M., and Ulrich, A.C. 2009. Characterization of Oil Sands Naphthenic Acids in Oil Sands Process-Affected Waters Using Fluorescence Technology. In Proceedings, 62nd Canadian Geotechnical Conference, Halifax, Nova Scotia, September 20-24, 2009.

Bro, R. 1997. PARAFAC Tutorials and Applications. Chemometrics and Intelligent Laboratory Systems. 38(2):149-171.

Clemente, J.S. and Fedorak, P.M. 2004. Evaluation of the analyses of tert-butyldimethysilyl derivatives of naphthenic acids by gas chromatography – electron impact mass spectrometry. Journal of Chromatography, 1047: 117-128.

Clemente, J.S. and Fedorak, P.M. 2005. A review of the occurrence, analyses, toxicity, and biodegradation of naphthenic acids. Chemosphere, 60(2005): 585-600.

Díaz-García, M.E., and Badía-Líaño, R. 2005. Fluorescence: Overview. 97-106.

Fan, T.P. 1991. Characterization of naphthenic acids in petroleum by Fast Atom Bombardment Mass Spectrometry. Energy & Fuels, 5: 371-375.

Goncalves, H., Medonca, C., Esteves da Silva, J.C.G. 2009. PARAFAC analysis of the quenching of EEM of fluorescence of glutathione capped CdTe quantum dots by Pb (II). Journal of Fluorescence, 19:141-149.

Grewer, D.M., Young, R.F., Whittal, R.M., and Fedorak, P.M. 2010. Naphthenic Acids and other acid-extractables in water samples from Alberta: What is being measured? Science of the Total Environment, 408(23): 5997-6010.

Hao, C., Headley, J.V., Peru, K.M., Frank, R., Yang, P., and Solomon, K.R. 2005. Characterization and pattern recognition of oil sand naphthenic acids using comprehensive two dimensional gas chromatography/time of flight mass spectrometry. Journal of Chromatography, 1067: 277-284.

Han, X., MacKinnon, M.D., and Martin, J.W. 2009. Estimating the in situ biodegradation of naphthenic acids in oil sands process waters by HPLC/HRMS. Chemosphere, 76: 63-70.

Headley, J.V. and McMartin, D.W. 2004. A Review of the occurrence and fate of naphthenic acids in aquatic environments. Journal of Environmental Science and Health, A39(8): 1989-2010.

Headley, J.V., Peru, K.M., and Barrow, M.P. 2009. Mass spectrometric characterization of naphthenic acids in environmental samples: A Review. Mass Spectrometry Reviews, 28: 121– 134.

Holowenko, F., MacKinnon, M. and Fedorak, P. 2002. Characterization of naphthenic acids in oil sands wastewaters by gas chromatography-mass spectrometry. Water Research, 36, 2843–2855.

Janfada, A., Headley, J.V., Peru, K.M., and Barbour, S.L. 2006. A laboratory evaluation of the sorption of oil sands naphthenic acids on organic rich soils. Journal of Environmental Science and Health, A41: 985-997.

Jivraj, M., M. Mackinnon, and B. Fung. 1995. Naphthenic acid extraction and quantitative analysis with FT- IR Spectroscopy. In Syncrude Analytical Manuals, 4th Edition, Research Department, Syncrude Canada Ltd., Edmonton, AB.

Kavanagh, R.J., Burnison, B.K., Frank, R.A., Soloman, K.R., and Van deer Kraak, G. 2009. Detecting oil sands process-affected waters in the Alberta oil sands region using synchronous fluorescence spectroscopy. Chemosphere, 76: 120–126.

McMartin, D.W., Headley, J.V., Friesen, D.A., Peru, K..M., and Gillies, J.A. 2004. photolysis of naphthenic acids in natural surface water. Journal of Environmental Science and Health, A39(6): 1361-1383.

Mohammed, M.H., Wilson, L.D., Headley, J.V., and Peru, K.M. 2008. Screening of oil sands naphthenic acids by UV-Vis absorption and fluorescence emission spectrophotometry. Journal of Environmental Science and Health, Part A 43: 1700–1705.

Seifert, W., and Teeter, R. 1969. Preparative thin-layer chromatography and High Resolution Mass Spectrometry of crude oil carboxylic acids. Analytical Chemistry, 41(6): 786-795.

Seifert, W., Teeter, R., Howells, W.G., and Cantow, M. 1969. Analysis of crude oil carboxylic acids after conversion to their corresponding hydrocarbons. Analytical Chemistry, 41(12): 1639-1647.

Scott, A.C., Young, R.F., and Fedorak, P.M. 2008. Comparison of GC-MS and FTIR methods for quantifying naphthenic acids in water samples. Chemosphere, **73**: 1258-1264.

Slavcheva, E., Shone, R., and Turnbull, A., 1999. Review of naphthenic acid corrosion in oil refining. British Corrosion Journal, 34: 125–131.

Rho, J.H., and Stewart, J.L. 1978. Automated Three-Dimensional plotter for fluorescence measurements. Analytical Chemistry, 50(4): 620-625.

Vo-Dinh, T. 1978. Multicomponent analysis by synchronous luminescence spectrometry. Analytical Chemistry, 50(3): 396-401.

Yen, T.W., Marsh, W.P., MacKinnon, M.D., and Fedorak, P.M. 2004. Measuring naphthenic acids concentrations in aqueous environmental samples by liquid chromatography. Journal of Chromatography A, 1033 (2004) 83–90.

Zhenbo, L.,Songbai, T., Yuchun, Z., Yi., D., and Lihong, Z. 2005. Determination of naphthenic acids in crude oil by chemical ionization mass spectrometry. Chinese Journal of Geochemistry, 24(1): 67-72.

3. Fluorescence of Process-Affected Water

3.1 Introduction

Process-affected water from the oil sands tailings ponds will produce a characteristic fluorescence signal when exposed to ultraviolet (UV) light in the wavelength range of 260 to 450 nm. Fluorescence has been used as an analytical tool for petroleum compounds in previous research. The signal produced from process-affected water is complex and overlapping, and indicates there are multiple species that contribute to the overall signal. The signals produced are called excitation-emission matrices, and are made up of different wavelengths and intensity of signals. Previous research has studied the correlation between fluorescence signal and naphthenic acids; naphthenic acids are a large group of complex carboxylic acids found in process-affected water. Mohammed et al. (2008) demonstrated a linear response in UV light absorbed and naphthenic acid concentration from 1-100 mg/L. The intensities at various excitation wavelengths were also observed and tracked for various concentrations of process-affected water and naphthenic acids. Brown et al. (2009) observed how peak intensity at a specific excitation wavelength decreased without shifting in the emission spectrum for a dilution series of process-affected water. Similar intensity peaks were observed by Kavanagh et al. (2009) and found to correlate with naphthenic acid concentrations determined from Fourier Transform Infrared spectroscopy.

The signals from process-affected water from various sources were evaluated to determine if fluorescence was a suitable analytical technique to detect naphthenic acids. Extractions were performed on process-affected water in order to determine if the fluorescence signal was produced by basic, neutral or acidic compounds. Samples were examined from various oil sands operations to determine if the fluorescence signals differed when the source was changed. The change in fluorescence signal was examined over three different sources of water over various levels of process-affected water concentration. Several defining

characteristics of the fluorescence signals were examined in detail in order to narrow down and define a characteristic that was distinctive of the process-affected water. Three characteristic properties were examined; the volume intensity of the matrix, the area of intensity under a particular excitation wavelength and the peak intensity of a particular excitation wavelength. The fluorescence properties were then correlated with known naphthenic acid quantification techniques.

3.1.1 Materials and Methods

3.1.2 Sources and preparation of samples

For this study process affected water samples were obtained from three different oil sand operations. Process-affected water from Syncrude was obtained from the West In-Pit tailings pond and from Suncor was obtained from the South Tailings Pond. Samples from Albian were obtained directly from their oil sands tailings pond. Samples were refrigerated at 4^{o}C and stored in plastic containers. Prior to analysis, samples were filtered using vacuum filtration and 0.45 µm nylon filters to remove suspended particles in the samples that cause light scatter during measurement.

A dilution series was prepared for each water source. Each water source was diluted with deionized water for contents of 75%, 50%, 25% and 10% process-affected water content including an undiluted sample. An Excitation-Emission Matrix was generated for each sample using fluorescence. In addition, naphthenic acid concentrations were determined using Fourier Transform Infrared spectroscopy.

3.1.3 Fluorescence and Absorbance Measurements

An Eclipse model Varian Cary spectrometer was used for fluorescence measurements using the 90^{o} detection setup. Samples were analyzed in clear

quartz cuvettes measuring 1.24x1.24x4.5 cm, requiring approximately 5 mL sample volume. Excitation-Emission Matrices were generated using Varian Cary Eclipse software at a scan rate of 600 nm/min. Emission wavelengths were collected from 240 to 600 nm with 1 nm increments at excitation wavelengths ranging from 250 to 450 nm with 10 nm increments. The bandwidth (slit width) was 10 nm and 5 nm for excitation and emission, respectively. Both excitation and emission filters were set to automatic. Absorbance measurements were recorded using a Shimadzu UV2401-PC UV-VIS Recording Spectrophotometer and were obtained for wavelengths from 250 to 600 nm with 1 nm increments.

3.1.4 Fourier Transform Infrared Spectroscopy

Naphthenic acid concentration was determined using a Perkin Elmer Spectrum 100 Fourier Transform Infrared (FTIR) spectrometer. Filtered process-affected water samples of 500 mL were prepared for the respective dilution series of each water source. The FTIR requires the organic acid fraction to be extracted prior to analysis. The extraction method used is outlined in Appendix A. For this research basic and neutral fractions were extracted in addition to the acid fraction. This is a modified extraction method similar to the industry standard used (Jivraji et al. 1995). The FTIR equipment then measures the absorbance of the monomeric and dimeric forms of the carbonyl groups at their respective wavelengths of 1743 and 1706 cm^{-1}. The results are then quantified by calibration curves derived from the commercially available Sigma Aldrich naphthenic acids. The FTIR method and raw data acquired for the calibration curve are found in Appendix B.

3.1.5 Other Analytical Methods

Undiluted process-affected water samples from each oil sands operation were analyzed for naphthenic acid concentrations using high resolution mass spectrometry (HRMS) at the division of analytical and environmental toxicology

at the University of Alberta. Additionally dissolved organic carbon content was analyzed at the Biogeochemical Analytical Laboratory, also at the University of Alberta.

3.2 Results and discussion

3.2.1 Excitation Emission Matrix

When process-affected water is subjected to ultraviolet light in the wavelength range of 260 to 450 nm, a fluorescence signal is produced. This signal represents the combination of excitation and emission wavelengths and intensities from fluorescent species present in the sample. A fluorescence species will emit intensity based on the excitation and emission wavelengths it is exposed to and the concentration of the species present in the sample (Goncalves et al. 2008). The data is arranged to form an excitation-emission matrix (EEM). The EEM is a three way array of fluorescence intensity, the emission spectrum, and the excitation spectrum. The intensity that is obtained from the spectrometer is recorded as arbitrary units, and is comparable between samples exposed to the same amount of energy, determined by the slit width (Lakowicz 2006).

The resulting EEMs from process-affected water are complex and overlapping, allowing the data to be viewed in several different methods. There are several factors that can affect the overall EEM. Inner filter effects cause the intensity recorded by the optics detector to be reduced and can be divided into primary and secondary inner filter effects (Tucker et al. 1992). The primary inner filter effect occurs when the intensity of the excitation beam is lost before it is viewed by the optics detector due to the right angle set up of the spectrometer. The secondary inner filter effect is a result of absorption of the emission beam due to high fluorescence. This is accounted for by recording the absorbance of the sample and applying a correction factor. Further explanation and necessary equations for the correction factor are included in Appendix C. Light scatter is another factor

that affects the EEM signal. Particles in the samples cause the light to deviate from its original path and spread out (Anderson and Bro 2003). Light scatter is not part of the signal and the amount of light scatter present will depend on the sample. Light scatter is manually deleted from the signal during data processing.

There are several different ways to visualize the EEM. The entire EEM can be graphed three dimensionally, examples illustrating two EEMs of the same process-affected water sample are shown in Figure 3.1. The first EEM shows the intensities obtained from the spectrometer before applying the correction factor, and include the light scatter. The light scatter appears as a diagonal line, and in this instance is over powering the signal. The second EEM has been corrected for inner filter effects and the light scatter has been removed.

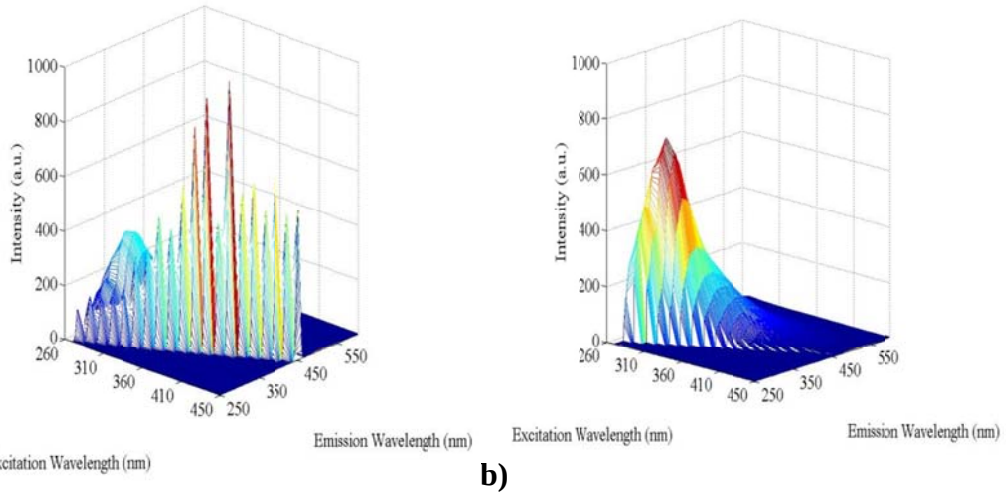

Figure 3.1: Three dimensional Excitation-Emission Matrix of process-affected water a) prior to absorbance correction and light scatter removal; b) after correction for absorbance and light scatter removal.

Another method of viewing EEMs is through contour plots. Taking the same data presented in Figure 3.1 the intensities are plotted as contours (visually it is the aerial view of the EEMs in Figure 3.1). Figure 3.2 shows the two EEMs

compared side by side with the first EEM showing the raw data and the second showing the corrected intensities with the light scatter removed.

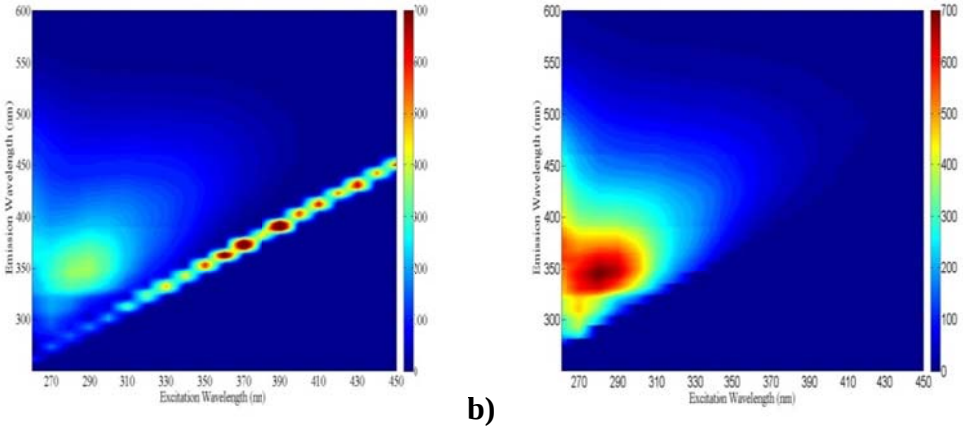

a) **b)**

Figure 3.2: Contour plot of Excitation-Emission Matrix of process-affected water a) prior to absorbance correction and light scatter removal; b) after correction for absorbance and light scatter removal.

The last graphical method presented is a two dimensional plot of the emission wavelengths and the corresponding intensities recorded for each excitation wavelength evaluated. Each excitation wavelength is graphed as a separate line. As before the same data is plotted and presented in Figure 3.3. The first EEM represents the raw data that is not corrected for absorbance and includes the light scatter, while the second EEM has been corrected for absorbance and the light scatter is removed. When the light scatter is removed it is not recorded as a zero; zero indicates a value of intensity, at these locations there is no value recorded.

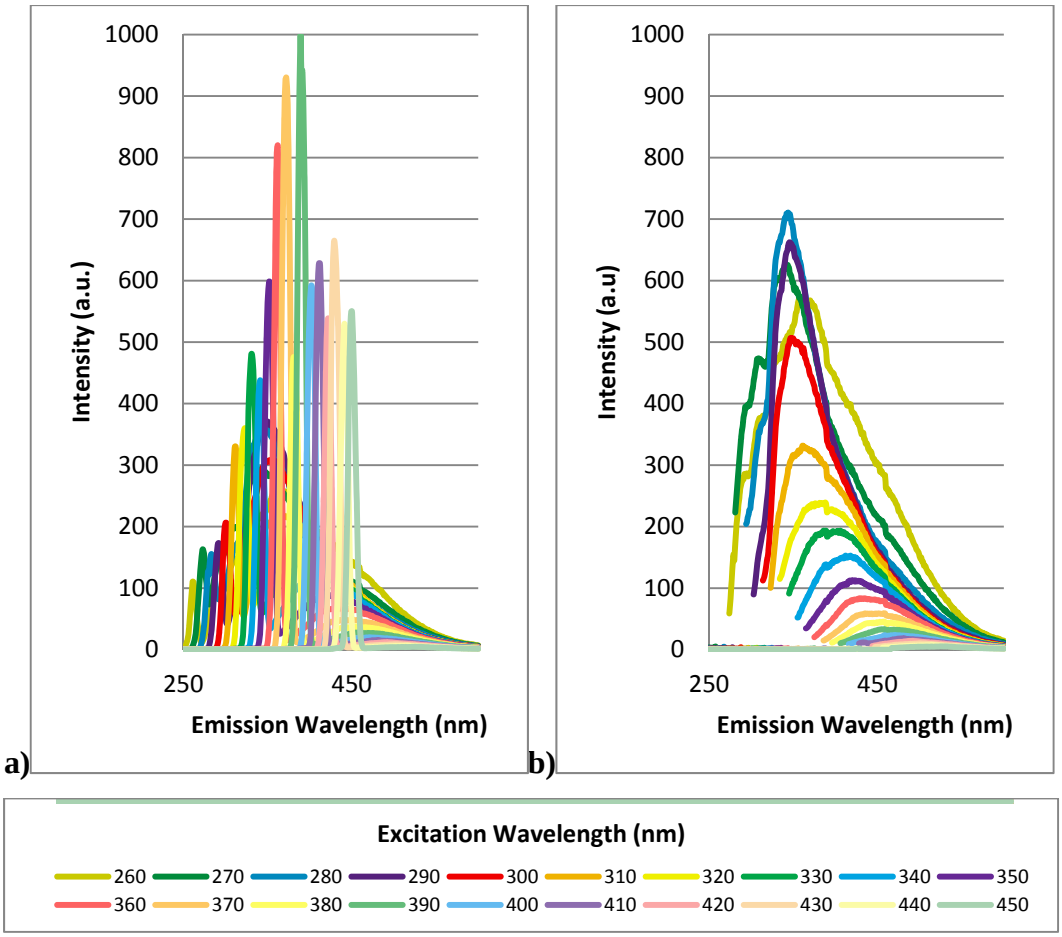

Figure 3.3: Emission spectra of process-affected water a) prior to absorbance correction and light scatter removal; b) after correction for absorbance and light scatter removal.

There are several characteristics of the EEM that can be examined, including the volume of the EEM, the area of intensity under a specific excitation wavelength, and the peak intensity of a specific excitation wavelength. Three-dimensional plotting of an EEM (Figure 3.1) is the most effective visual representation of the volume of the EEM. Using this method of graphing the area of intensity appears as a band, with the peak intensity being the highest point. The contour plot (Figure 3.2) is unable to convey these characteristics as effectively as the three-dimensional plot, however demonstrates where majority of the signal is produced for process-affected water. Majority of the signal produced is found in the lower excitation and emission wavelengths. Absorbance is found to be higher in these lower wavelengths, which reports a lower intensity. Since a majority of the signal

is in this area the correction for inner filter effects becomes important. The last graphical method is an effective method for depicting the peak intensity. The area of intensity appears as the region underneath the outline of an individual excitation wavelength. In samples where the light scatter is abundant the signal and peaks are difficult to view, necessitating removal for data analysis.

3.2.2 Extractions

In order to further understand what compounds were responsible for the fluorescence signal in process-affected water, extractions were performed to separate out the basic, neutral and acidic fractions. The extraction method used is outlined in Appendix A. The end products of the extractions were then diluted with dichloromethane (DCM) to approximately the same concentration levels that would be expected in the process-affected water tailings ponds. The extractions were performed on process-affected water from three water sources; Syncrude, Suncor and Albian. The basic and neutral fractions did not produce any signal for any of the three sources. Signals were produced in the acid fraction for all three sources. The EEMs of each fraction for each respective water source is contained in Appendix D. Comparison of a sample of process-affected water and an acid extract from the same source is shown in Figure 3.4. These EEMs have not been corrected for absorbance and the light scatter has not been removed.

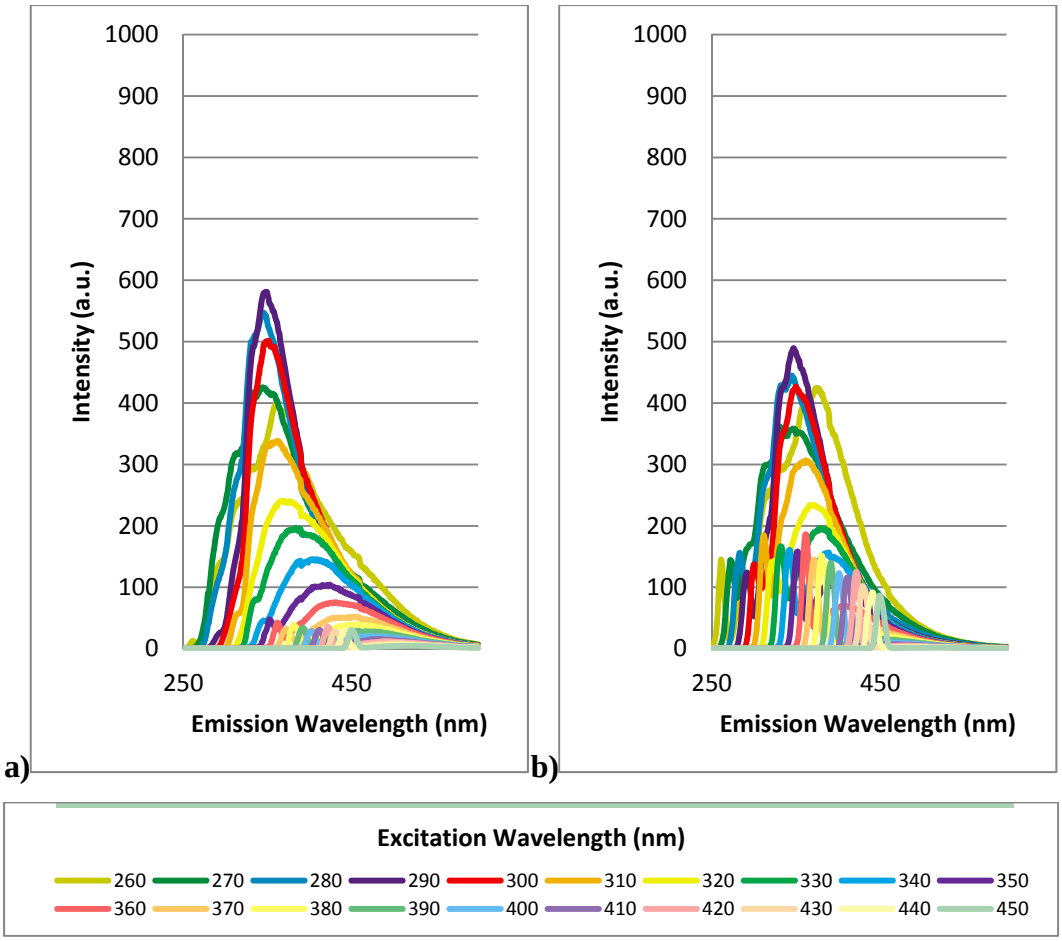

Figure 3.4: Emission spectra over excitation wavelengths 260-450nm of a) process-affected water b) acid extraction.

The two samples produce fluorescence signals of approximately the same shape, with prominent peaks occurring at the same excitation wavelengths in similar emission wavelength locations. The most prominent peaks occur at the 290 nm excitation wavelength, with another pronounced peak slightly below at the 280 nm. The difference in intensities can be attributed to the dilution factor of the acid extract. This narrows down the chemical composition of the possible fluorescent compound or compounds in the process-affected water and aides in further analysis as the fluorescence signal can be attributed entirely to the acid fraction of process-affected water.

3.2.2.1 Solvents

The extraction solvent, DCM, was fluoresced under the same conditions prior to analysis to determine if there was any influence on the EEM signal. Aside from light scatter, DCM did not produce any signal. Deionized water was used to dilute the process-affected water to various levels for fluorescence signals. Like DCM, deionized water gave no signal aside from light scatter. In order to determine whether another solvent would be a suitable choice, methanol was also scanned. Methanol is a common solvent in other applications, and is able to dissolve commercially available naphthenic acids. In this case methanol produced a weak signal, under 30 arbitrary units (a.u.), most significantly in the lower excitation wavelengths. This can become significant when the fluorescent compound content is low. The resultant EEMs are found in Appendix E.

3.2.3 Fluorescence Dilution Series

Process-affected water samples were acquired from three water sources; Syncrude, Suncor and Albian. Each sample was fluoresced in order to determine how the variation in location and extraction process affected the fluorescence signal. The signals obtained were corrected for absorbance and the light scatter removed, as shown in Figure 3.5. The EEMs prior to and following absorbance correction and light scatter removal are contained in Appendix F. Samples were filtered to 0.45 µm in order to remove particulate matter that cause increased light scatter. At this filter size a small amount of light scatter was observed in the Syncrude and Suncor samples. However, large amounts of light scatter were observed with the Albian sample. Samples were then filtered a second time through 0.2 µm filters. While the amount of light scatter was reduced, most noticeably in the Albian sample, the overall signal shapes and intensities were not significantly altered. This adds an unnecessary second filtering step, as the light scatter is removed for analysis. A comparison of EEMs filtered to 0.45 µm and 0.2 µm are shown in Appendix G.

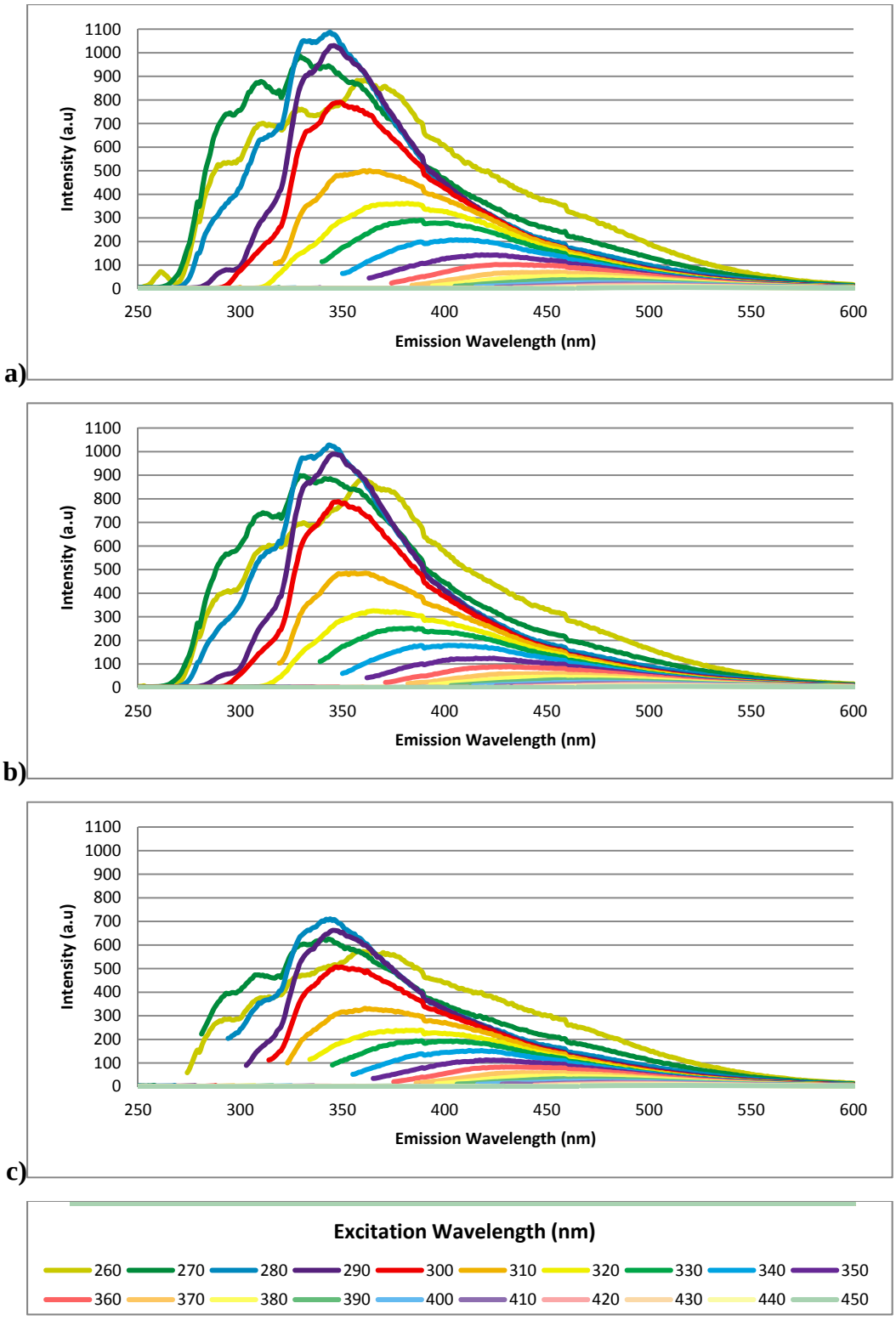

Figure 3.5: Emission spectra of process-affected water from various water sources over excitation wavelengths 260-450 nm a) Syncrude b) Suncor c) Albian.

The signals produced from the various water sources exhibited similar shapes with prominent peaks occurring at similar emission and excitation wavelengths. Prior to correction for absorbance, a characteristic peak occurs at the 290 nm excitation wavelength, and approximately the 346 nm emission wavelength. When the inner filter effects are accounted for the 280 nm excitation wavelength becomes more pronounced at approximately 343 nm emission wavelength. The most evident variation between the water sources was in intensity. The similar shape of the EEMs indicates that process-affected waters from each company contain the same fluorescent species; the variation in intensity indicates that the species are in different concentrations.

In order to determine the effect of process-affected water concentration on the signal intensity, a dilution series was prepared for each water source. Each source was diluted to 75%, 50%, 25% and 10% process-affected water content. Within each dilution series the EEM signal retained the shape and locations of the peak intensities, without shifting the peak to other wavelengths. As the process-affected water content was decreased, the peak intensities observed were also decreased. The fluorescence signals obtained for each sample within each dilution series are contained in Appendix H. Examining the 280 nm excitation wavelength within a dilution series the preservation of the peak is demonstrated for the Syncrude dilution series in Figure 3.6. The Suncor and Albian dilution series displayed the same trend; similar preservation was evident for all excitation wavelengths. The conservation of the intensity peak throughout the dilution series demonstrates the correlation between fluorescence intensity and process-affected water concentration.

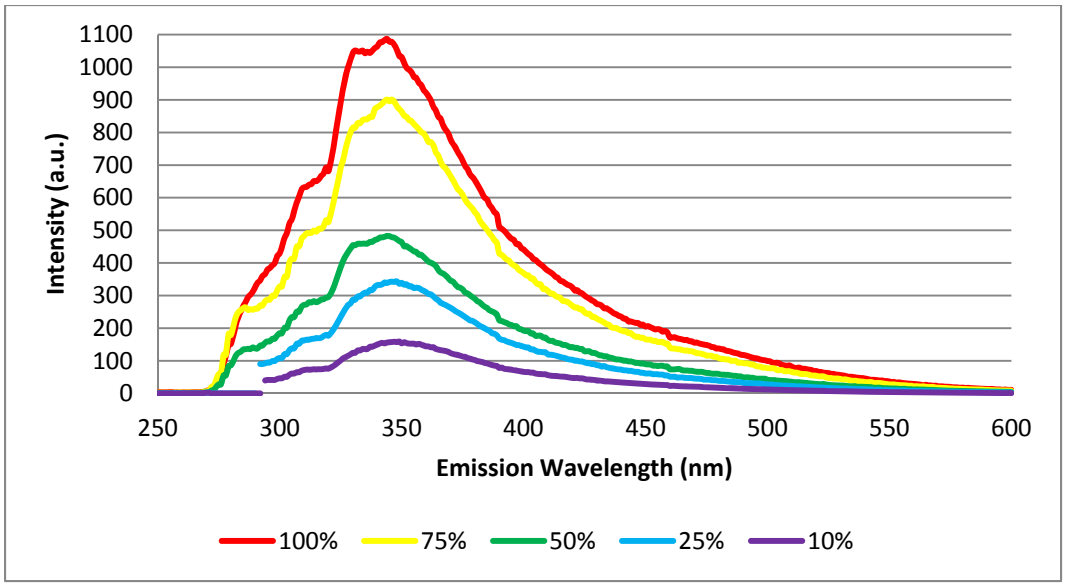

Figure 3.6: Emission spectra of Syncrude process-affected water dilution series at excitation wavelength 280 nm.

3.2.4 Quantification of Excitation-Emission Matrices

The EEMs produced from process-affected water are complex and can be quantified by several different methods. In order to determine which method was best suited for process-affected water, three characteristic properties of the EEMs were examined in relation to the process-affected water concentration and the water source; the volume intensity of the EEM, the area of intensity under the 280 nm excitation wavelength and the peak intensity at the 280 nm excitation wavelength. The 280nm wavelength was chosen for the area and peak intensity analysis as it was the most prominent in all samples after correction for absorbance.

The first characteristic examined was the volume intensity of the EEM. This incorporates all recorded intensities for all excitation and emission wavelengths and takes the overall shape of the EEM into account. The relationship between the volume intensity and process-affected water content is shown for the three water sources in Figure 3.7. The volume intensities take the inner filtering effects into account and do not include light scatter.

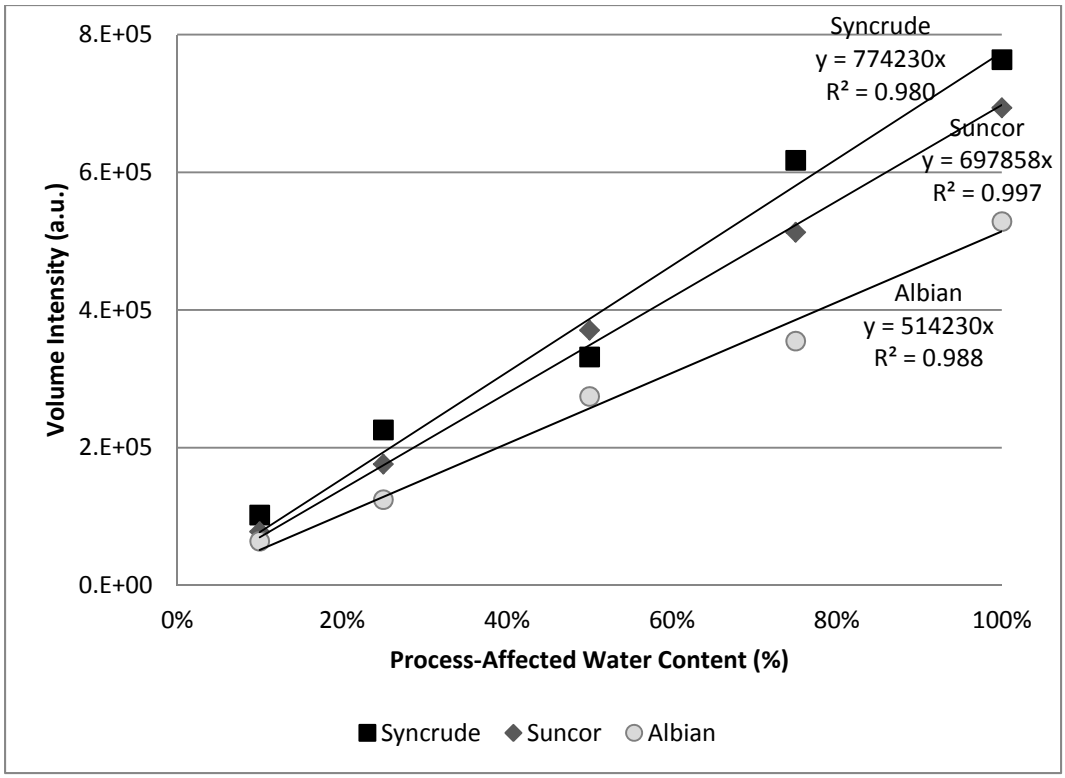

Figure 3.7: Volume intensity of process-affected water at various levels of dilution for three water sources.

The second characteristic examined was the area of intensity under the 280 nm excitation wavelength. After the correction factor was applied to the EEMs, the 280 nm was consistently the highest peak within the signal. The area of intensity is the result of the integration over the emission spectra of the 280 nm excitation wavelength. The resulting relationship between the area of intensity and the process-affected water content are shown in Figure 3.8. The area of intensity presented takes the inner filtering effects into account and excludes the light scatter.

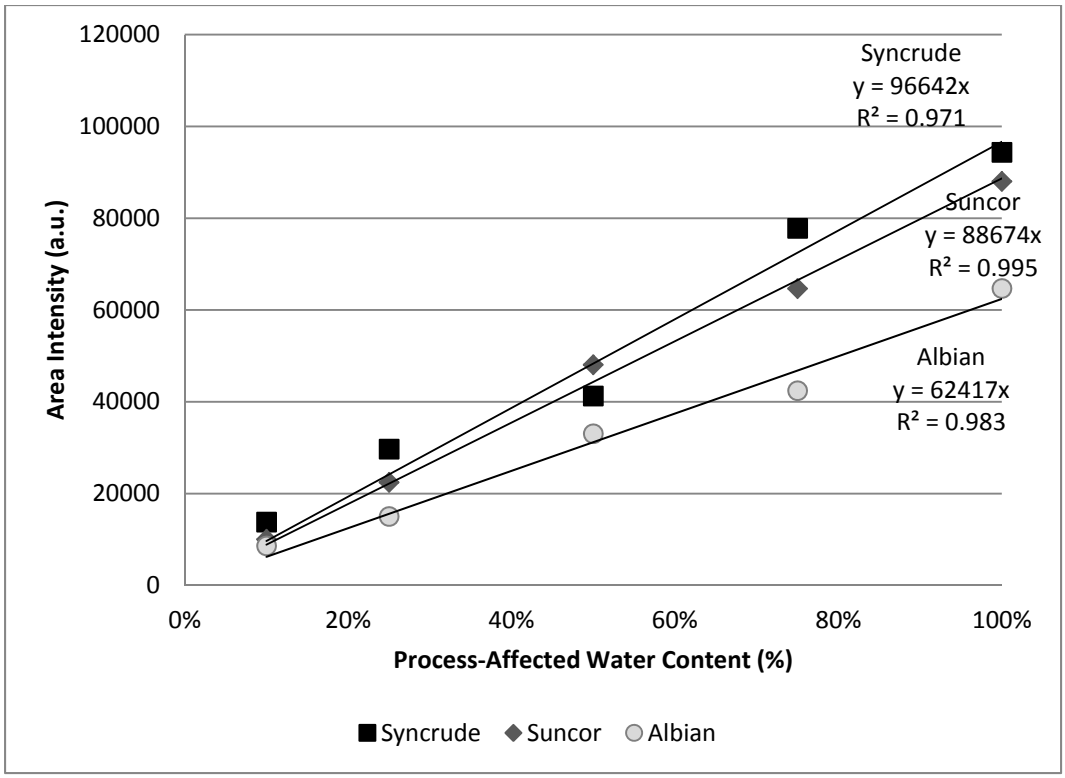

Figure 3.8: Intensity area under 280nm excitation wavelength of process-affected water at various levels of dilution for three water sources.

The final characteristic examined was the peak intensity at the 280 nm excitation wavelength and approximately the 343 nm emission wavelength. The peak observed was a singular response observed to be the most prominent after absorbance correction for all samples analyzed. The correlation between the peak intensity observed and the process-affected water content is shown in Figure 3.9. These peak intensities have been corrected for inner filtering effects. For this characteristic, light scatter is not an issue as it occurs prior to the 343 nm emission wavelength.

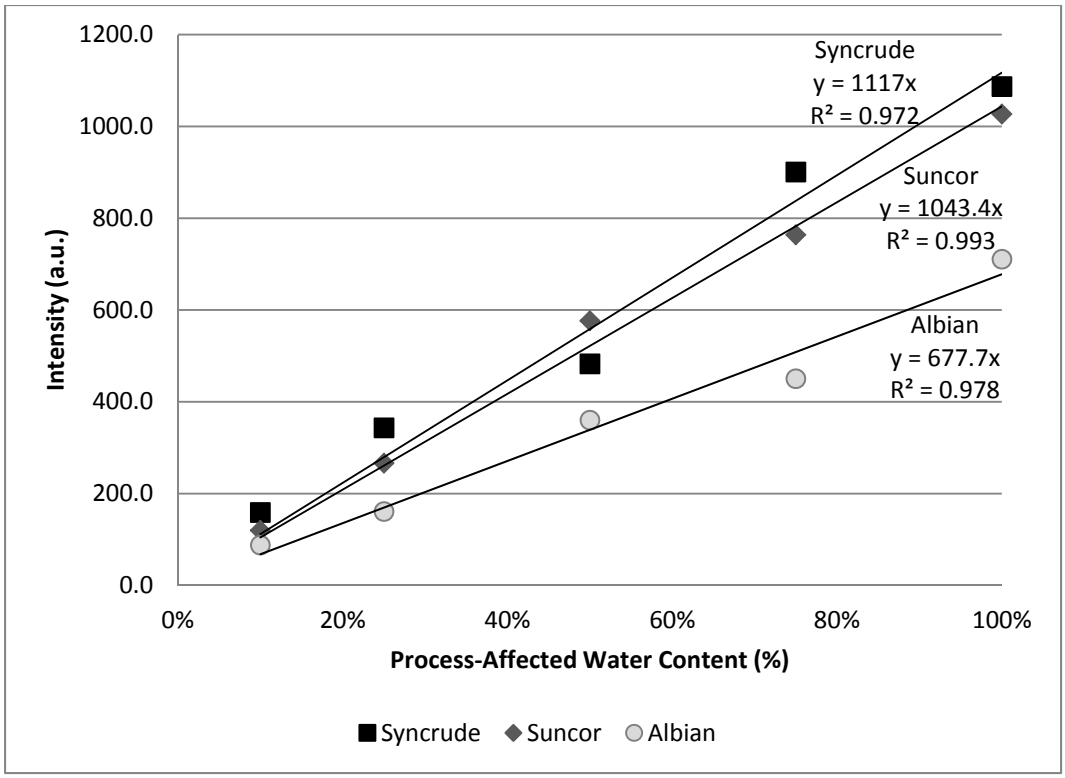

Figure 3.9: Peak intensity observed at 280nm excitation wavelength of process-affected water at various levels of dilution for three water sources.

When assessing the relationship between the characteristics examined, it was observed that all three characteristics displayed a strong linear correlation with the process-affected water content. The linear regression model determined for all characteristics was set through zero, as this represents no fluorescence intensity observed when the process-affected water content is zero. For all three process-affected water sources examined, the volume intensity showed the highest linear correlation and the peak intensity was the lowest. However, the lowest coefficient of determination, R^2, was above 0.96; this indicates there is still a very strong linear relationship between the peak intensity and the amount of process-affected water present. Using the peak intensity has many advantages over the volume and area intensity. After correction, the peak intensity is easily identified; it requires no data processing and the light scatter does not affect the value.

Assessing the water sources as a collective group for each characteristic found that the linear correlation was reduced from when each water source was examined individually. The water sources were also examined in groups of two for each characteristic. The R^2 values for each scenario evaluated are shown in Table 3.1.

Table 3.1: Linear regression R^2 values for EEM characteristics.

	Peak intensity (280nm)	Area intensity (280nm)	Volume intensity
Syncrude & Suncor	**0.977**	**0.978**	**0.979**
Suncor & Albian	0.843	0.917	0.893
Syncrude & Albian	0.794	0.831	0.854
Syncrude, Suncor & Albian	0.848	0.880	0.897

Though each scenario evaluated showed reasonable linear correlation, the Syncrude and Suncor water sources showed they were well correlated with each other when the Albian samples were excluded. This indicates that the fluorescent components of process-affected water for Syncrude and Suncor are more closely related than the Albian contents. The fluorescent species present may be at similar concentrations within the Syncrude and Suncor samples and lower in the Albian samples or this also suggests that one or more fluorescent components are present in Syncrude and Suncor that are missing from the Albian samples. This is also evident in the light scatter present in Albian samples; though the particles that cause light scatter may not induce fluorescence, it suggests the chemical makeup of Albian differs from that of Syncrude and Suncor.

The peak intensity observed during the 280 nm exciation wavelength was observed to be linear with process-affected water content for all source waters. In order to determine if the linearity was maintained for higher concentrations an acid extraction was performed on Syncrude water. The dried extract was concentrated with DCM to 5x the levels currently found in the tailings ponds.

The 280 nm excitation peak intensity is observed in Figure 3.10 for both corrected and uncorrected intensities.

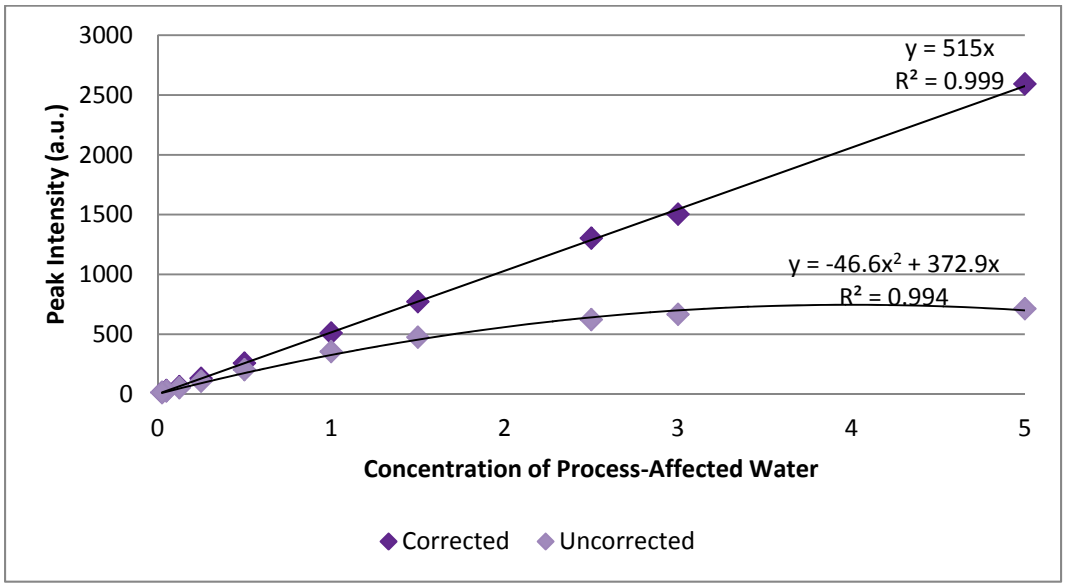

Figure 3.10: Peak intensities at 280 nm excitation wavelength for acid extract concentrated with DCM.

When the peak intensities were corrected for absorbance the linear correlation was maintained for concentrations 5x what is currently found in the tailings ponds. However when the peak intensities were not corrected the intensities leveled out and were best fit with a polynomial regression model. At the higher concentrations of process-affected water the secondary inner filter effect becomes more prominent and intensity is lost due to reabsorption. This was not observed for the fluorescent content currently found in tailings ponds; intensities that were uncorrected for absorbance still showed linear correlation in this range.

3.2.5 Commercial Naphthenic Acids

The fluorescence signal can be attributed exclusively to the acid fraction, which is the fraction that is used in Fourier Transform Infrared (FTIR) spectroscopy analysis of naphthenic acids. In FTIR analysis commercial naphthenic acids are used to quantify the process-affected water naphthenic acids. A stock solution for

200 mg/L was prepared using 20 mg of Sigma Aldrich naphthenic acids and 100 mL of methanol. An EEM of the stock solution after correction for absorbance is shown in Figure 3.11. As previously mentioned there is a slight affect from methanol on the EEM, however the Sigma Aldrich naphthenic acids are not soluble in deionized water.

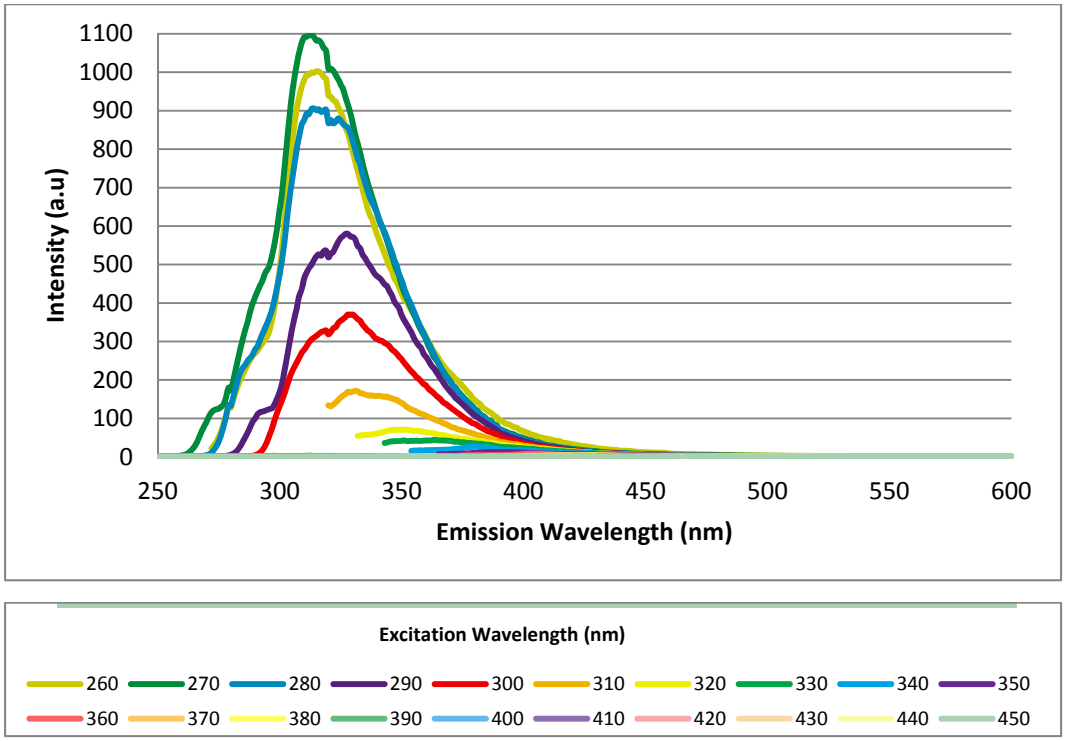

Figure 3.11: Emission spectra of Sigma Aldrich commercial naphthenic acids over excitation wavelengths 260-450 nm.

Unlike the signals produced from process-affected water the intensities from Sigma Aldrich were more prominent in the lower wavelengths. The main peak was found to be at the 270 nm excitation and 310 nm emission wavelengths. At an excitation wavelength of 280 nm a singular peak response was still observed, however it was shifted from 343 nm to 314 nm emission wavelength. In general the emission spectra for all excitation wavelengths had peaks shifted to this area. A significant amount of intensity was observed in the lower excitation wavelengths and was not as evident in the higher wavelengths. For the process-affected water signals the 290 nm excitation intensity peaks were close in relation

to the 280 nm excitation peak; the 290 nm excitation peak was significantly lower in relation to the 280 nm excitation peak for the Sigma Aldrich signal.

A dilution series was prepared from the 200 mg/L stock solution with methanol in order to prepare a calibration curve. Like the process-affected water signals the Sigma Aldrich EEMs retained their shape and prominent peaks throughout the dilution series, which are located in Appendix J. The calibration curve was created using the 280 nm excitation intensity peaks, as it has been determined to be a strong characteristic of the process-affected water and was still fairly prominent in the Sigma Aldrich EEMs. Figure 3.12 shows the calibration curve; the effect of the methanol signal has been removed for comparison.

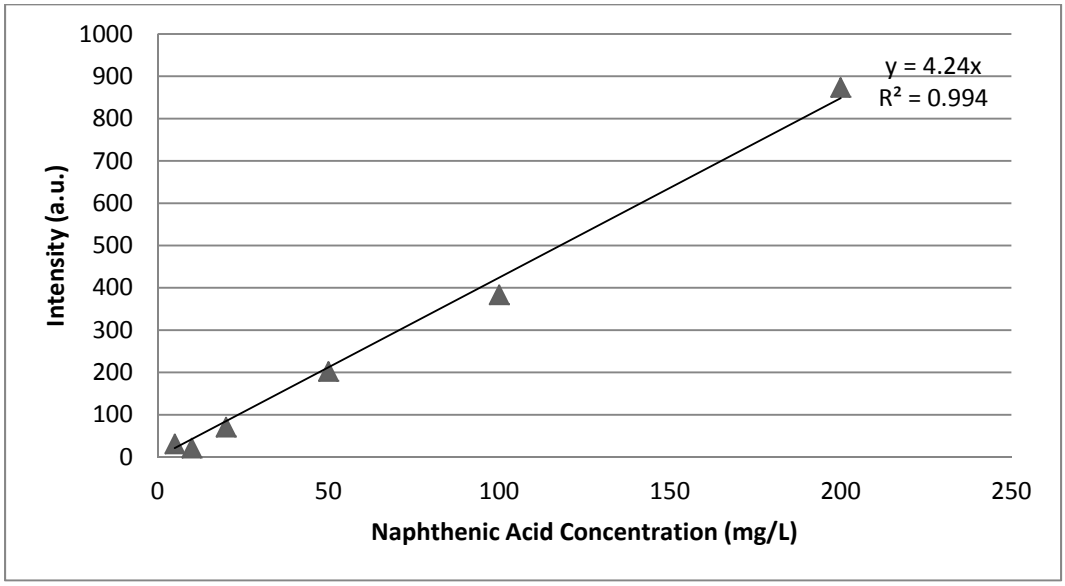

Figure 3.12: Sigma Aldrich commercial naphthenic acids 280 nm excitation fluorescence calibration curve.

Despite the variation from the process-affected water signals, the Sigma Aldrich also displayed strong linear correlation between the 280 nm excitation intensity peak and the naphthenic acid concentration. Using the calibration equation the concentrations of naphthenic acids were estimated for each of the undiluted process-affected water sources and are displayed in Table 3.2.

Table 3.2: Estimated naphthenic acid concentrations from Sigma Aldrich fluorescence calibration curve.

Source	280nm Peak Intensity (a.u.)	Estimated Concentration (mg/L)
Syncrude	1087	256
Suncor	1027	242
Albian	711	167

The estimated concentrations using the intensity peaks from Sigma Aldrich naphthenic acids were far outside of the expected concentrations that have been determined by FTIR analysis. Concentrations of naphthenic acids within the tailings ponds have been found in the range of 40-120 mg/L (Holowenko et al. 2001). Similar calibration curves were prepared using the volume and area intensity parameters and are contained in Appendix H. Due to the smaller shape of the Sigma Aldrich EEMs, the volume parameter greatly overestimated the naphthenic acid concentration. Similarly, the area of intensity under the 280 nm excitation wavelength estimated naphthenic acid concentration outside of the range though not as high as the volume parameter, but higher than predicted by peak intensities. It is evident that the fluorescent species within the commercially prepared naphthenic acids are different than the fluorescent species which are found in the process-affected water. However the fluorescence of the commercial naphthenic acids indicates that naphthenic acids could be a contributing source to the overall process-affected water signal.

3.2.6 Fourier Transform Infrared (FTIR) Spectroscopy

The current method used by the oil sands industry operators to quantify naphthenic acids is through Fourier Transform Infrared (FTIR) spectroscopy. In order to further investigate whether naphthenic acids contribute to the fluorescence signal from process-affected water, concentrations of naphthenic acids were determined by FTIR and compared to the observed 280 nm excitation

peak. Naphthenic acids are carboxylic acids that are considered to be of the general form $C_nH_{2n+z}O_2$, which indicates that fluorescence would not occur. However naphthenic acids in the tailings ponds process-affected water have been shown to contain various levels of substitution and potentially misclassified by the industry standard FTIR analysis.

The previously discussed fluorescence dilution series was used for FTIR analysis and consisted of process-affected water from the three water sources diluted to 75%, 50%, 25% and 10% process-affected water content. An extraction was performed on each sample and the organic acid fraction was analyzed by FTIR for naphthenic acid concentration; the raw data is contained in Appendix K. The resulting naphthenic acid concentration for the process-affected water dilution series based on FTIR is shown in Figure 3.11.

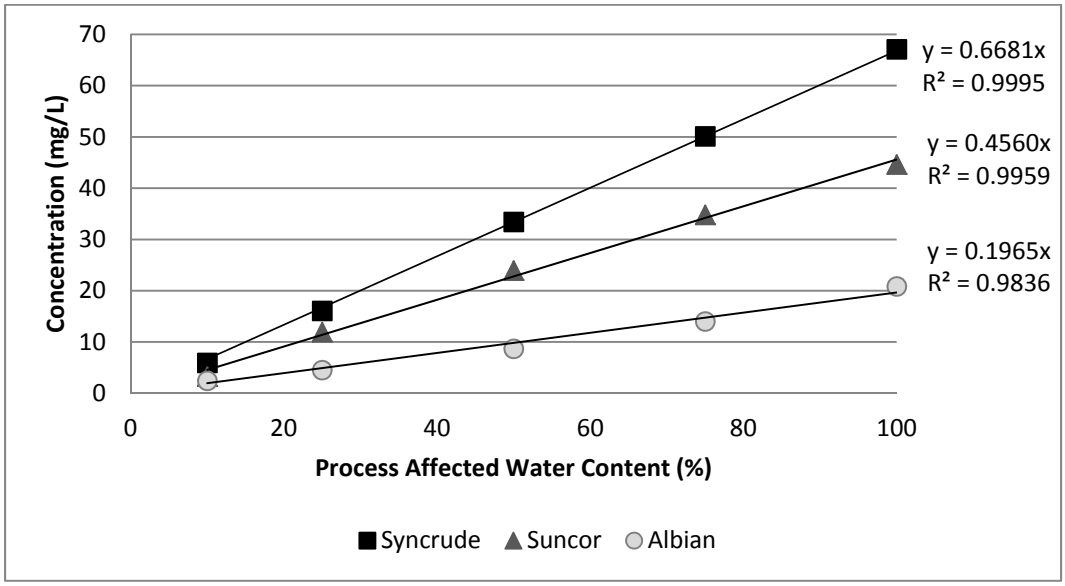

Figure 3.13: Naphthenic acid concentration as determined by FTIR for various levels of dilution of process-affected water for three water sources.

All three water sources showed a strong linear response to process-affected water content and naphthenic acid concentration, as was expected. Syncrude water showed the highest naphthenic acid concentration while Albian water showed the lowest and Suncor water was in between.

The peak intensity values from the 280 nm excitation wavelength determined in the fluorescence series were then compared to the naphthenic acid concentrations determined from the FTIR. The results are shown in Figure 3.12.

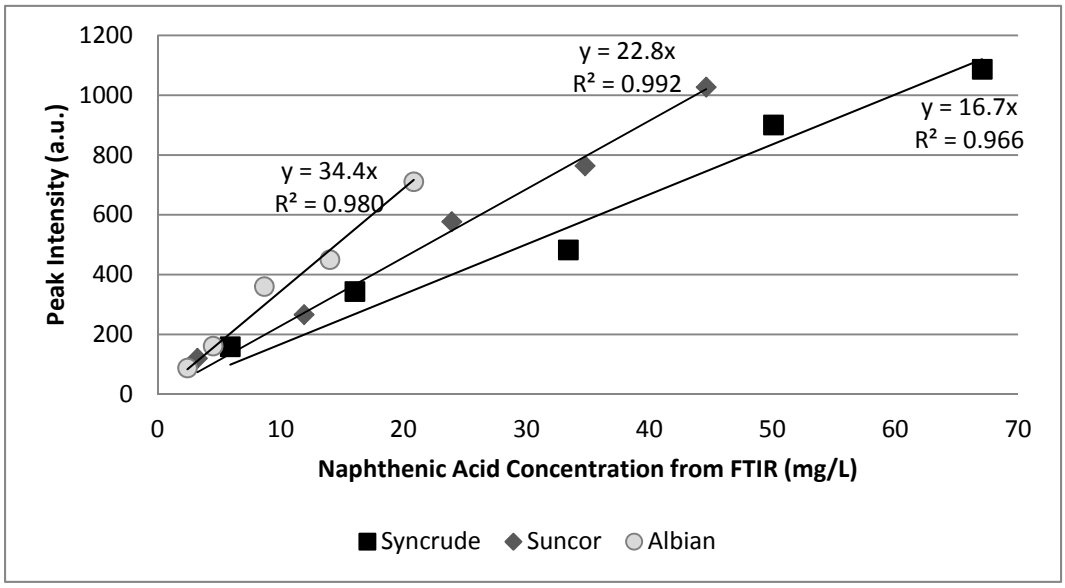

Figure 3.14: Naphthenic acid concentration as determined by FTIR and 280 excitation wavelength peak intensity for process-affected water at various dilution levels for three water sources.

Looking at each water source individually there was strong linear correlation between the peak intensity from the 280 nm excitation wavelength and the naphthenic acid concentration determined from FTIR. As the fluorescence signal was determined to be exclusively related to the organic acid fraction of process-affected water, there is evidence to support that the 280 nm excitation peak intensity is related to the naphthenic acid concentration determined from that fraction.

When the water sources were examined collectively the linear regression model did not show as strong of a correlation as when the sources were studied individually; the R^2 value dropped to 0.80 whereas individually R^2 values were above 0.96. As previously discussed, the Syncrude and Suncor process-affected water showed similar fluorescence trends. When considered together the

correlation increased, however not substantially. Though there is indication that the fluorescence signal is related to naphthenic acid concentration, it does not describe the discrepancy noted in Albian process-affected water composition, and is more likely attributed to a different fluorescent species.

3.2.7 Other Naphthenic Acid Analytical Methods

Additional analytical techniques have been used to gain more insight into the complex nature of naphthenic acids. High resolution mass spectrometry (HRMS) has been used to identify naphthenic acid profiles by carbon number and ring structure, as well as determine a total concentration (Han et al. 2009). Using this technique naphthenic acids with three to five oxygens, instead of two commonly associated with naphthenic acids, were found (Bataineh et al 2006; Han et al. 2009). These oxy naphthenic acids can be misclassified as higher molecular weight classical naphthenic acids (Clemente and Fedorak 2004). Undiluted samples of each process-affected water source were analyzed by HRMS to obtain a total naphthenic acid concentration. Additionally the dissolved organic carbon (DOC) of each process-affected water sample was determined, as naphthenic acids fall under this category. Table 3.3 compares the 280 nm excitation peak obtained from fluorescence to the concentrations of naphthenic acids as determined by HRMS and FTIR, as well as to the amount of dissolved organic carbon.

Table 3.3: Comparison of analytical methods for naphthenic acids

	Fluorescence 280nm Peak (a.u.)	HRMS (mg/L)	FTIR (mg/L)	DOC (mg/L)
Syncrude	1087	20.1	67.1	56.6
Suncor	1027	13.6	44.6	43.8
Albian	711	6.6	20.8	38.4

Naphthenic concentrations determined from HRMS analysis were found to be more than three times lower than those that were determined by FTIR analysis for all three process-affected water sources. Consistent with FTIR concentrations Syncrude water showed the highest naphthenic acid concentration while Albian water showed the lowest and Suncor water was in between. The 280 nm excitation peak is also consistent with these results. Naphthenic acids fall under the dissolved organic carbon classification, which includes all compounds that contain organic carbon that would be found in the process-affected water. Rationally, the naphthenic acid concentration must be lower or equal to the DOC as the DOC is a much broader group classification. The FTIR values for Syncrude and Suncor have naphthenic acid concentrations that register higher than the DOC content. This further suggests that FTIR analysis overestimates the actual naphthenic acid concentration.

Further HRMS analysis was completed on Suncor water samples that had been diluted to 60% and 20% process-affected water content. The 280 nm excitation peaks were then compared to the naphthenic acid concentrations as determined by HRMS, as shown in Figure 3.15.

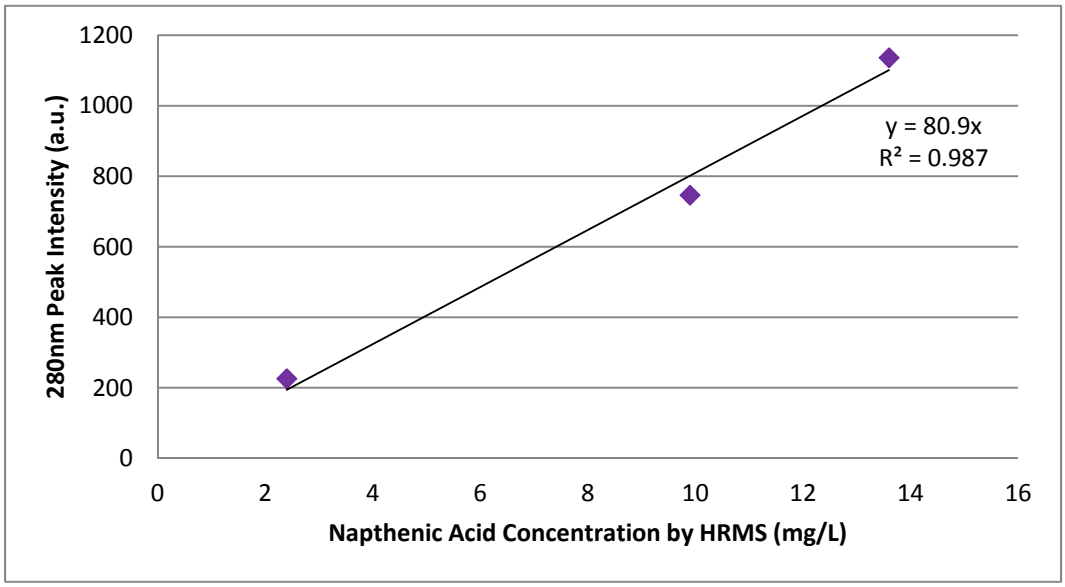

Figure 3.15: Naphthenic acid concentration as determined by HRMS and 280 excitation wavelength peak intensity for Suncor process-affected water at various dilution levels.

The naphthenic acid concentrations determined from HRMS showed strong linear correlation when compared to the 280 nm excitation peak from the Suncor samples, similar to the concentrations determined by FTIR. This indicates that while FTIR is potentially overestimating naphthenic acid concentration, the more rigorously defined concentration is still linked to the fluorescence signal.

Previously published literature has demonstrated the existence of the prominent 280nm excitation peak for process-affected water samples and has correlated fluorescence signals to naphthenic acid concentration. Mohammed et al. (2008) observed the emission spectra from excitation wavelengths ranging from 250 nm to 380 nm at a fixed concentration. Like this study the 280 nm excitation wavelength was found to produce higher intensities than the 290 nm excitation wavelength; however the authors chose to use the 290 nm excitation wavelength to demonstrate linearity between naphthenic acid concentration and fluorescence signal. Similar to this study Brown et al. (2009) observed the linear relationship between the excitation peak, area and EEM volume for a particular oil sands operation (not named) for the 290 nm excitation peak and area. The 280 nm excitation wavelength was chosen over the 290 nm excitation wavelength that was examined in studies completed by Mohammed et al. (2008) and Brown et al. (2009) as it consistently displayed higher intensities once corrected for absorbance. Kavanagh et al. (2009) used synchronous fluorescence spectroscopy, a fluorescence technique where the excitation and emission wavelengths are scanned simultaneously at a fixed wavelength interval. Peak intensities were determined at 282.5 nm and 320 nm excitation wavelengths. While the 282.5 nm peak is consistent with this study, the larger 320 nm peak was not observed in the process-affected water signals. The tailings pond samples utilized by Kavanagh et al. (2009) were obtained from different tailings ponds than the ones used in this study.

3.3 Conclusions

Process-affected water produces fluorescence signals when exposed to UV light in the wavelength range of 260 to 450 nm. This signal can be attributed exclusively to the organic acid fraction, which is known to contain naphthenic acids. Samples from various oil sands operations exhibit similar shaped EEMs and varied by intensity. The variation in intensity indicates that the fluorescent species are in different concentrations within each water source. The conservation of the intensity peak location and retention of the EEM shape throughout the dilution series demonstrates the correlation between fluorescence intensity and process-affected water concentration. Several characteristics were examined in order to determine which would be best suited to identify process-affected water and correlate to naphthenic acid concentration. Volume and area intensity of the process-affected water EEMs are suitable characteristics which maintain linearity over a dilution series. Peak intensity is observed at an excitation wavelength of 280nm and approximately 343nm emission wavelength and also displays a linear correlation with process-affected water content. This characteristic has many advantages over the volume and area intensity as it does not require light scatter to be removed and is easily observed without data manipulation. All three characteristics showed strong linear correlation when examining individual sources of water. Collectively the correlation was not as strong; however Syncrude and Suncor showed similar fluorescence signatures that did not appear in Albian samples indicating that one or more fluorescent components are potentially missing, or not at the same concentration.

When comparing the peak intensity to naphthenic acid concentration determined by the industry standard analytical method, FTIR, there was strong linear correlation between individual water sources. When the water sources were

assessed as a collective group the linear correlation was reduced. Using another analytical method, HRMS, and the DOC values it is evident that FTIR overestimates the naphthenic acid concentration. Fluorescence peak intensity values were still strongly correlated with naphthenic acid concentrations determined by HRMS. Overall, fluorescence as an analytical method can be used to indicate the presence of naphthenic acids in the acid extractable fraction of process-affected water; though there is indication of more than one fluorescent species, and all fluorescent species are not fully defined.

3.4 References

Anderson C.M., and Bro. R. 2003. Practicial aspects of PARAFAC modeling of fluorescence excitation-emission data. Journal of Chemometrics, 17:200-215.

Bataineh, M., Scott, A.C., Fedorak, P.M., and Martin, J.W. 2006. Capillary HPLC/QTOF-MS for characterizing complex naphthenic acid mixtures and their microbial transformation. Analytical Chemistry, 78: 8354-8361.

Brown, L. D., M. Alostaz, A. C. Ulrich. 2009. Characterization of oil sands naphthenic acids in oil sands process-affected waters using fluorescence technology. In 62nd Canadian Geotechnical Conference, Halifax, Nova Scotia, 1–7.

Clemente, J.S. and Fedorak, P.M. 2004. Evaluation of the analyses of tert-butyldimethysilyl derivatives of naphthenic acids by gas chromatography – electron impact mass spectrometry. Journal of Chromatography, 1047(2004): 117-128.

Goncalves, H., Medonca, C., Esteves da Silva, J.C.G. 2009. PARAFAC analysis of the quenching of EEM of fluorescence of glutathione capped CdTe quantum dots by Pb (II). Journal of Fluorescence, 19:141-149.

Holowenko F, MacKinnon M and Fedorak P. 2001. Naphthenic acids and surrogate naphthenic acids in methanogenic microcosms. Water Resources, 35:2596–606.

Jivraj, M., M. Mackinnon, B. Fung (1995). Naphthenic acid extraction and quantitative analysis with FT- IR spectroscopy. In Syncrude Analytical Manuals, 4th Edition, Research Department, Syncrude Canada Ltd., Edmonton, AB

Kavanagh, R.J., Burnison, B.K., Frank, R.A., Soloman, K.R., Van deer Kraak, G. 2009. Detecting oil sands process-affected waters in the Alberta oil sands region using synchronous fluorescence spectroscopy. Chemosphere, 76: 120–126.

Lakowicz, J.R. 2006. Principles of Fluorescence Spectroscopy, 3rd Ed. Springer Science+Business Media, LLC, New York, NY.

Mohammed, M.H., Wilson, L.D., Headley, J.V., and Peru, K.M. 2008. Screening of oil sands naphthenic acids by UV-Vis absorption and fluorescence emission spectrophotometry. Journal of Environmental Science and Health Part A, 43: 1700–1705.

Tucker, S.A., Amszi, V.L., Acree, W.E. 1992. Primary and secondary inner filtering: Effect of K2Cr2O7 on fluorescence emission intensities of quinine sulphate. Journal of Chemical Education, 69(1), A8-A12.

4. Parallel Factor Analysis of Process-Affected Water

4.1 Introduction

The fluorescence signals obtained from process-affected water are complex and overlapping, indicating the possibility of multiple fluorescent species contributing to the overall signal. For these conditions a decompositional method can be used, such as parallel factor analysis (PARAFAC). This multivariable statistical procedure can be used to decompose fluorescence data and differentiate the underlying fluorescent components of a mixture. If the fluorescent species in question is known, PARAFAC can be used to determine unknown concentrations in samples (Valverde et al. 2006). Conversely, PARAFAC can be used to determine how many fluorescent species are in a sample when different concentrations of the fluorescent species are used. Fluorescent organic matter has been analyzed using PARAFAC to track concentrations and movement within aquatic environments, as well as identify interactions been the organic matter and trace metals (Wedborg et al. 2007; Yamashita and Jaffe 2008). PARAFAC has also been used to identify petroleum hydrocarbons within soil (Alostaz et al. 2008a) and used to monitor photodegradation in petroleum hydrocarbons in the environment (Bosco 2006).

PARAFAC models were created to determine how many fluorescent species were contributing to the overall signal of process-affected water. Process-affected water was obtained from three oil sands operations and the optimal number of components was determined for each water source. The resulting emission spectrum of each component was then compared for each water source in order to determine if there was any variation in fluorescent species between oil sands operations. PARAFAC models were also determined for commercial naphthenic acids, as it has been previously established in Chapter 3 there is an indication that naphthenic acids contribute to the overall fluorescence signal.

4.2 Background

When a fluorescence signal is obtained the data is arranged to form an excitation-emission matrix (EEM). The EEM is a three dimensional array of fluorescence intensity, the emission spectrum and the excitation spectrum. The data collected from an EEM can be classified as multi-way data, where several sets of data variables are measured in a crossed fashion. PARAFAC transforms these possibly correlated variables into smaller uncorrelated variables (Bro 1997). For process-affected water it is unknown how many species are contributing to the fluorescence signal, or what fluorescent species are present within the samples. The related equations of the PARAFAC model have been previously discussed in Chapter 2, section 2.5. PARAFAC creates a model matrix based on EEMs of process-affected water at different concentrations by breaking it down into three loading matrices and a matrix of error. The first loading matrix is the estimated concentration (or fluorescence intensity), the second is the matrix of excitation wavelengths and lastly is the emission wavelengths. The removal of light scatter is important prior to PARAFAC analysis as light scatter is not bilinear and will affect the convergence of the PARAFAC algorithm (Hall 2006). The regions of light scatter are set to Not a Number (NaN) which leaves the value undefined (not as a zero). Because the light scatter appears diagonally throughout the matrix each row is able to be approximated in the algorithm, as an entire row is not set as undefined (Hall 2006). This allows the algorithm to minimize the least squares error term, as there is no value expected (Anderson and Bro 2000).

4.3 Materials and Methods

4.3.1 Parallel Factor Analysis (PARAFAC)

PARAFAC requires a series of Excitation-Emission Matrices of the analyte in question in different concentrations. For this study the EEMs of the process-affected water dilution series that were utilized in Chapter 3 were analysed using the PARAFAC method. The required arrays were prepared using MATLAB

R2009b and the additional PARAFAC toolbox version 5.2 add on. The EEMs for the dilution series are displayed in Appendix F. The intensities used were all corrected for inner filter effects prior to MATLAB analysis.

The EEMs of each dilution is imported to MATLAB separately. The EEMs are arranged so that the intensities are stacked to form a large dataset. The command history for MATLAB data analysis is included in the Appendix for each source. Once a successful dataset is built there are several options that require specification within the program. The stop criterion for relative change and absolute change was set to $1.0x10^{-6}$. The algorithm was set to stop after 10000 iterations or 3600 seconds was reached if neither of the two previous stop criterions were reached. Constraints were set for each of the three loadings matrices so that values were nonnegative. These constraints aid in the convergence of the model and are based on prior knowledge that fluorescence intensity, concentrations and wavelengths are not possible (Bro 1997)

4.4 Results and Discussion

4.4.1 Optimal Components

Multiple models were generated for each process-affected water source with varying number of components. A component in PARAFAC represents a fluorescent contribution to the overall signal. The contribution can be from a singular fluorescent species or from a class of fluorescent species (Hall 2006). The optimal number of fluorescent components and subsequently most appropriate model is determined using three different criteria. Distinct fluorescent peaks can be observed in both the excitation and emission matrix plots, indicating a component that fluoresces at a unique signature. Additionally the residual matrix of the PARAFAC model should describe noise and not systematic variation in the data. The last criterion is known as the core consistency. The core consistency diagnostic determines if there is an extra

component that does not describe systematic variation and is non- trilinear (Bro 1998).

4.4.2 Fluorescent Components of Process-Affected Water

Process-affected water was obtained from three oil sands operations. As previously discussed in Chapter 3 the fluorescence signals from process-affected water is complex and overlapping. Using the statistical method PARAFAC the EEMs obtained were broken down in order to determine how many underlying fluorescent components were contributing to the overall signal.

Syncrude

The Syncrude dilution series presented in Chapter 3 was used to generate PARAFAC models with increasing components from one component to seven components. The three loading matrices for each model are shown in Appendix J. Models with six and seven components did not produce distinct excitation and emission peaks, and had weak core consistency plots. The optimal number of components for Syncrude process-affected water was determined to be five. The estimated relative concentrations within each dilution are shown for the five components in Figure 4.1.

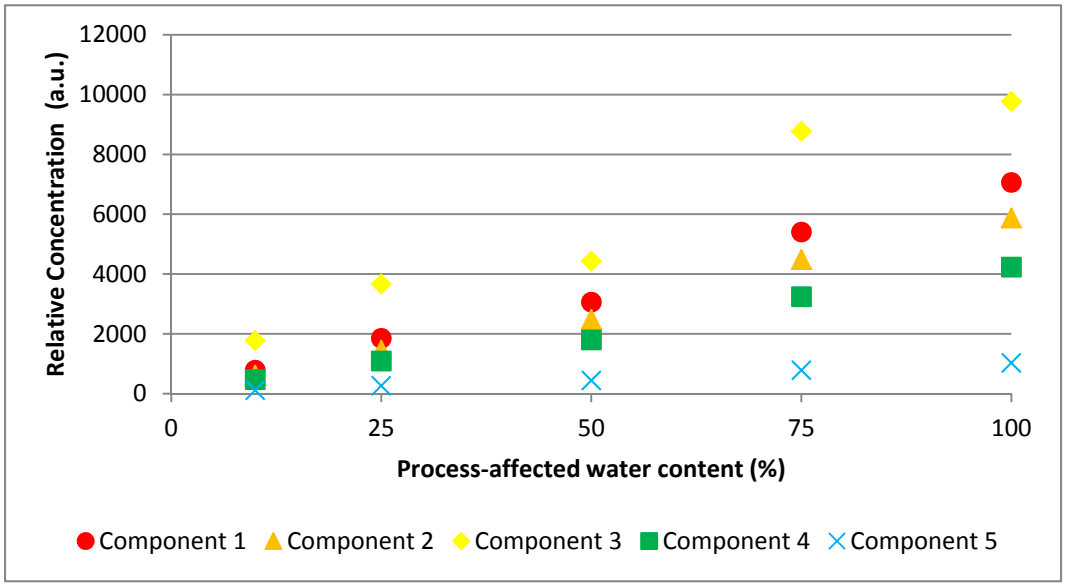

Figure 4.1: Estimated relative concentration for five components of Syncrude process-affected water determined by PARAFAC.

The PARAFAC model found that the relative concentration of fluorescent components decreased with the process-affected water dilutions. The PARAFAC model labels components based on their abundance within the sample (component 1 is the most abundant whereas component 5 is the least abundant) however for comparison purposes discussed in 4.4.3 the fluorescent species were rearranged. For the Syncrude process-affected water the highest relative concentrations were found in component 3, then successively through the rest of the components. It is not necessary for each component to have a different concentration within each sample; should the components have the same concentration it indicates that they are in equal concentration within the sample but have different fluorescent properties.

PARAFAC does not take into consideration the dilution content of the individual EEMs that are stacked within the dataset. The concentrations of each component were normalized for comparison to the undiluted sample and shown in Table 4.1.

Table 4.1: Relative Concentrations of Syncrude Components Normalized.

Dilution	Component 1	Component 2	Component 3	Component 4	Component 5
100%	1	1	1	1	1
75%	0.76	0.76	0.90	0.77	0.76
50%	0.43	0.42	0.45	0.43	0.43
25%	0.26	0.25	0.37	0.26	0.26
10%	0.11	0.10	0.18	0.11	0.11

Overall the relative concentrations determined from PARAFAC aligned with the dilution series. There was noticeable overestimation within component 3 in most of the dilutions and for the 50% dilution sample all components were estimated to be slightly lower.

The second loading matrix obtained from the PARAFAC model is the excitation wavelength trends. The calculated emission spectra for each of the five determined components for Syncrude process-affected water are shown in Figure 4.2.

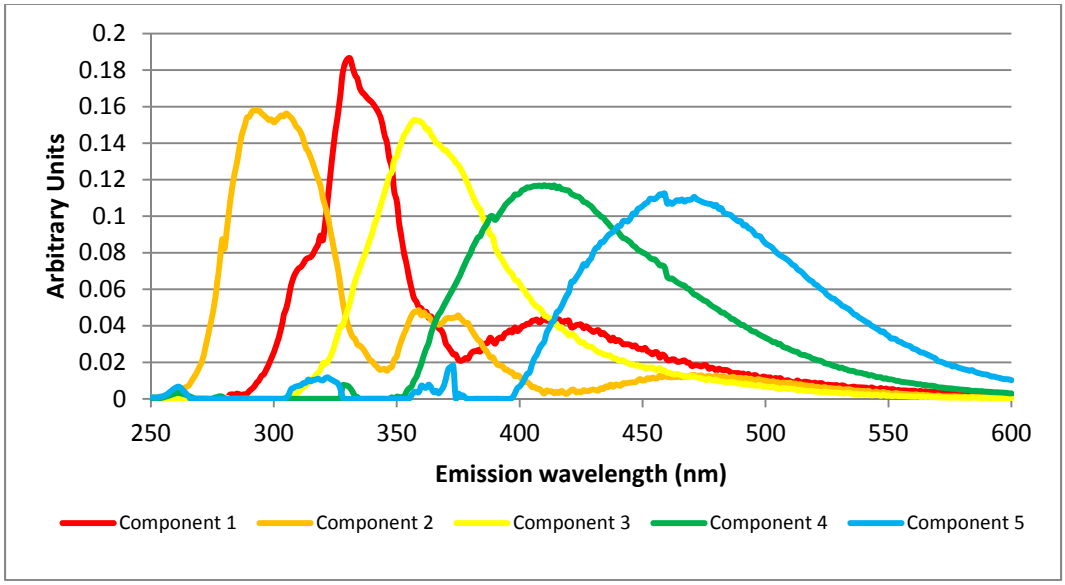

Figure 4.2: Emission spectra of five components for Syncrude process-affected water determined by PARAFAC.

The emission spectrum shown has five distinct peaks for each fluorescent component identified. The modelled emission spectrum does not have a specified excitation wavelength but shows trends as a function of the emission wavelengths (Alostaz 2008b). The third loading matrix depicts the excitation spectra. Similar to the emission spectra calculated in the second loading matrix, PARAFAC represents the excitation spectra as a function of excitation wavelengths, and not a specific emission wavelength. The excitation spectra is another way of representing the florescent species and can be used to compare to known excitation spectrums; for this work the emission spectrum was used for this comparison.

Suncor

Similar to the Syncrude analysis, the Suncor dilution series presented in Chapter 3 was used to generate PARAFAC models. Models were generated for one component increasing up to seven components. The resulting three loading matrices for each of the models are shown in Appendix K. The Suncor models for six and seven components did not produce distinct excitation and emission peaks, and had weak core consistency plots. The optimal number of components for Suncor process-affected water was determined to be five. Figure 4.3 depicts the estimated relative concentrations within each dilution for the five components.

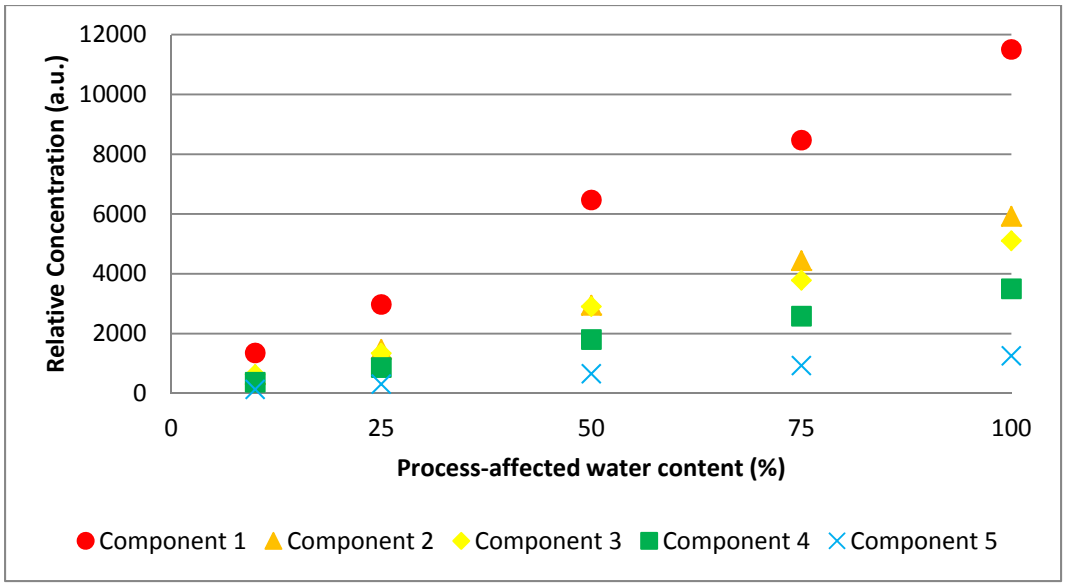

Figure 4.3: Estimated relative concentration for five components of Suncor process-affected water determined by PARAFAC.

Like the Syncrude model the PARAFAC model for the Suncor process-affected water found that the relative concentration of fluorescent components decreased with process-affected water content. Component 1 was found to be in the highest concentration with each successive component having lower concentrations. Components 2 and 3 were found to have very similar concentrations in this case. The concentrations were again normalized for comparison to the undiluted sample, the results are shown in Table 4.2.

Table 4.2: Relative Concentrations of Suncor Components Normalized.

Process-affected water content	Component 1	Component 2	Component 3	Component 4	Component 5
100%	1	1	1	1	1
75%	0.74	0.75	0.74	0.74	0.74
50%	0.56	0.50	0.57	0.52	0.52
25%	0.26	0.25	0.26	0.25	0.25
10%	0.12	0.11	0.12	0.11	0.11

The PARAFAC model determined the relative concentrations to be correlated with the expected values from the dilution series. There were several instances

where the relative concentrations were overestimated, most noticeably for the 50% sample.

As previously described for the Syncrude dilution series, the second loading matrix for the Suncor dilution series is the emission spectrum. The calculated emission spectra for each of the five determined components for Suncor process-affected water are shown in Figure 4.4.

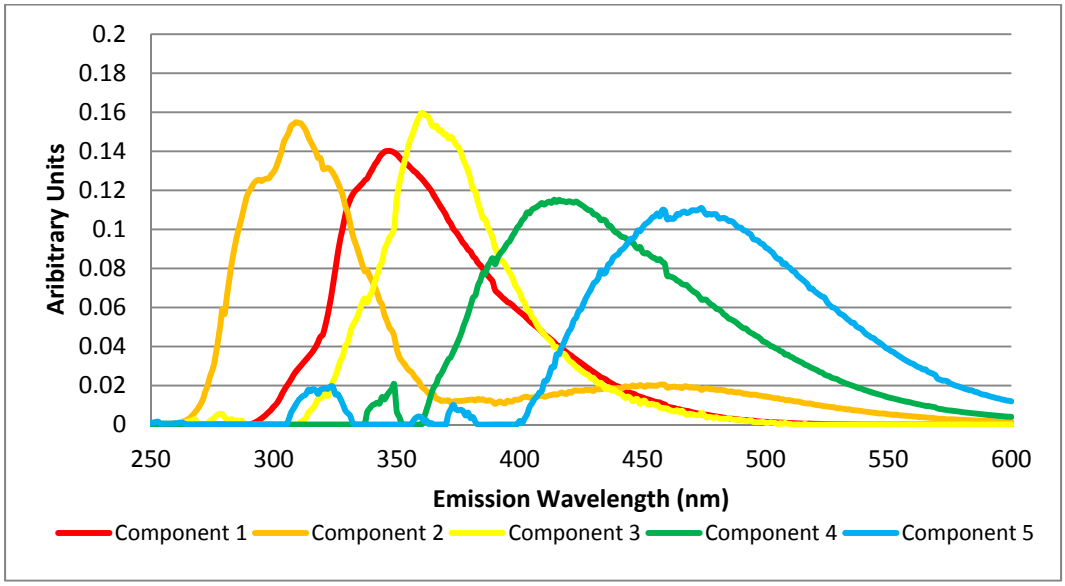

Figure 4.4: Emission spectra of five components for Suncor process-affected water determined by PARAFAC.

Each component modelled displayed a distinct peak at a different emission wavelength. As previously mentioned the resulting emission spectra does not occur at a specific excitation wavelength, but shows the general trend of the fluorescent species. The third loading matrix shows similar results for the excitation spectra, there are five distinct peaks present. The excitation spectrum is contained in Appendix K.

Albian

Like the previous two water sources the Albian dilution series presented in Chapter 3 was used to generate PARAFAC models. Models with components from one to seven were generated, and the resulting three loading matrices for each model are shown in Appendix L. The optimal number of components for Albian process-affected water was also determined to be five. Models of six and seven components were unable to produce distinct peaks in the emission and excitation spectra, and had weak core consistency plots. The estimated relative concentrations of the five components for each sample in the dilution series are shown in Figure 4.5.

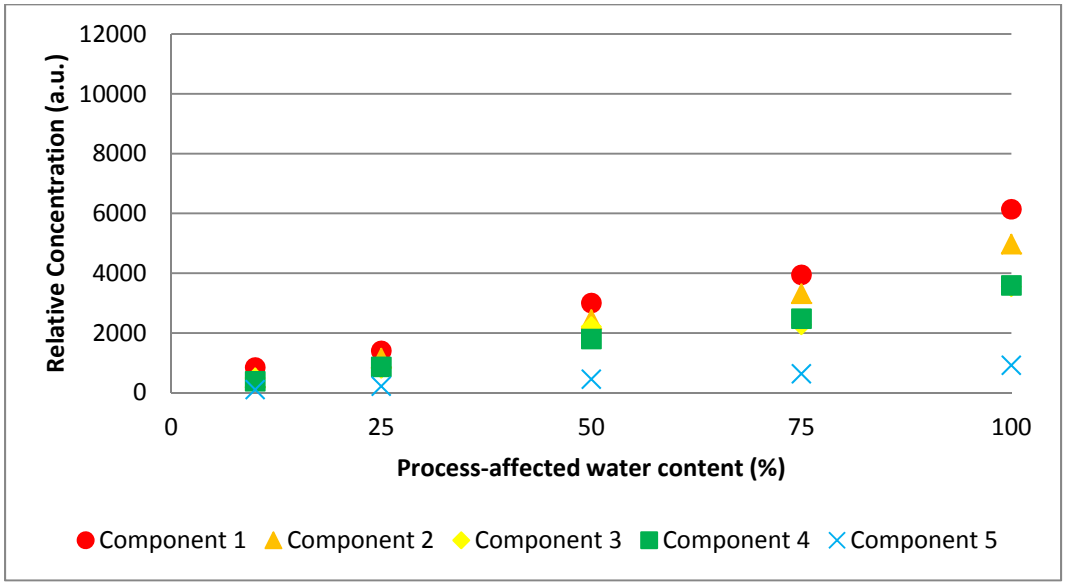

Figure 4.5: Estimated relative concentration for five components of Albian process-affected water determined by PARAFAC.

The estimated relative concentrations for the Albian PARAFAC model followed the same trend as the Syncrude and Suncor models; as the process-affected water content decreased the estimated concentration correspondingly decreased. Like the Suncor model component 1 was found to have the highest concentration with each successive component having lower concentrations. The Albian model

found that components 3 and 4 were very close in concentration. Table 4.3 shows the concentrations when normalized for comparison to the undiluted sample.

Table 4.3: Relative Concentrations of Albian Components Normalized.

Process-affected water content	Component 1	Component 2	Component 3	Component 4	Component 5
100%	1	1	1	1	1
75%	0.64	0.67	0.64	0.69	0.69
50%	0.49	0.49	0.62	0.50	0.49
25%	0.23	0.23	0.23	0.24	0.24
10%	0.14	0.10	0.14	0.11	0.11

The estimated concentrations for the Albian PARAFAC model were correlated with the expected values from the dilution series, with some noticeable discrepancies. The 75% sample was found to be estimated lower than expected for all components, and component 3 showed overestimation for the 50% and 10% samples.

As previously described for the Syncrude and Suncor dilution series, the second loading matrix calculated by PARAFAC is the emission spectrum. The calculated emission spectra for each of the five determined components for Albian process-affected water are shown in Figure 4.6.

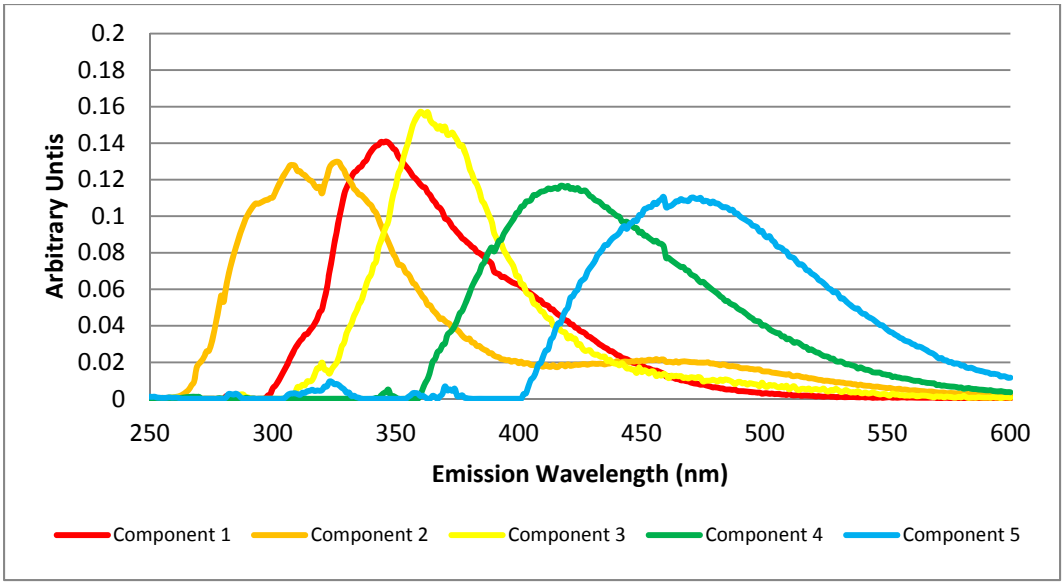

Figure 4.6: Emission spectra of five components for Albian process-affected water determined by PARAFAC.

Again, like the previous two models the Albian PARAFAC model found five distinct components in the emission spectrum. Regardless of where the process-affected water was obtained from PARAFAC found that five fluorescent components were optimal. The relative concentrations of each component were found to be correlated with the expected values of the dilution series for the respective water source. The PARAFAC models produced an emission spectrum for each water source that displayed five distinct peaks. How the relative concentrations and emission spectra compare between each company is discussed in the next section, 4.4.3.

4.4.3 Comparison of Components Between Process-Affected Water

PARAFAC determined five distinct fluorescent components for each of the three water sources examined. In order to determine if the fluorescent components varied between each water source the emission spectra from the second loading matrix of the PARAFAC models was examined. The locations of the peaks within the emission spectra were compared between each process-affected water source. Similar general trends of the modelled emission spectrum between water

sources indicates that the fluorescence signal were produced by similar fluorescent species. The five components were matched by peak location and emission spectra trend for all three water sources. The individual components are compared between each source in Figure 4.7.

The PARAFAC models found that components 3, 4, and 5 (Figures 4.7c-e) were strongly matched between the sources. The emission spectra showed the same general trends and peaks occurred in the same emission wavelength locations. Component 2 (Figure 4.7b) showed slight variation. Suncor and Albian displayed the same general trend in the emission spectra though the peak locations were marginally different. The peak location for component 2 for Syncrude was in the same general area, however the emission spectra shows a second much lower peak that is not present in the models from Suncor and Albian. The largest variation was found in component 1. Suncor and Albian were strongly matched in peak location and emission spectra trend, however the peak location of component 1 for Syncrude was noticeably shifted to lower emission wavelengths.

The relative concentrations for each component were compared between the undiluted samples for each process-affected water source. The results are shown in Figure 4.8. The component with the highest concentration was not the same for each water source. Syncrude had the highest concentration in component 3, whereas Suncor and Albian had the highest concentration in component 1. However the relative concentration of component 1 within the Suncor sample was almost double that which was found in the Albian sample. The relative concentrations for all three water sources for component 2 were all in the same order of magnitude. The same trend was observed for components 4 and 5, but at different magnitudes for each component. The relative concentrations determined in component 3 found that Syncrude was significantly higher than both Suncor and Albian.

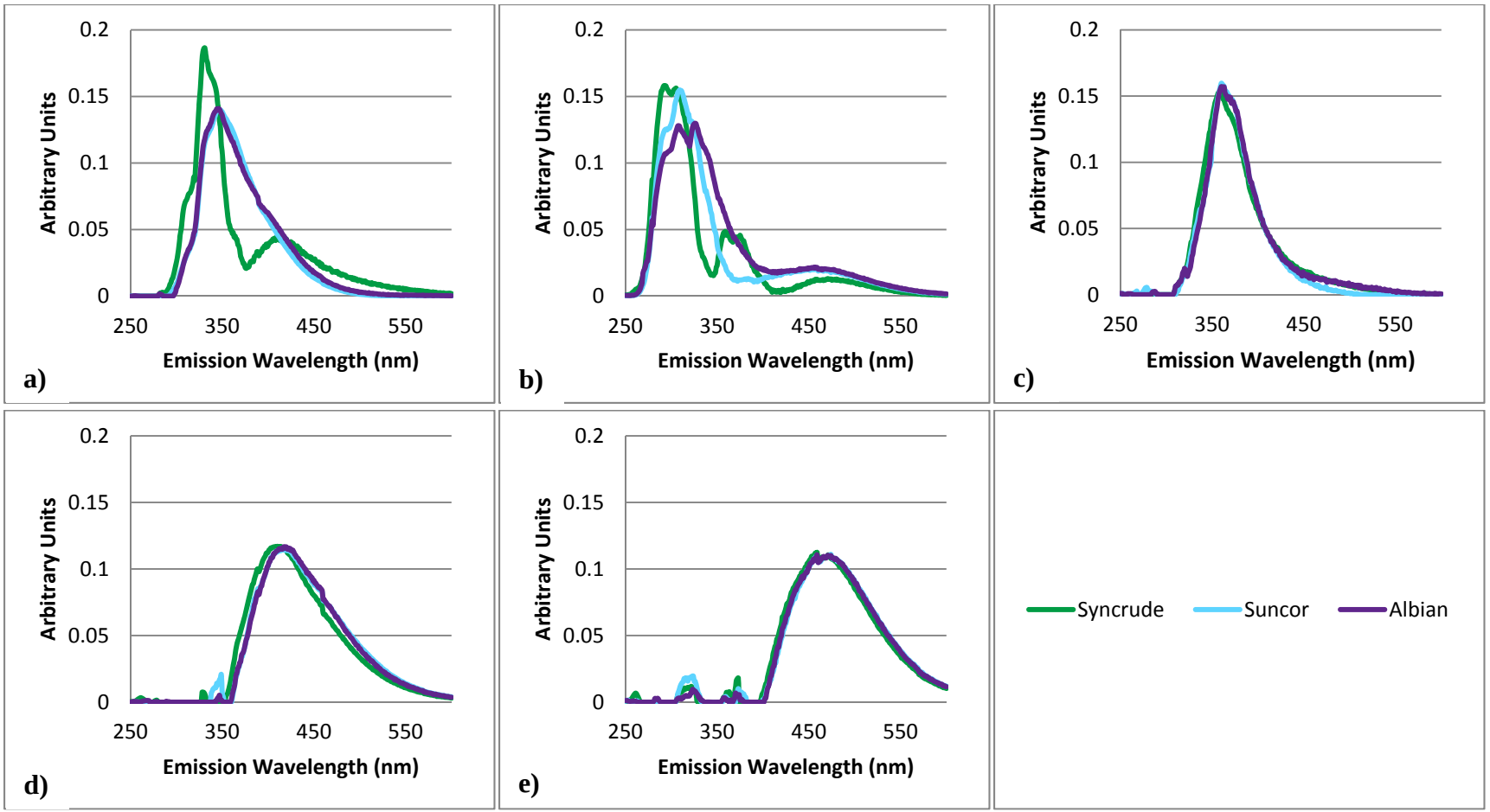

Figure 4.7: Comparison of PARAFAC Components between Syncrude, Suncor and Albian a) Component 1; b) Component 2; c) Component 3; d) Component 4; and e) Component 5.

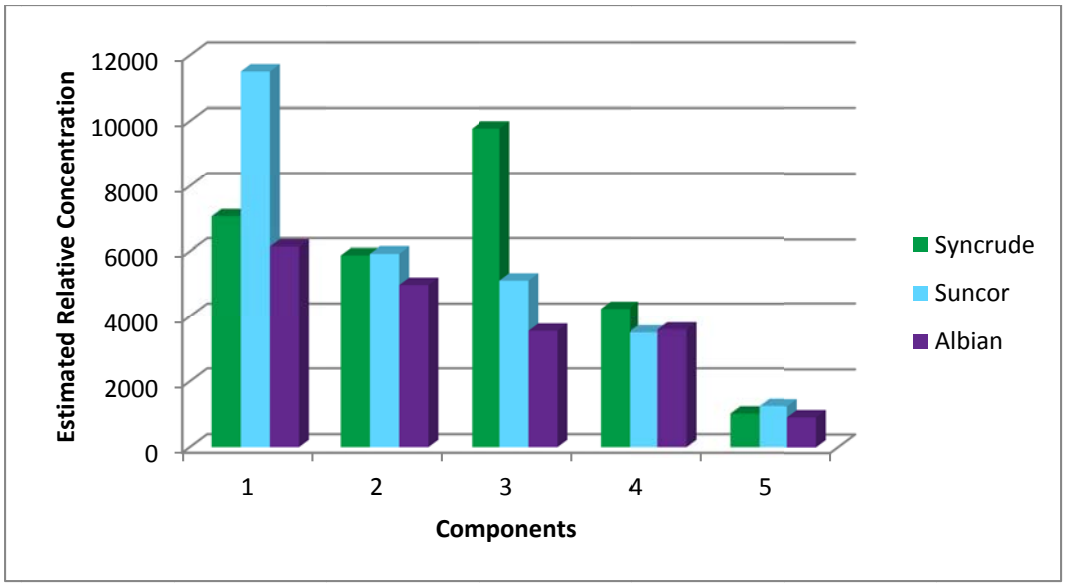

Figure 4.8: Comparison of estimated relative concentration of PARAFAC Components between Syncrude, Suncor and Albian.

The five components that were determined from PARAFAC models for each process-affected water source were found to have similar emission spectra trends and peaks in similar emission wavelength locations. The most evident variation was between the component 1 calculated for Syncrude and the component 1 calculated for Suncor and Albian. The Syncrude peak was noticeably shifted from the Suncor and Albian peak location. The presence of similar underlying fluorescent species explains how the overall shape of the EEMs is consistent between companies. The estimated relative concentrations within each component were found to vary between each of the water sources. The variation in concentration explains the difference in intensity between companies.

4.4.4 Fluorescent Components of Commercial Naphthenic Acids

Naphthenic acids are a known constituent of process-affected water. The fluorescence signal has previously been determined to be exclusively related to the organic acid fraction of process-affected water, which naphthenic acids belong to. In Chapter 3, section 3.1.4, found that naphthenic acid concentration was linked to the fluorescence signal in process-affected water. PARAFAC models

were created for the Sigma Aldrich naphthenic acid dilution series shown in Appendix H. Models were created with increasing components from one to four. The four component model reached the maximum number of iterations, indicating the model could not reach the convergence stop criteria for either relative or absolute change. The optimal number of fluorescent components determined from the commercial naphthenic acids was three. The estimated relative concentrations within each dilution sample for the three components are shown in Figure 4.9.

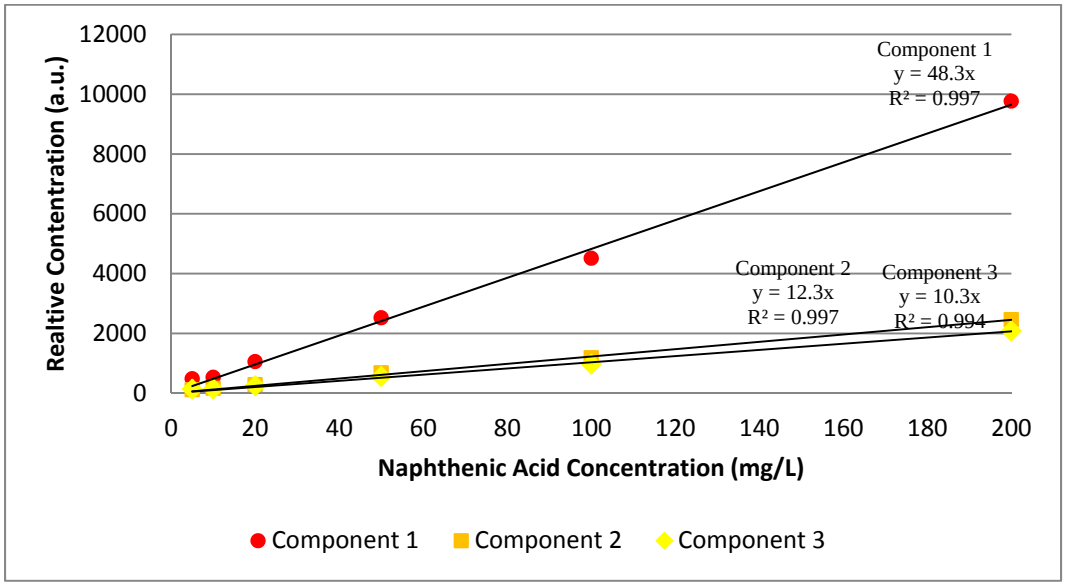

Figure 4.9: Estimated relative concentration for three components of Sigma Aldrich commercial naphthenic acids determined by PARAFAC.

As with the process-affected water models the estimated relative concentrations decreased with the naphthenic acid content. The PARAFAC model found that component 1 had the highest concentration, and components 2 and 3 had nearly identical concentrations. The second loading of the PARAFAC model, found that there were three distinct peaks and components 2 and 3 clearly had different emission spectra. The emission spectra for all three components are shown in Figure 4.10.

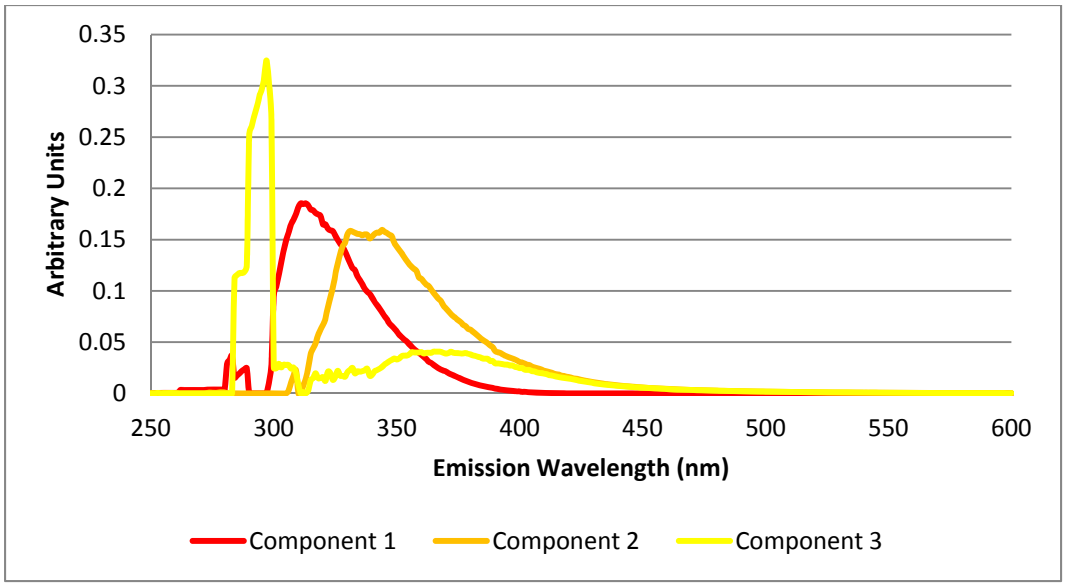

Figure 4.10: Emission spectra of three components for Sigma Aldrich commercial naphthenic acids determined by PARAFAC.

The emission spectra of the three components found that the peak locations were located at shorter emission wavelengths than the fluorescent components for process-affected water. The average emission wavelength and intensity for the three process-affected water sources for each fluorescent component was determined and compared to the Sigma Aldrich naphthenic acids. The intensities and peak locations are compared in Table 4.4.

Table 4.4: Comparison of peak location and intensity for PARAFAC components of process-affected water and Sigma Aldrich naphthenic acids.

Process-affected Water Components	Intensity (a.u.)	Emission Wavelength (nm)	Sigma Aldrich Naphthenic Acid Components	Intensity (a.u.)	Emission Wavelength (nm)
1	0.145	346	2	0.159	344
2	0.138	303	1	0.182	310
3	0.155	360			
4	0.116	413			
5	0.111	458	3	0.325	297

When compared to the PARAFAC components found for process-affected water the components 1 and 2 of the Sigma Aldrich model were fairly close. Component 2 of Sigma Aldrich was a close match to component 1 of the process-affected water in both peak intensity and emission wavelength location. Component 1 of Sigma Aldrich appeared in a similar emission wavelength location as the second component of process-affected water, however the peak intensity was higher. The last component of Sigma Aldrich was found at the shortest emission wavelength of any of the PARAFAC components and had a significantly higher intensity. There was no comparison to components found for the process-affected water.

Using the relative concentrations for components 1 and 2 of the Sigma Aldrich PARAFAC model as a calibration curve the naphthenic acid concentration was calculated for the three process-affected water sources. The relative concentrations of undiluted process-affected water were compared to the relative concentrations of Sigma Aldrich according to the component matches shown in Table 4.4. The estimated concentrations are shown in Table 4.5.

Table 4.5: Estimated Naphthenic Acid concentrations for Process-affected water.

Sigma Aldrich Component 1

	Relative Concentration (a.u.)	Estimated Concentration (mg/L)
Syncrude	5877	122
Suncor	5926	123
Albian	4972	103

Sigma Aldrich Component 2

	Relative Concentration (a.u.)	Estimated Concentration (mg/L)
Syncrude	7067	576
Suncor	11507	937
Albian	6139	500

Using the relative concentrations of Sigma Aldrich component 1 as a calibration curve the naphthenic acid concentrations for undiluted process-affected water samples were overestimated from those determined in Chapter 3. The concentrations are just in the high part of the 40-120 mg/L range that has been found in tailings ponds (Holowenko et al. 2001). However analysis from FTIR and HRMS of the undiluted samples found that naphthenic acid concentrations should be lower. When component 2 was used to estimate naphthenic acid concentration, the results were greatly exaggerated, and not indicative of what is known to be in process-affected water.

The underlying fluorescent components of Sigma Aldrich naphthenic acids that were determined from PARAFAC had several features that were comparable to the components determined for process-affected water. Two of the three Sigma Aldrich components matched process-affected water components. However the concentrations of the fluorophores were not a match when the intensities of the components were compared. Commercial naphthenic acids are used as a standard to quantify naphthenic acids in analytical methods such as FTIR and HRMS. The complexities of petroleum derived naphthenic acids are not accurately represented by these commercial naphthenic acids. PARAFAC found three fluorescent components not present in the Sigma Aldrich samples, and possibly one component that appears in the Sigma Aldrich samples that does not appear in the process-affected water.

4.5 Conclusions

PARAFAC was used to create models to determine the underlying fluorescent components that contribute to the EEMs generated by process-affected water and commercial naphthenic acids. Process-affected water was obtained from three different oil sands operations. Models for each company found that the optimal number of components was five. Each fluorescent component was found to have a distinct peak in the emission spectrum and have a relative concentration that decreased similarly to the dilution series.

The five PARAFAC components were compared between companies to determine if the underlying fluorescent components were similar. Three of the components were well matched in both peak intensity location and emission spectra displayed. The other two components displayed many similarities but were not as well matched. The relative concentrations of each component had different distributions within each company. The similar underlying fluorescent components explain how the overall shape of the EEMs is consistent between companies. The variation of each components relative concentration describes the variation in intensities shown in the three companies EEMs.

PARAFAC models were also created for Sigma Aldrich naphthenic acids, which are commercial naphthenic acids used for analysis of process-affected water. The optimal number of components that was determined was three. When these components were compared to the fluorescent components of process-affected water, two of the three components matched. The estimated concentrations and known concentrations of the Sigma Aldrich samples were used to approximate the naphthenic acid concentration in process-affected water. The naphthenic acid concentration could not be correlated to a specific Sigma Aldrich component, and greatly overestimated naphthenic acid concentrations previously determined by FTIR. The fluorescent components identified by PARAFAC for the commercial naphthenic acids do not accurately describe the fluorescent components that PARAFAC identified for process-affected water.

4.6 References

Alostaz, M., Biggar, K., Donahue, R., and Hall, G. 2008a. Petroleum contamination characterization and quantification using fluorescence emission excitation matrices (EEMs) and parallel factor analysis (PARAFAC). Journal of Environmental Engineering and Science, 7: 183–197.

Alostaz, M., Biggar, K., Donahue, R., and Hall, G. 2008b. Soil type effects on petroleum contamination characterization using ultraviolet induced fluorescence excitation-emission matrices (EEMs) and parallel factor analysis (PARAFAC). Journal of Environmental Engineering and Science, 7: 661–675.

Anderson C.M., and Bro. R. 2000. The *N*-way Toolbox for MATLAB. Chemometrics and Intelligent Laboratory Systems,. 1–4

Anderson C.M., and Bro. R. 2003. Practical aspects of PARAFAC modeling of fluorescence excitation-emission data. Journal of Chemometrics, 17:200-215.

Bosco, M.V., and Larrechi, M.S. 2006. PARAFAC and MCR-ALS applied to the quantitative monitoring of the photodegradation process of polycyclic aromatic hydrocarbons using three-dimensional excitation emission fluorescent spectra comparative results with HPLC. Talanta, 71: 1703–1709.

Bro, R. 1997. PARAFAC Tutorials and Applications. Chemometrics and Intelligent Laboratory Systems, 38(2):149-171.

Bro, R. 1998. Multi-way analysis in the food industry: Models, Algorithms, and Applications. PhD thesis, University of Amsterdam.

Goncalves, H., Medonca, C., Esteves da Silva, J.C.G. 2009. PARAFAC analysis of the quenching of EEM of fluorescence of Glutathione Capped CdTe Quantum Dots by Pb (II). Journal of Fluorescence, 19:141-149.

Hall, G. 2006. Chemometric characterization and classification of estuarine water through multidimensional fluorescence. PhD thesis, Tufts University.

Valverde, R. S., Gil Garcia M. D., Martinez Galera, M., and Goicoechea H. C. 2006. Highly collinear three-way photoinduced spectrofluorimetric data arrays modelled with bilinear least-squares: Determination of tetracyclines in surface water samples. Talanta, 70: 774–783.

Wedborg M., Persson T., and Larsson, T. 2007. On the distribution of UV-blue fluorescent organic matter in the Southern Ocean. Deep-Sea Research, 54: 1957–1971.

Yamashita, Y., and Jaffe,R. 2008. Characterizing the interactions between trace metals and dissolved organic matter using Excitation-Emission Matrix and Parallel Factor Analysis. Journal of Environmental Science and Technology, 42: 7374–7379.

5. Conclusions and Future Recommendations

5.1 Summary of Results

Process-affected water from oil sands operations produce fluorescence signals when exposed to UV light in the wavelength range of 260 to 450 nm. A distinct peak was observed at approximately the 343 nm emission wavelength when scanned at a wavelength of 280 nm. This peak was consistent in location throughout samples obtained from three different oil sands operations, and throughout a series of dilutions. Comparing each water source, the EEMs obtained displayed similar shapes and varied by intensity. The variation in intensity indicates that the fluorescent species are in different concentrations within each water source, while the similar EEM shape indicates that similar fluorescent species are present in each sample. The conservation of the intensity peak location and retention of the EEM shape throughout the dilution series demonstrates the correlation between fluorescence intensity and process-affected water concentration. The fluorescence signal was narrowed down to exclusively the organic acid fraction of process-affected water, which is known to contain naphthenic acids.

The characteristic 280 nm peak intensity was compared to naphthenic acid concentration determined by the industry standard analytical method, FTIR, and displayed strong linear correlation between individual water sources. Examining process-affected water regardless of source the correlation was reduced. Other analytical methods for naphthenic acids indicate overestimation of the naphthenic acid FTIR concentration, however peak intensities were still strongly correlated to naphthenic acid concentrations determined by HRMS.

The EEMs generated by process-affected water are complex and indicate more than one fluorescent species present. Using models created by PARAFAC it was determined that the fluorescence signal from process-affected water could be

broken down into five different fluorescence species for samples from each oil sands operation. Of the five species, three of the species were well matched between each water source. The other two components displayed many similarities, but were not as closely related. This indicates that the fluorescent species are very similar regardless of source, and is supported by the similar overall EEM shape displayed. The relative concentrations of each fluorescent species differed between each water source, indicating that while similar fluorescent species are present, they are not distributed the same. The variation of each components relative concentration describes the variation in intensities shown in the three companies EEMs. The fluorescence signal from commercial naphthenic acids was attributed to three fluorescent species according to PARAFAC models. Two of the three fluorescent species correlated with the species determined for process-affected water. The naphthenic acid concentrations determined from FTIR were unable to be correlated to a specific fluorescent species, and thus unable to estimate the naphthenic acid concentration in the process-affected water samples.

Overall, fluorescence as an analytical method can be used to indicate the presence of naphthenic acids in the acid extractable fraction of process-affected water. The fluorescent species identified by PARAFAC indicate that process-affected water contains similar species regardless of source, though in varying concentrations. Commercial naphthenic acids, like those used in FTIR analysis, have different fluorescence properties and do not describe those found in process-affected water.

5.2 Applications to Industry

This research has added to the understanding of naphthenic acids in process-affected water from the oil sands industry. The fluorescence signal produced from process-affected water can be attributed exclusively to the organic acid fraction which contains naphthenic acids. The current industry standard analytical method for quantifying naphthenic acids, FTIR, is time consuming and

shows indication of overestimating the total concentration. The concentration determined by FTIR is unable to distinguish between molecular structure of naphthenic acids groups or identify individual species. The strong correlation between the 280 nm excitation peak and FTIR naphthenic acid concentration shows that fluorescence can be used to identify changing concentrations and distribution within an oil sands operation. Fluorescence offers many advantages over the current industry and research analytical methods for naphthenic acids as it is rapid and requires little sample preparation. Currently fluorescence is able to determine naphthenic acid concentration when compared to a calibration curve that is based off of FTIR values for a particular oil sands company. While this does raise similar concerns of naphthenic acid concentration overestimation, fluorescence offers several advantages over FTIR. Using fluorescence for naphthenic acid detection eliminates much of the sample preparation and analysis time that is associated with FTIR, and requires a much smaller sample volume that is not destroyed during the analysis and can be retained for future use. Further research in this area can narrow down the fluorescent species present in process-affected water and provide more insight into naphthenic acids quantification and characterization.

5.3 Recommendations for Future Work

It is recommended that further research should be continued on using fluorescence as an analytical tool for process-affected water. The fluorescence signals indicate that there are more than one species, or group of species that contribute to the overall fluorescent signal, however the exact chemical makeup of these species remains unknown. High performance liquid chromatography (HPLC) can be used in conjunction with fluorescence and aid in further identifying the molecular weights and structures of compounds fluorescing within the process-affected water mixture. This analytical method has previously been used to characterize naphthenic acid concentration (Yen et al. 2004), which as stated previously is a known constituent of the fluorescent fraction.

There is currently a great deal of ongoing research in the area of characterization and quantification of naphthenic acids as they are a compound of interest due to their toxic and corrosive properties. New analytical methods have identified various degrees of deviation from the classical naphthenic acid formula to include compounds such as nitrogen, sulphur, sodium and higher amounts of oxygen (Grewer et. al 2010). Currently the chemical structures of the naphthenic acids that contribute to the toxic and corrosive properties have not been identified. As more insight is gained into the chemical makeup of naphthenic acids and the extractable organic acid fraction the species which contribute to fluorescence signal can be identified.

The principle fluorescent components identified by PARAFAC can subsequently be utilized in a second statistical technique, soft independent method of class analogy (SIMCA). SIMCA allows for data from an unknown sample to be compared to the determined principle components and subsequently assess the similarities between the two datasets. Using this method the fluorescent components can be statistically matched between oil sands companies. Additionally samples obtained from other source waters, for example groundwater, can be analyzed to identify if they contain the fluorescent species present in the tailings ponds. SIMCA can also aid in the identification of fluorescent species by comparing known fluorescent contaminants to the process-affected water.

The process-affected water that was used for this work was obtained from tailings ponds that are considered active. Some of the oil sands companies have multiple tailings ponds, which includes older tailings ponds which are no longer active and were excluded from this work. Previous research has shown that naphthenic acids will biodegrade over time (Allen 2008). The effect that biodegradation and the degree of aging have on the overall fluorescence signal should be observed. An experiment comparing aged process-affected water to fresh process-affected water

could aid in identification of the reduction of all fluorescent species or a certain fluorescent species.

One of the advantages of fluorescence as an analytical tool is the development of a field portable fluorescence sensor by the University of Alberta Electrical Engineering department. Portable fluorescence sensors have been used to identify petroleum hydrocarbons in previous research (Alostaz 2008). The portable sensor developed for naphthenic acid identification has the ability to scan at six excitation wavelengths over the full emission spectra (Taschuk et al. 2010). The current sensor scans at excitation wavelengths:

- 265 nm;
- 280 nm;
- 295 nm;
- 310 nm;
- 320 nm; and
- 340 nm.

Experiments with the portable sensor should include obtaining fluorescence signals from process-affected water similar to the sources used in this research. Similar to this research the field program should include observing the change in fluorescence signal between each oil sands company and for various concentrations of process-affected water. In addition the signals from the field spectrometer should be compared to the signals obtained from the laboratory spectrometer.

This future work will aid to the application of fluorescence as an analytical tool in the oil sands industry and further the understanding of naphthenic acids. The identification of the fluorescent compounds and their chemical makeup within process-affected water will help identify the relationship between fluorescence signal and the organic acid fraction and naphthenic acids. The implementation of fluorescence as an analytical tool aids the oil sands industry as it is a quick analytical method that requires little sample preparation and can be used applied as both a laboratory and field technique.

5.4 References

Allen, E.W. 2008. Water treatment in Canada's oil sands industry I: Target pollutants and treatment objectives. Journal of Environmental Engineering and Science, 7: 123-128.

Grewer, D.M., Young, R.F., Whittal, R.M., and Fedorak, P.M. 2010. Naphthenic Acids and other acid-extractables in water samples from Alberta: What is being measured? Science of the Total Environment, 408(23): 5997-6010.

Taschuk, M.T., Wang, Q., Drake, S., Ewanchuk, A., Gupta, M., Alostaz, M., Ulrich, A.C, Sego, D.C., and Tsui, Y.Y. 2010. Portable Naphthenic Acid Sensor for Oil Sands Applications. In Proceedings of the Second International Oils Sands Tailings Conference, Edmonton, Alberta, 5-8 December 2010. pp. 213-221.

Yen, T.W., Marsh, W.P., MacKinnon, M.D., and Fedorak, P.M. 2004. Measuring naphthenic acids concentrations in aqueous environmental samples by liquid chromatography. Journal of Chromatography A, 1033 (2004) 83–90.

APPENDIX A: Extraction Method

In order to analyze the naphthenic acid fraction from the tailings pond process-affected water using the Fourier Transform Infrared (FTIR) spectroscopy method it is required to do an extraction first. This method is based on the method outlined by Jivraji et al. (1995).

1. Rinse all glassware necessary with dichloromethane (CH_2Cl_2)
2. Filter water sample through 0.45 µm for a total of 500 mL
3. Record mass of sample
4. Record initial pH of sample

Base Extraction

5. Add concentrated sodium hydroxide (NaOH) until sample reaches pH of 11.5
6. Move sample to sepratory funnel
7. Add 25 mL of dichloromethane
8. Shake sepratory funnel, releasing pressure as necessary
9. Allow mixture to settle until distinct interface is observed
10. Drain dichloromethane layer
    a. Record mass of beaker
11. Repeat steps 7-10 twice for a total of 75 mL of dichloromethane removed
12. Allow extracted base components to dry
    a. Mass of extracted components can then be determined
13. Transfer water layer back to a beaker

Acid Extraction

14. Add concentrated hydrochloric acid (HCl) until sample reaches pH of 2
15. Move sample to sepratory funnel
16. Add 25 mL of dichloromethane
17. Shake sepratory funnel, releasing pressure as necessary
18. Allow mixture to settle until distinct interface is observed
19. Drain dichloromethane layer
    a. Record mass of beaker
20. Repeat steps 7-10 twice for a total of 75 mL of dichloromethane removed
21. Discard water layer
22. The extracted components can then either be:
    a. Allowed to dry. The mass of extracted components can then be determined
    b. Used to determine neutral components.

Neutral Extraction

23. Prepare a 500 mL sample of deionized water
24. Record mass of sample
25. Record initial pH of sample
26. Add concentrated sodium hydroxide (NaOH) until sample reaches pH of 11.5
27. Move deionized water sample to sepratory funnel
28. Add extracted acid components in 75 ml of dichloromethane from step 22
29. Shake sepratory funnel, releasing pressure as necessary
30. Allow mixture to settle until distinct interface is observed
31. Drain dichloromethane layer
    a. Record mass of beaker
32. Allow extracted neutral components to dry
    a. Mass of extracted components can then be determined

Acid Extraction (after Neutral)

33. Transfer deionized water layer back to a beaker
34. Add concentrated hydrochloric acid (HCl) until sample reaches pH of 2
35. Move sample to sepratory funnel
36. Add 25 mL of dichloromethane
37. Shake sepratory funnel, releasing pressure as necessary
38. Allow mixture to settle until distinct interface is observed
39. Drain dichloromethane layer
    a. Record mass of beaker
40. Repeat steps 7-10 twice for a total of 75 mL of dichloromethane removed
41. Discard water layer
42. Allow extracted acid components to dry
    a. Mass of extracted components can then be determined

APPENDIX B: FTIR Method

After the extract is allowed to dry it is ready for analysis. The instrument used was a Perkin Elmer Spectrum 100 FTIR spectrometer.

Instrument

1. Select the following parameters
    a. Wavelength:
        i. Start: 4000 cm^{-1}
        ii. End: 400 cm^{-1}
    b. Measurement unit: Absorbance
    c. Accumulation of scans: 32
    d. Resolution: 4
2. Collect background spectrum
    a. Rinse KBr cell with dichloromethane (CH_2Cl_2) five times
    b. Fill KBr cell with CH_2Cl_2, ensuring the cell is free of air bubbles
    c. Select "Collect background"

Calibration Curve

1. Prepare a 1000 mg/kg stock solution of Sigma Aldrich commercial naphthenic acids
    a. 0.2 g of naphthenic acids
    b. 200 g of dichloromethane (CH_2Cl_2)
2. Prepare 300, 250, 200, 150, 100, 50, 25, 20, 10 and 1 mg/kg standards from the stock solution
3. Use the sample parameters as described above
4. Scan each sample three times
    a. Rinse KBr cell with CH_2Cl_2 five times between each sample
5. Record height at each peak (1743 cm^{-1} and 1706 cm^{-1})
6. Sum the peak heights for a total height
    a. Take the average of the three scans
7. Prepare a standard calibration curve of concentration versus average total peak height

Sample Analysis

1. Samples require extraction method
2. Use sample parameters as described above
3. Dissolve the acid fraction with approximately 20 g of CH_2Cl_2
    a. Adjust amount to concentrate within curve
    b. Record actual mass of CH_2Cl_2 added
4. Rinse KBr cell with sample twice

5. Scan three times
6. Record height at each peak (1743 cm^{-1} and 1706 cm^{-1})
7. Sum the peak heights for a total height
    a. Take the average of the three scans
8. Determine concentration from calibration curve

The data collected to create the calibration curve used for the results in this thesis are shown in Table B1. Each standard was run three times according to the parameters described above and the average height was used to create the calibration curve. The resulting calibration curve is shown in Figure B1.

Table B1: FTIR Calibration Curve Data

Concentration (mg/Kg)	Mass of NAs added (g)	Mass of CH_2Cl_2 added (g)	Actual (mg/Kg)	1743 cm^{-1} Height	1706 cm^{-1} Height
1000	0.2082	203.8	1021.6	0.39085	0.34220
				0.39830	0.33043
				0.40598	0.32433
			Average	0.398377	0.33232
			Total	**0.730697**	
	Mass of Stock Solution (g)	Mass of CH_2Cl_2 added(g)	Actual (mg/Kg)	1743cm^{-1} Height	1706cm^{-1} Height
300	29.85	99.79	305.6	0.17328	0.078934
				0.17353	0.074116
				0.17437	0.072754
			Average	0.173727	0.075268
			Total	**0.248995**	
250	25.6	105.35	248.2	0.13410	0.050133
				0.13444	0.047048
				0.13568	0.046490
			Average	0.13474	0.04789033
			Total	**0.18263**	
200	20.61	107.05	196.7	0.10480	0.034024
				0.10933	0.033380
				0.10940	0.033100
			Average	0.107843	0.03350133
			Total	**0.141345**	

150	15.17	100.17	154.7	0.088692	0.025155
				0.089322	0.024202
				0.090453	0.023946
			Average	0.089489	0.02443433
			Total	**0.113923**	
100	10.65	101.14	107.6	0.065582	0.016189
				0.065324	0.015027
				0.06574	0.01504
			Average	0.065549	0.01541867
			Total	**0.080967**	
50	5.5	108.38	51.8	0.033153	0.0052233
				0.033301	0.0054448
				0.033783	0.005314
			Average	0.033412	0.00532737
			Total	**0.03874**	
25	2.59	110.06	24.0	0.017102	0.0032801
				0.016078	0.0016199
				0.015886	0.00121
			Average	0.016355	0.00203667
			Total	**0.018392**	
20	2.07	113.37	18.7	0.011598	0.00014354
				0.011756	0.0001547
				0.01204	0.0002563
			Average	0.011798	0.00018485
			Total	**0.011983**	
10	1.38	102.58	13.7	0.009605	0.0012823
				0.008248	-0.000226
				0.008542	-0.0001511
			Average	0.008798	0.00030175
			Total	**0.0091**	
1	0.32	102.19	3.2	0.002014	6.3246E-07
				0.001252	-0.0009847
				0.00166	-0.0009779
			Average	0.001642	-0.000654
			Total	**0.000988**	

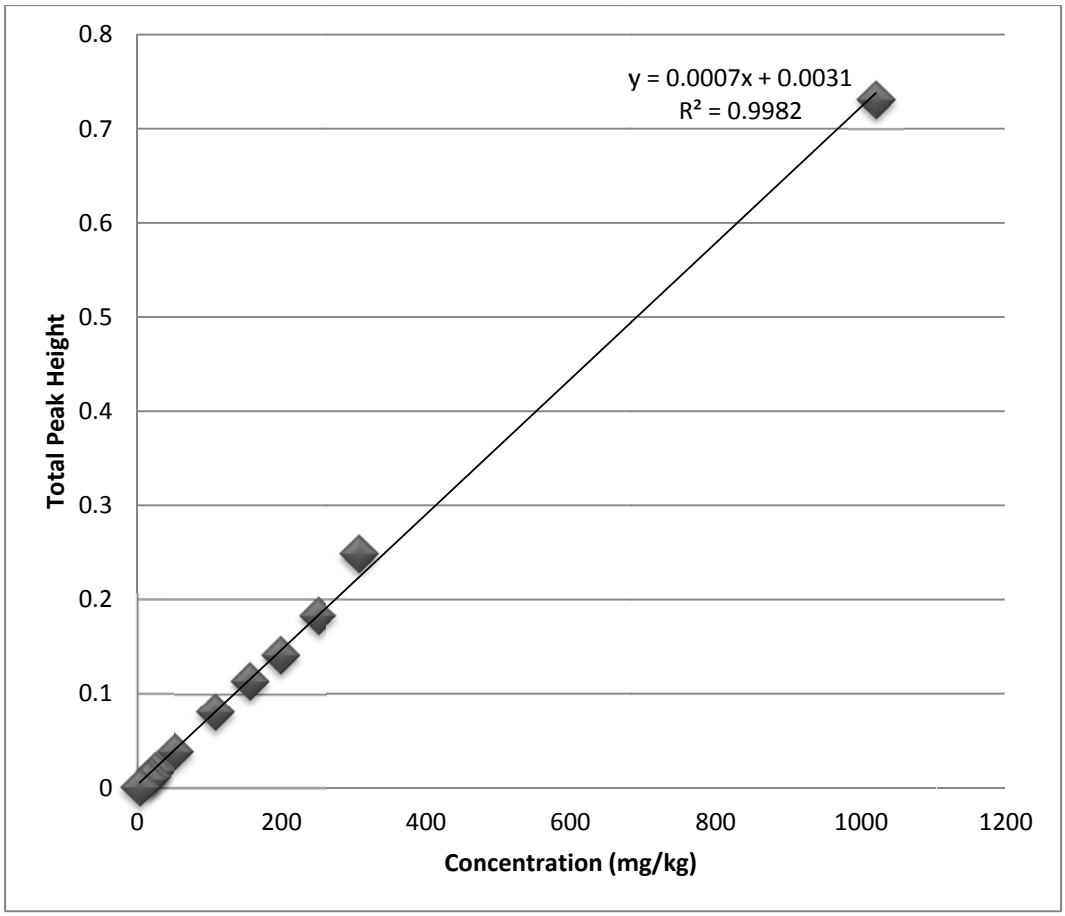

Figure B1: FTIR Calibration Curve. The total height from the dominant peaks is plotted against the concentration of the commercial naphthenic acids.

Appendix C: Correction Calculations

The instrument used for fluorescence is the Varian Cary Eclipse fluorescence spectrophotometer. The spectrometer is a single cell holder set up for right angle fluorometry, as shown in Figure F1. When samples are not optically dilute (Absorbance $cm^{-1} < 0.01$) inner filtering becomes a problem (Tucket et al 1992). While the set up reduces stray radiation, only fluorescence emissions from the center of the sample cell are collected. Process-affected water is not considered optically dilute, most significantly at lower excitation wavelengths, so it must be corrected for both primary and secondary inner filter effects.

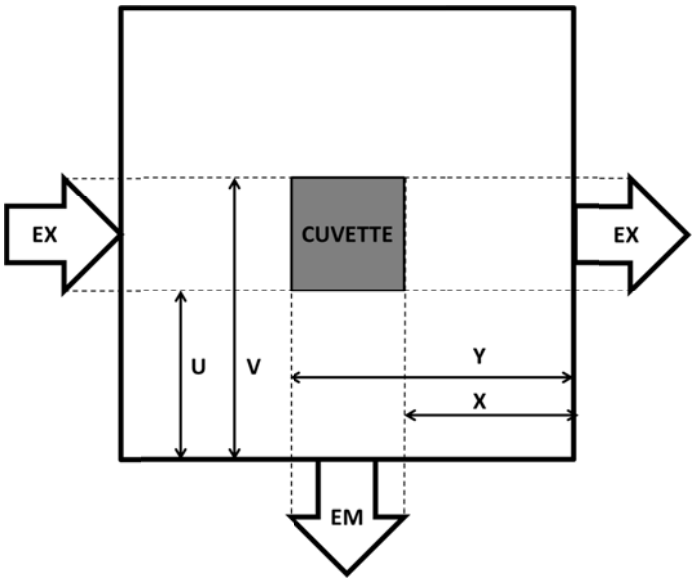

Figure C1: Cell configuration in the Varian Cary Eclipse Spectrometer

As shown in Figure F1, (x,y) and (u,v) are window parameters. The window parameters were recorded as follows:

$U: 0.174cm$
$V: 1.066cm$
$X: 0.174cm$
$Y: 1.066cm$

In right angry fluorometry, the cuvette is placed as in the figure. The emission detector is at 90^o with respect to the incoming excitation beam. The excitation beak is attenuated before reaching the detection optics. This is called primary inner filtering. The correction factor for primary inner filtering is:

$$Correction\ Factor\ for\ primary\ inner\ filtering: f_{prim}$$

$$f_{prim} = \frac{F^{corr}}{F^{obs}} = \frac{2.303\ A(Y-X)}{10^{-AX}-10^{-AY}} \quad (1)$$

Where F^{obs} is the fluorescence intensity observed, F^{corr} is the fluorescence intensity after correction and A is the absorbance recorded at the excitation wavelength.

The second correction factor is due to the absorption of emitted fluorescence in large quantities. The correction factor for secondary inner filtering is:

$$Correction\ Factor\ for\ secondary\ inner\ filtering: f_{sec}$$

$$f_{sec} = \frac{F^{corr}}{F^{obs}} = \frac{(V-U)(1/b)\ln T}{T_{at\ V/b} - T_{at\ U/b}} \quad (2)$$

Where b is the cell path length (1cm in this case), and T is the transmittance recorded at the emission wavelength. The two equations can then be arranged to get the corrected florescence intensity:

$$F^{corr} = f_{prim} f_{sec} F^{obs} \quad (3)$$

The following calculations show how to obtain the corrected intensity using the observed intensity at an excitation wavelength of 290nm and an emission wavelength of 346nm for a Syncrude sample.

F^{obs}=509.5481

The primary correction factor:
Absorbance A at 290nm: 0.395

$$f_{prim} = \frac{F^{corr}}{F^{obs}} = \frac{2.303\ A(Y-X)}{10^{-AX}-10^{-AY}}$$

$$f_{prim} = \frac{F^{corr}}{F^{obs}} = \frac{2.303\ (0.395\ cm^{-1})(1.066\ cm - 0.174\ cm)}{10^{-((0.395\ cm^{-1})(0.174\ cm))} - 10^{-((0.395\ cm^{-1})(1.066\ cm))}} = 1.7105$$

The secondary correction factor:
Absorbance A at 346nm: 0.119

$$f_{sec} = \frac{F^{corr}}{F^{obs}} = \frac{(1.066\ cm - 0.174\ cm)(1/1\ cm)\ln(10^{-0.119\ cm^{-1}})}{\left(10^{(-0.119\ cm^{-1})(1.066\ cm/1\ cm)}\right) - \left(10^{(-0.119\ cm^{-1})(0.174\ cm/1\ cm)}\right)} = 1.1822$$

The corrected value is then calculated as:

$$F^{corr} = f_{prim} f_{sec} F^{obs} = (1.7105)(1.1822)(509.5481) = 1030.3843$$

Appendix D: Acid Extracts

In order to determine if the fluorescing compounds were in the base, neutral or acid components of the process-affected water, an extraction was done following Appendix A. Undiluted samples were collected from each company and filtered to 0.45µm. The initial pH, base pH and acid pH were recorded for the process-affected water and deionized water samples, as well as the required mass of the 500mL samples. Table D1 contains the recorded values.

Table D1: Recorded pH levels and mass of process affected water for undiluted extractions

	Initial pH	Base pH	Acid pH	Mass of Container (g)	Mass of Container + Sample (g)	Mass of Sample (g)
Syncrude						
PA Water	8.50	11.62	2.03	171.42	667.75	496.33
Deionized Water	8.91	11.79	1.96	170.31	661.37	491.06
Suncor						
PA Water	8.55	11.57	2.05	166.90	662.48	495.58
Deionized Water	5.55	11.80	2.00	218.07	715.90	497.83
Albian						
PA Water	8.32	11.51	1.93	171.41	660.03	488.62
Deionized Water	6.60	11.79	2.13	166.20	655.80	489.60

Following the extraction procedure the dried extracts were measured to estimate the amount of extract. The acid extraction showed there was consistently more dried extract in the acid component than base and neutral components for each company. The results are in Table D2.

Table D2: Dried Extract Mass by Acid Neutral Base

	Mass of container +Extracts (g)	Mass of container (g)	Extracts (g)
Syncrude			
Acid	111.1157	111.0925	0.0232
Neutral	114.9219	114.9205	0.0014
Base	110.7214	110.7195	0.0019

	Mass of container +Extracts (g)	Mass of container (g)	Extracts (g)
Suncor			
Acid	102.5665	102.5477	0.0188
Neutral	107.0108	107.0107	0.0001
Base	109.0976	109.0959	0.0017
Albian			
Acid	108.1271	108.1158	0.0113
Neutral	114.0852	114.0836	0.0016
Base	116.1848	116.1841	0.0007

For fluorescence analysis these dried extracts were then dissolved in dichloromethane and diluted back to a concentration level that would be expected in a tailings pond. A stock solution was made by adding approximately 40g of DCM. From the stock solution 2g was then transferred to a new beaker and 23g of fresh DCM is added. This dilutes the extractions approximately to process affected water levels in the tailings pond, without reading 500mL of dichloromethane. The actual amounts of dichloromethane added are recorded in Table D3.

Table D3: Dichloromethane amounts added to dried extractions for fluorescence analysis.

	Mass of Extract (g)	Mass Extracted from Stock (g)	Mass of Stock (g)	Mass of Fresh DCM
Syncrude				
Acid	0.0232	5.23	51.74	28.03
Neutral	0.0014	5.20	42.00	19.75
Base	0.0019	2.03	40.10	24.70
Suncor				
Acid	0.0188	2.00	42.52	25.49
Neutral	0.0001	4.25	44.47	23.56
Base	0.0017	3.71	42.15	24.64
Albian				
Acid	0.0113	5.32	45.46	29.66
Neutral	0.0016	2.22	40.93	23.47
Base	0.0007	2.88	47.13	26.71

Fluorescence scans of the samples revealed that majority of the fluorescent compounds are found within the acidic component of the process-affected water. The scans for each extraction are shown in Figures D1-D3 for Syncrude, Suncor and Albian, respectively.

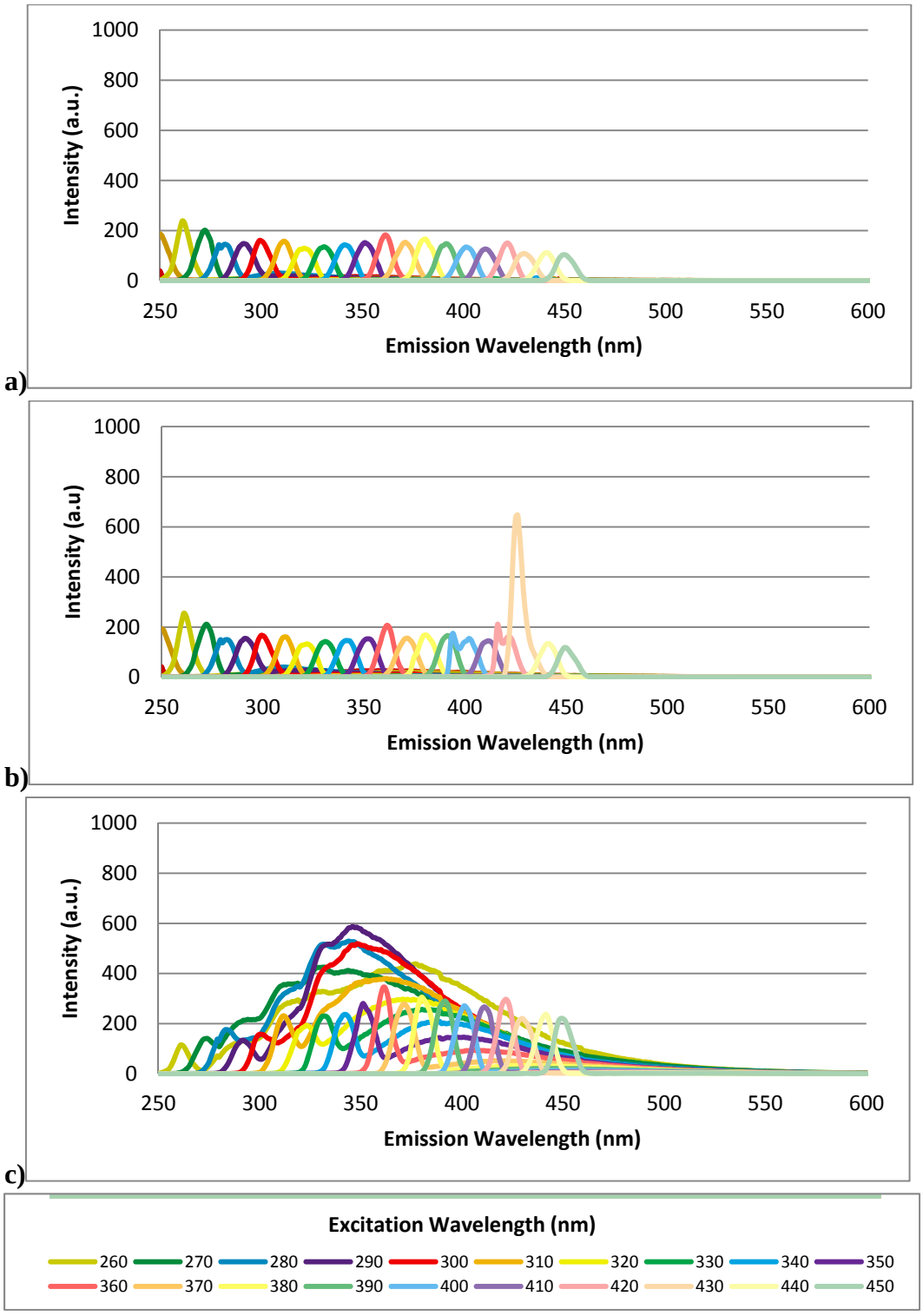

Figure D1: a) Base extraction b) Neutral extraction c) Acid extraction. Sample from Syncrude process-affected water dried extractions diluted to tailings pond concentration levels.

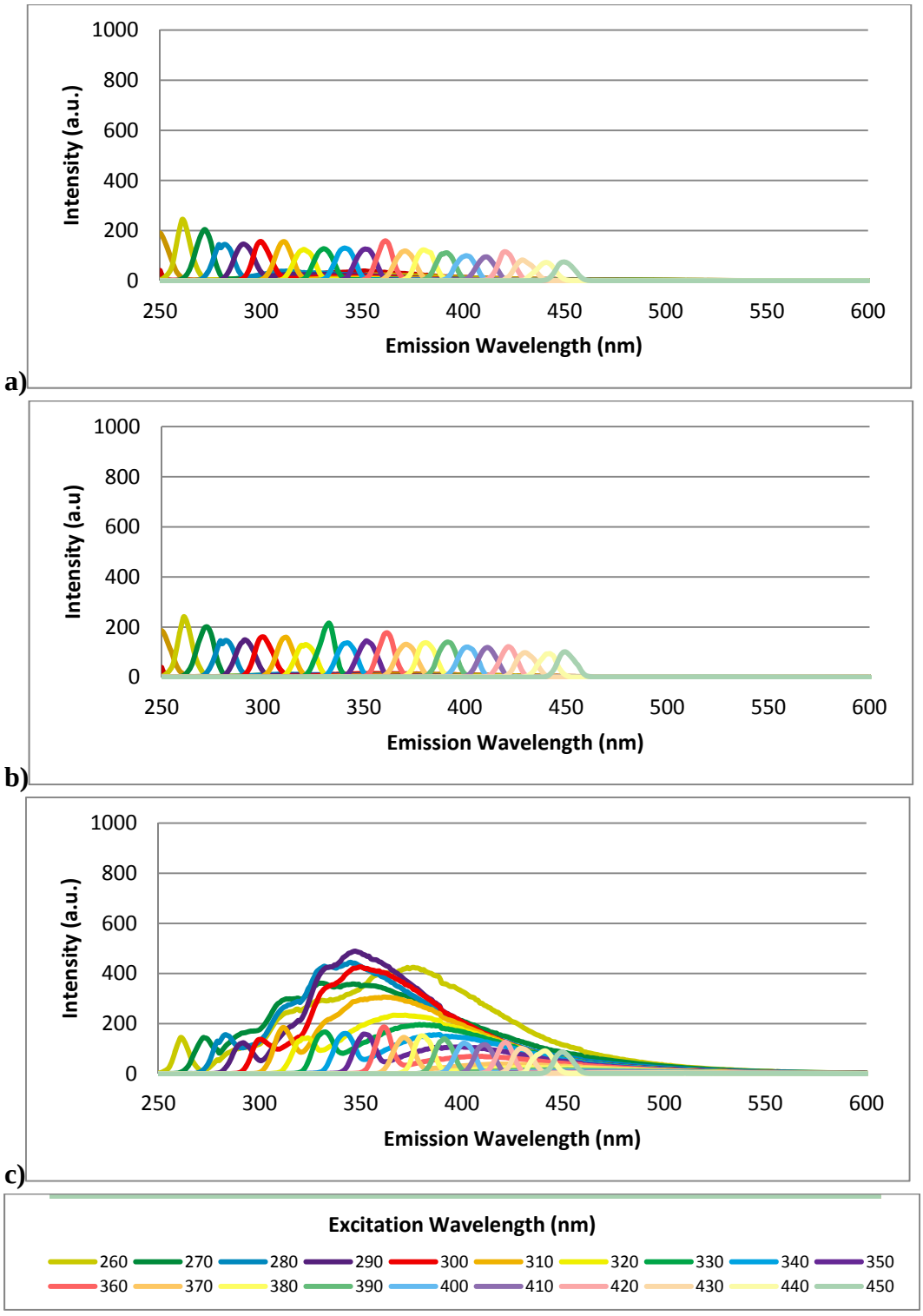

Figure D2: a) Base extraction b) Neutral extraction c) Acid extraction. Sample from Suncor process-affected water dried extractions diluted to tailings pond concentration levels.

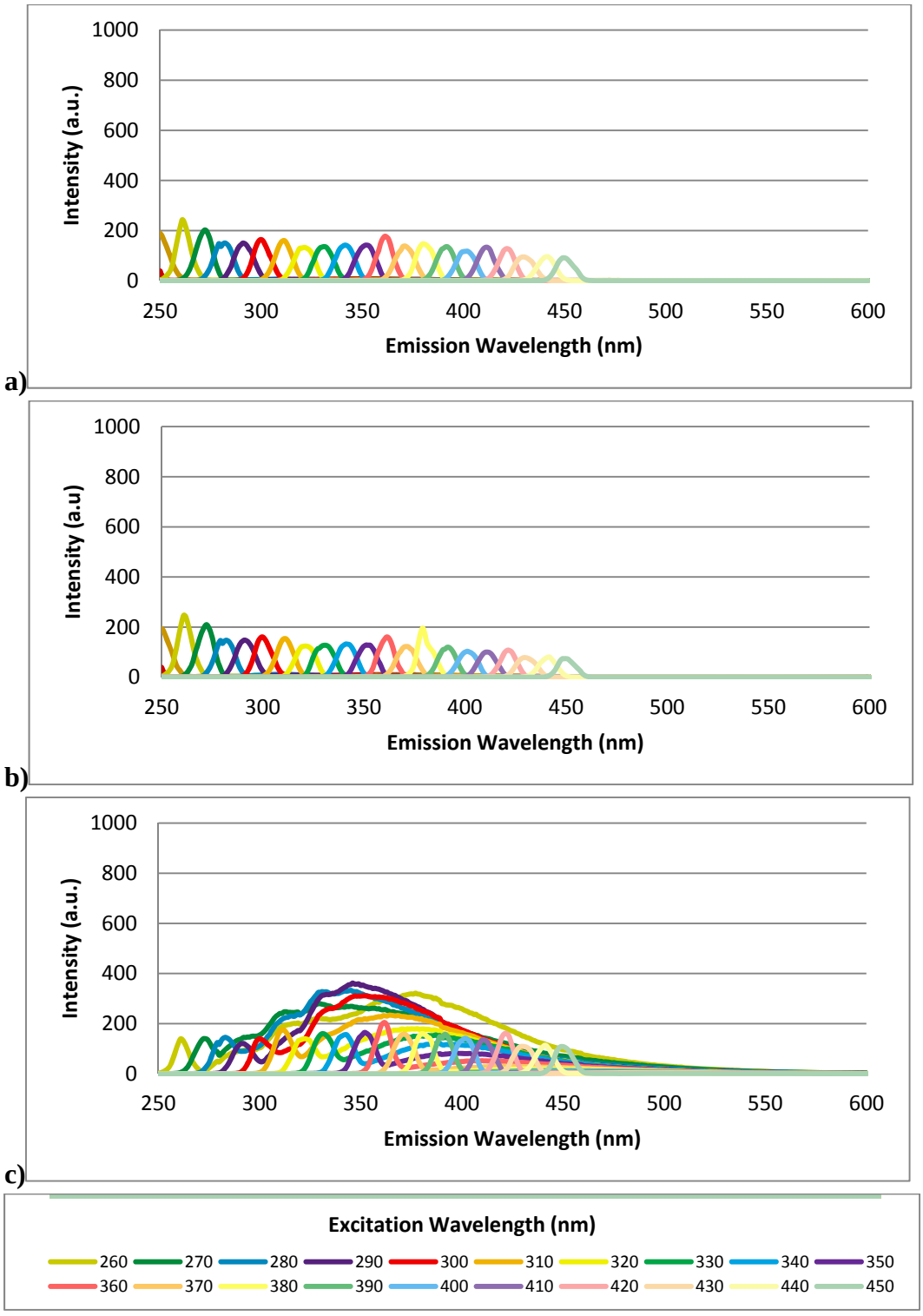

Figure D3: a) Base extraction b) Neutral extraction c) Acid extraction. Sample from Suncor process-affected water dried extractions diluted to tailings pond concentration levels.

Appendix E: Solvents

A Varian Cary Eclipse spectrometer was used for fluorescence measurements using the 90^{o} detection setup. Samples were analyzed in clear quartz cuvettes measuring 1.24x1.24x4.5 cm. Excitation-Emission Matrices were generated using Varian Cary Eclipse software at a scan rate of 600 nm/min. Emission wavelengths were collected from 240 to 600 nm with 1 nm increments at excitation wavelengths ranging from 250 to 450 nm with 10 nm increments. The bandwidth (slit width) was 10 nm and 5 nm for excitation and emission, respectively. Both excitation and emission filters were set to automatic.

Blanks of several different solvents were analyzed to determine their effect on the signal. Deionized water was scanned as it was used in several of the dilution series. The scan for deionized water is shown in Figure E1. The deionized water gave no signal aside from light scatter.

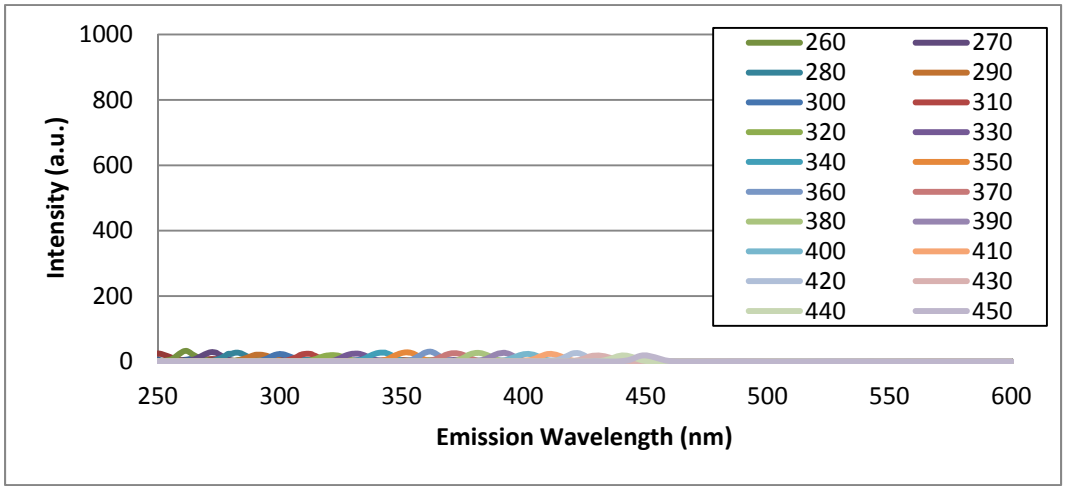

Figure E1: Fluorescence scan of deionized water

The solvent used for FTIR analysis is dichloromethane. The naphthenic acids are known to partition into this solvent. In order to determine the effect dichloromethane has on the fluorescence signal it was scanned using the above parameters. The EEM is shown in Figure E2. Like deionized water, dichloromethane does not give a signal aside from light scatter.

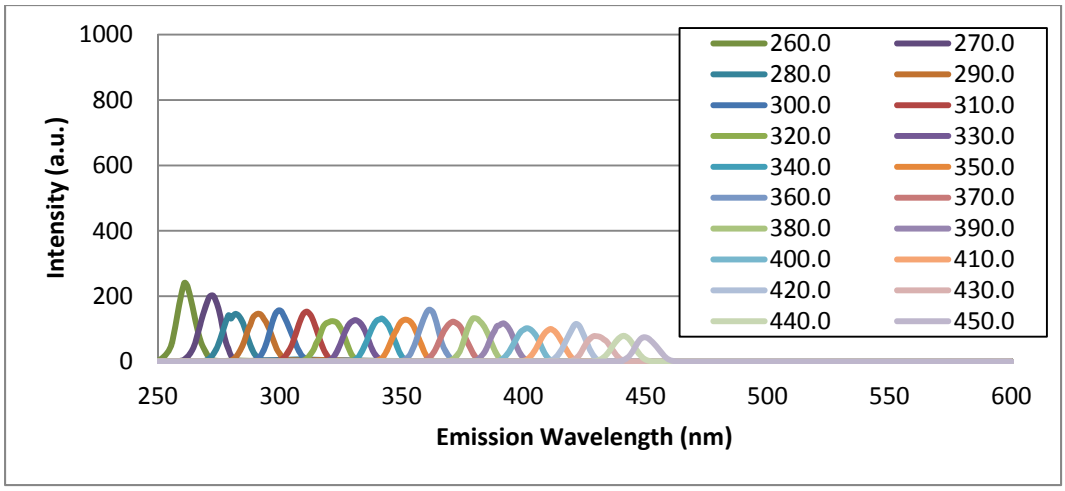

Figure E2: Fluorescence scan of dichloromethane

In order to determine if another solvent would be a suitable choice, methanol was also scanned. Methanol is a common solvent in other applications, and is able to dissolve commercially available naphthenic acids. The fluorescence scan of methanol is shown in Figure E3, with the light scatter included and with the light scatter removed inset. In this case methanol gives a small signal, most significantly in the lower excitation wavelengths.

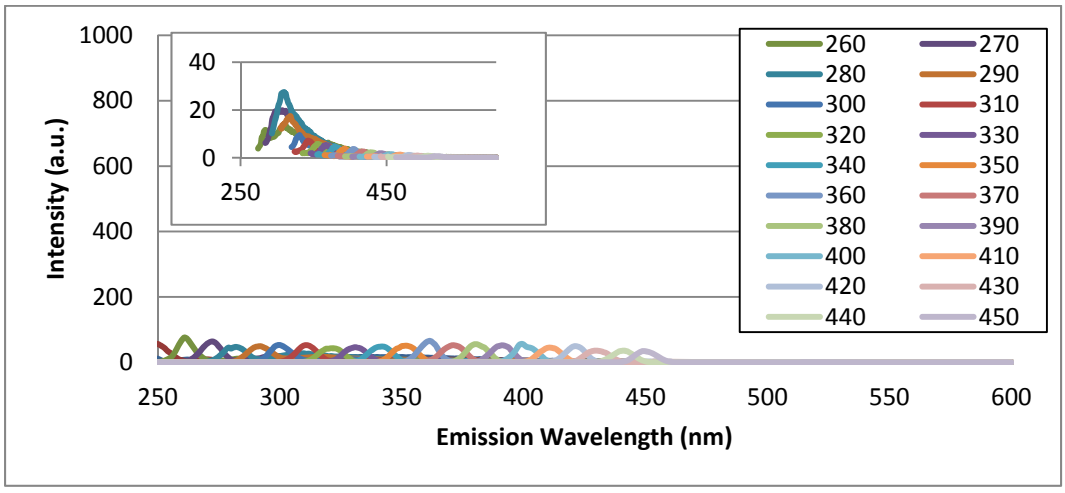

Figure E3: Fluorescence scan of methanol

Two acid extractions were performed on 500mL of Syncrude water filter to 0.45µm each, according to Appendix A. Stock solutions were created by adding 100mL of methanol and dichloromethane respectively which is approximately five times more diluted than the process-affected water levels in the tailings pond. A dilution series was prepared at 60%, 50%, 30%, 20%, 10%, 5%, 2.5%, 1% and 0.5% in 10mL flasks.

Appendix F: Fluorescence Dilution Series

Light scatter is an unavoidable product that occurs during fluorescence scanning. The fluorescence intensity is measured at a 90° angle, as shown in Figure F1. Consequently, some stray light is transmitted by the sample and picked up by the detection system. The stray light is referred to as light scatter; it is not part of the signal. The amount of light scatter is dependent on the sample scanned and must be manually removed for data analysis.

A dilution series for Syncrude, Suncor and Albian was prepared for fluorescence analysis. Five samples of 10mL were prepared with the process-affected water at 10%, 25%, 50%, 75% and 100% with deionized water. The process-affected water was filtered to 0.45µm before scanning. Unfiltered samples contain particles that will absorb excitation wavelengths and do not appear in the signal.

The following figures are the resulting excitation emission matrices (EEMs) for the dilution series. Figure A) shows the EEM with light scatter and intensity values uncorrected for primary and secondary inner filtering effects. Figure B) shows the EEM with light scatter and intensity values corrected for primary and secondary inner filtering effects. Figure C) shows the EEM with the light scatter removed and intensity values uncorrected for primary and secondary inner filtering effects. Figure D) shows the EEM with the light scatter removed and intensity values corrected for primary and secondary inner filtering effects. The Syncrude dilution series scans are shown in Figures 1-5, the Suncor dilution series scans shown in Figures 2-6, and the Albian dilution series scans are shown in Figures 7-11.

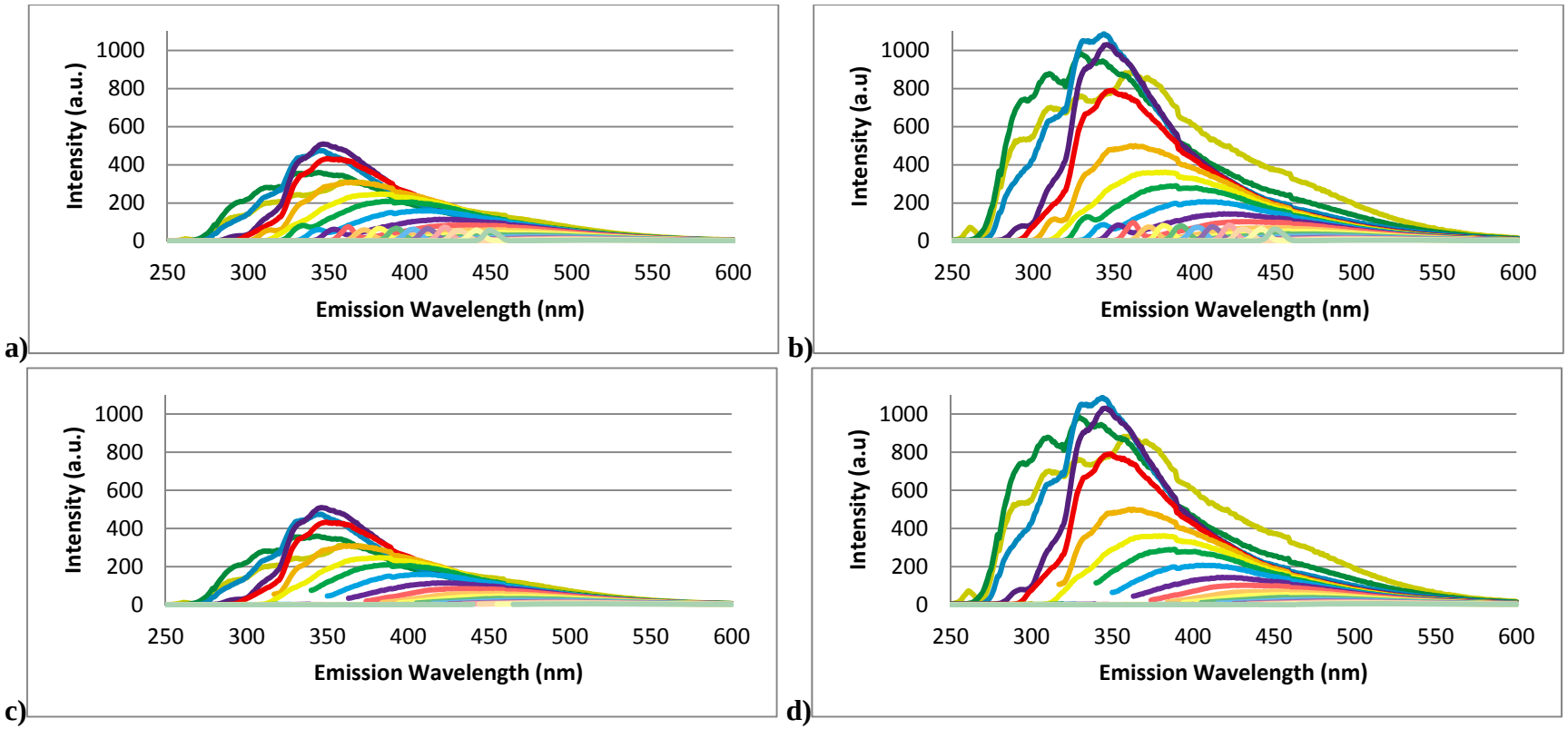

Figure F1:Syncrude process affected water filtered to .45µm and undiluted. A) Intensity values uncorrected for primary and secondary inner filtering effects with light scatter. B) Intensity values corrected for primary and secondary inner filtering effects with light scatter. C) Intensity values uncorrected for primary and secondary inner filtering effects without light scatter. D) Intensity values corrected for primary and secondary inner filtering effects without light scatter.

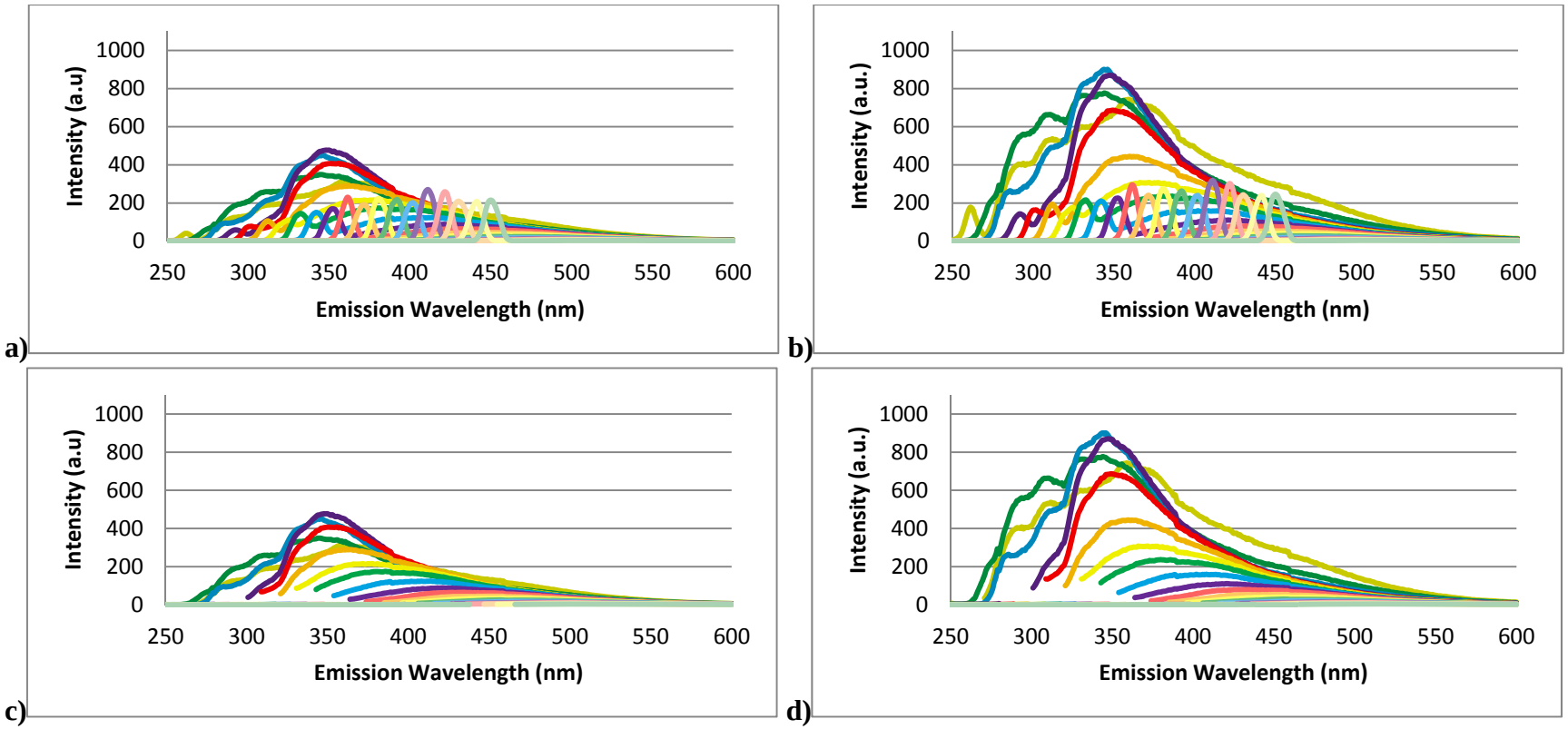

Figure F2: Syncrude process affected water filtered to .45µm and diluted to 75% with deionized water. A) Intensity values uncorrected for primary and secondary inner filtering effects with light scatter. B) Intensity values corrected for primary and secondary inner filtering effects with light scatter. C) Intensity values uncorrected for primary and secondary inner filtering effects without light scatter. D) Intensity values corrected for primary and secondary inner filtering effects without light scatter.

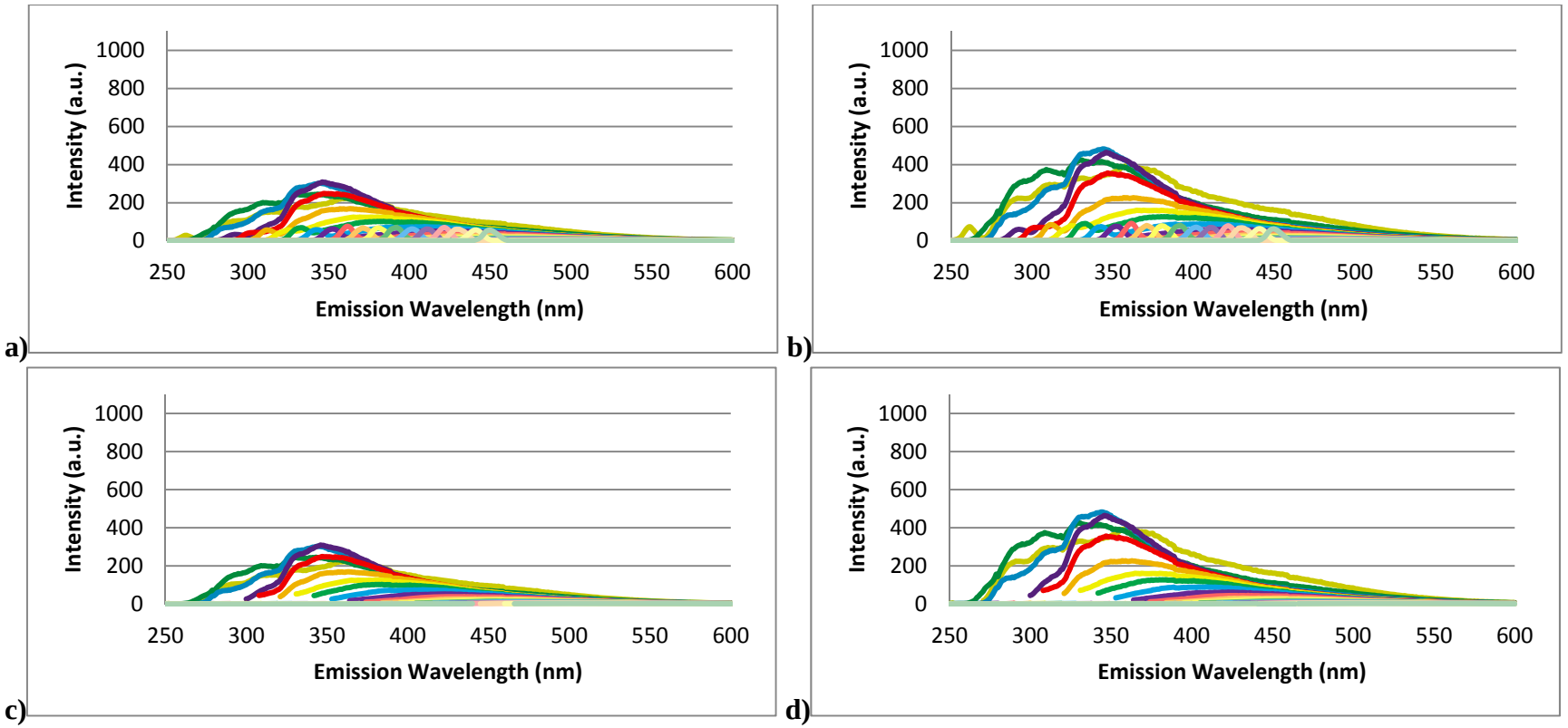

Figure F3: Syncrude process affected water filtered to .45µm and diluted to 50% with deionized water. A) Intensity values uncorrected for primary and secondary inner filtering effects with light scatter. B) Intensity values corrected for primary and secondary inner filtering effects with light scatter. C) Intensity values uncorrected for primary and secondary inner filtering effects without light scatter. D) Intensity values corrected for primary and secondary inner filtering effects without light scatter.

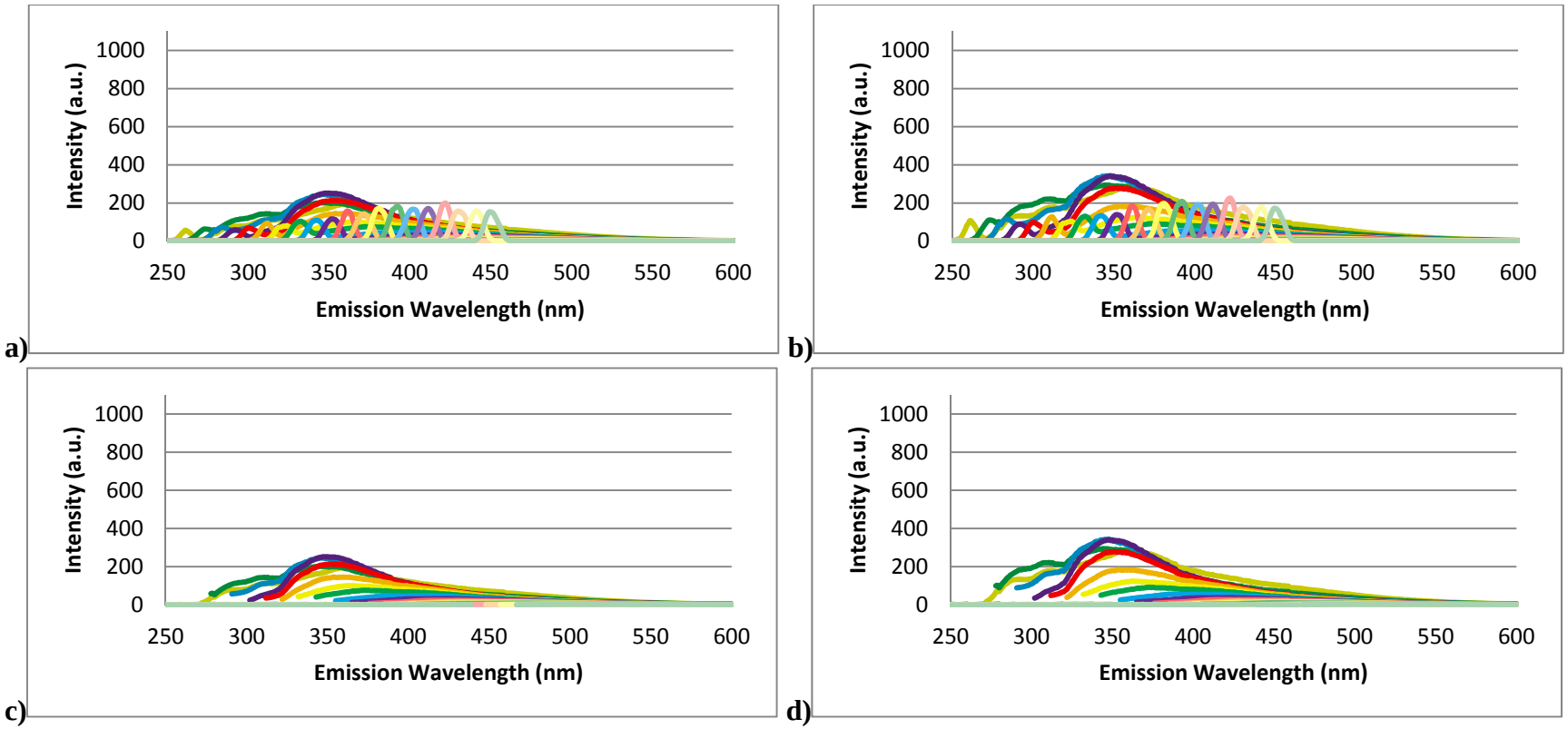

Figure F4: Syncrude process affected water filtered to .45µm and diluted to 25% with deionized water. A) Intensity values uncorrected for primary and secondary inner filtering effects with light scatter. B) Intensity values corrected for primary and secondary inner filtering effects with light scatter. C) Intensity values uncorrected for primary and secondary inner filtering effects without light scatter. D) Intensity values corrected for primary and secondary inner filtering effects without light scatter.

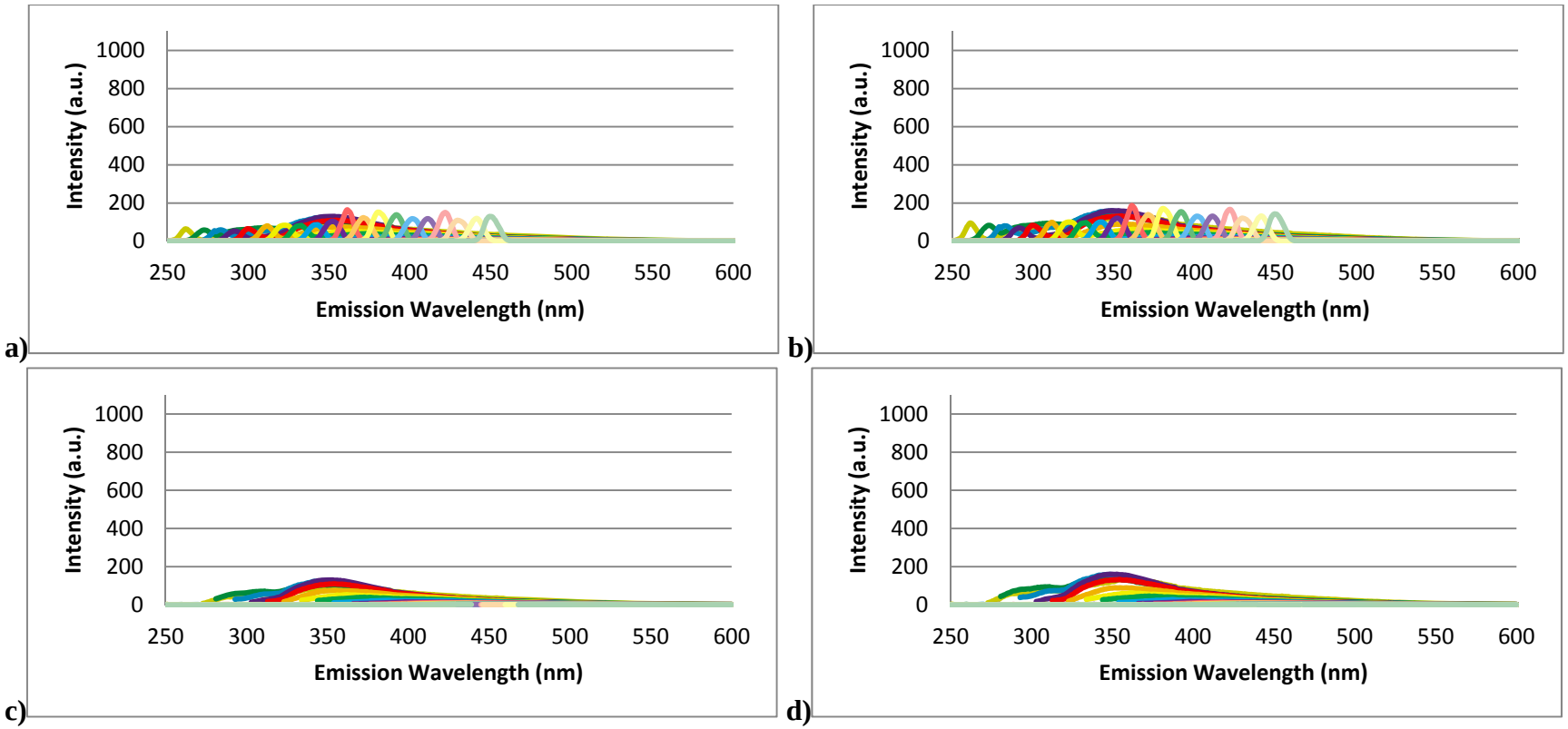

Figure F5: Syncrude process affected water filtered to .45µm and diluted to 10% with deionized water. A) Intensity values uncorrected for primary and secondary inner filtering effects with light scatter. B) Intensity values corrected for primary and secondary inner filtering effects with light scatter. C) Intensity values uncorrected for primary and secondary inner filtering effects without light scatter. D) Intensity values corrected for primary and secondary inner filtering effects without light scatter.

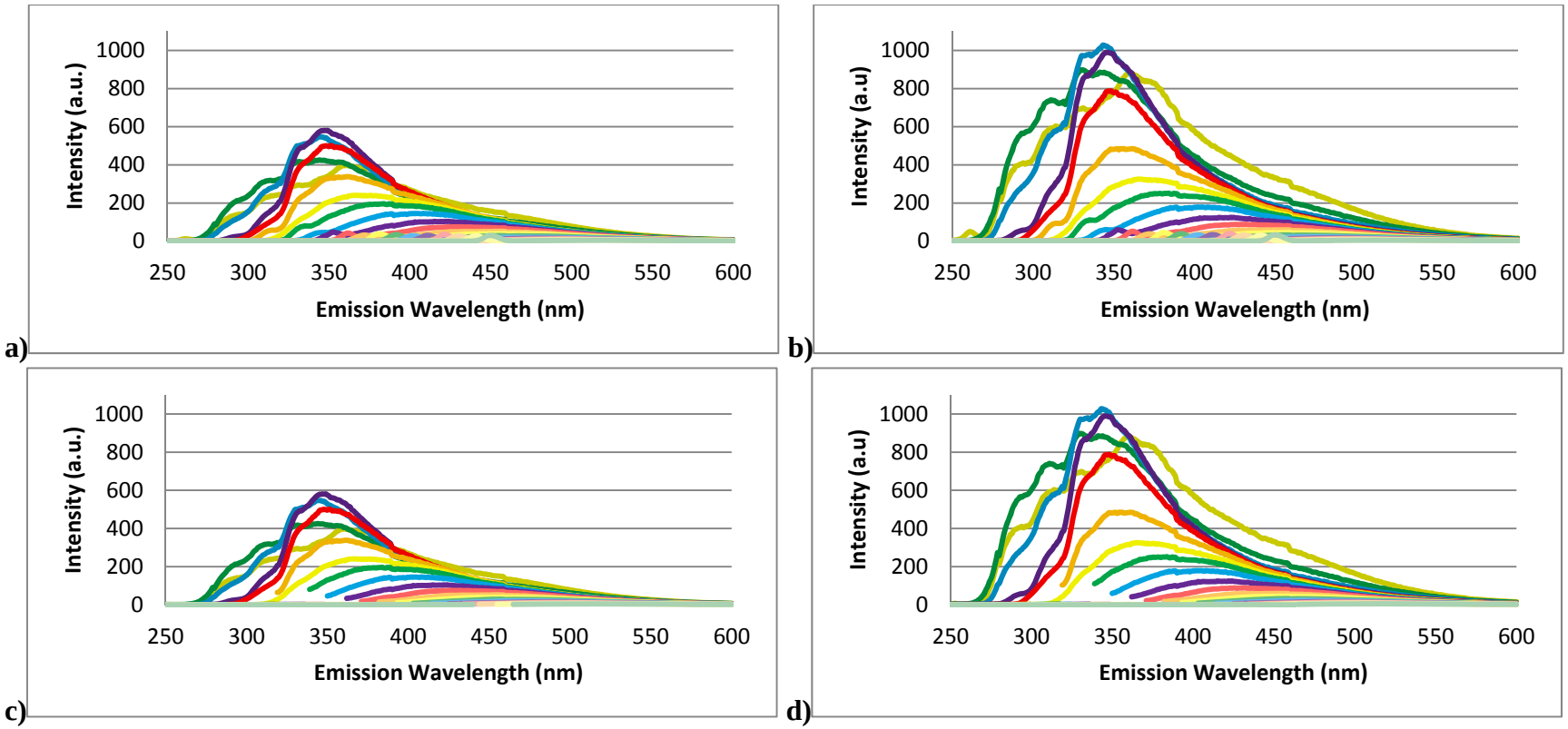

Figure F6: Suncor process affected water filtered to .45µm and undiluted. A) Intensity values uncorrected for primary and secondary inner filtering effects with light scatter. B) Intensity values corrected for primary and secondary inner filtering effects with light scatter. C) Intensity values uncorrected for primary and secondary inner filtering effects without light scatter. D) Intensity values corrected for primary and secondary inner filtering effects without light scatter.

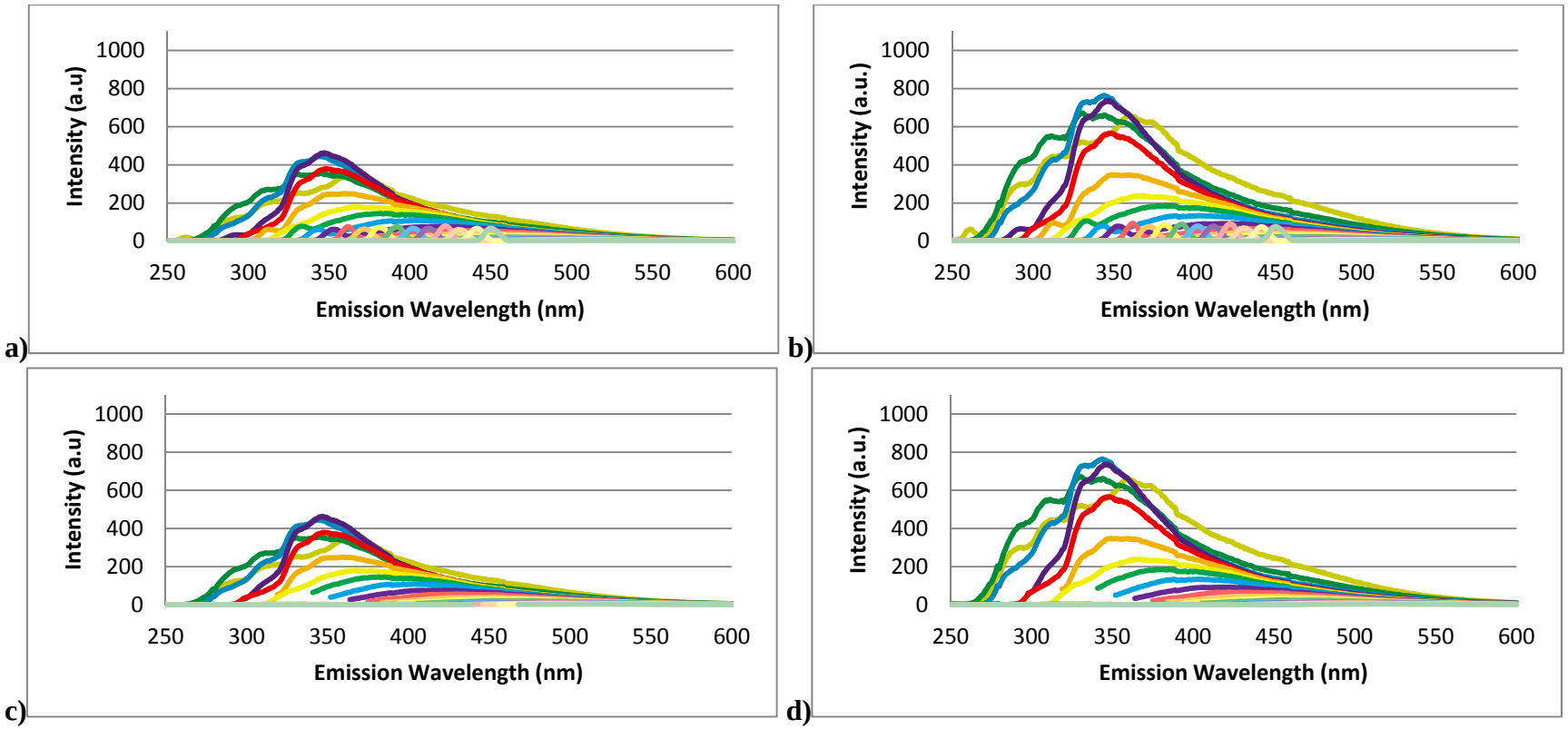

Figure F7: Suncor process affected water filtered to .45µm and diluted to 75% with deionized water. A) Intensity values uncorrected for primary and secondary inner filtering effects with light scatter. B) Intensity values corrected for primary and secondary inner filtering effects with light scatter. C) Intensity values uncorrected for primary and secondary inner filtering effects without light scatter. D) Intensity values corrected for primary and secondary inner filtering effects without light scatter.

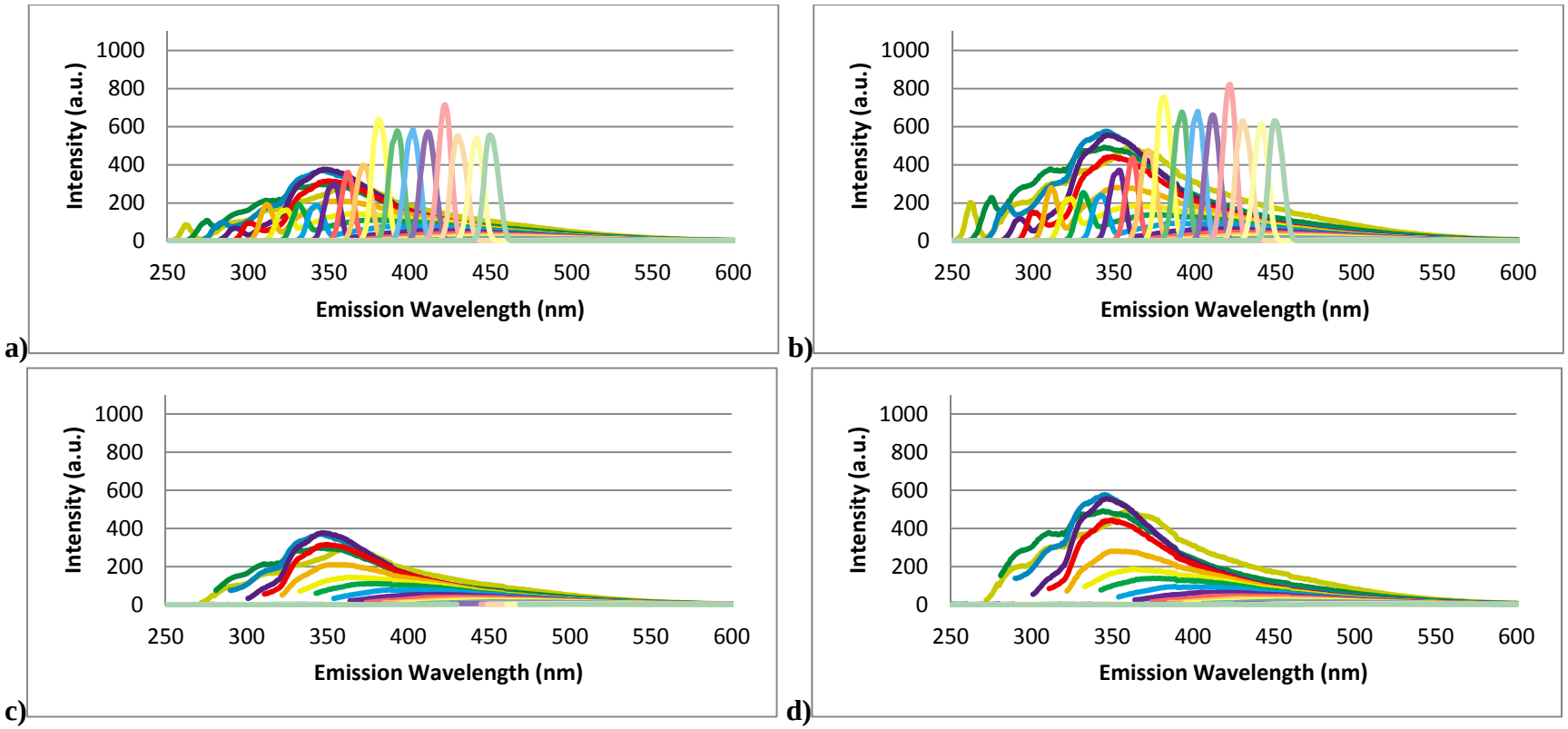

Figure F8: Suncor process affected water filtered to .45µm and diluted to 50% with deionized water. A) Intensity values uncorrected for primary and secondary inner filtering effects with light scatter. B) Intensity values corrected for primary and secondary inner filtering effects with light scatter. C) Intensity values uncorrected for primary and secondary inner filtering effects without light scatter. D) Intensity values corrected for primary and secondary inner filtering effects without light scatter.

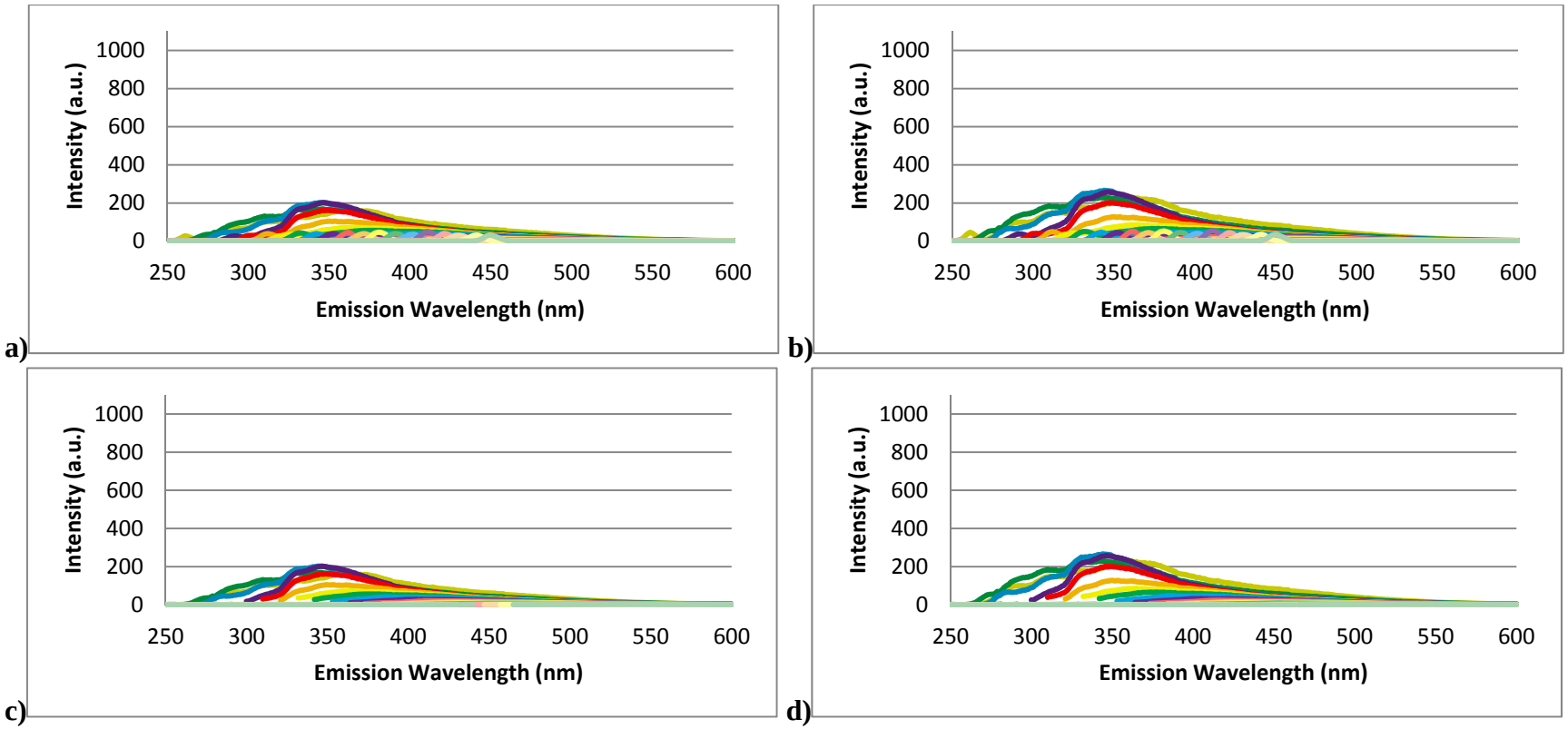

Figure F9: Suncor process affected water filtered to .45µm and diluted to 25% with deionized water. A) Intensity values uncorrected for primary and secondary inner filtering effects with light scatter. B) Intensity values corrected for primary and secondary inner filtering effects with light scatter. C) Intensity values uncorrected for primary and secondary inner filtering effects without light scatter. D) Intensity values corrected for primary and secondary inner filtering effects without light scatter.

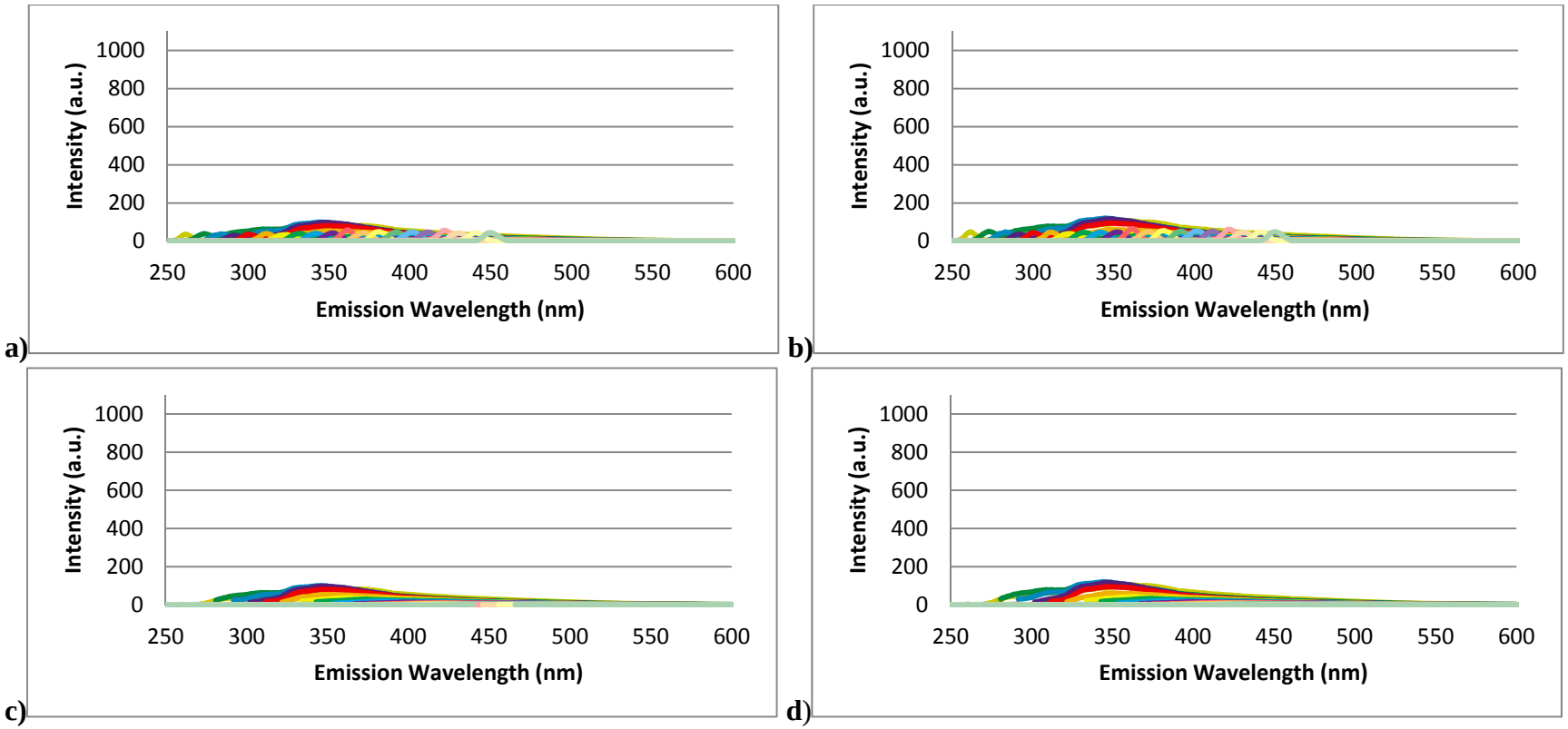

Figure F10: Suncor process affected water filtered to .45µm and diluted to 10% with deionized water. A) Intensity values uncorrected for primary and secondary inner filtering effects with light scatter. B) Intensity values corrected for primary and secondary inner filtering effects with light scatter. C) Intensity values uncorrected for primary and secondary inner filtering effects without light scatter. D) Intensity values corrected for primary and secondary inner filtering effects without light scatter.

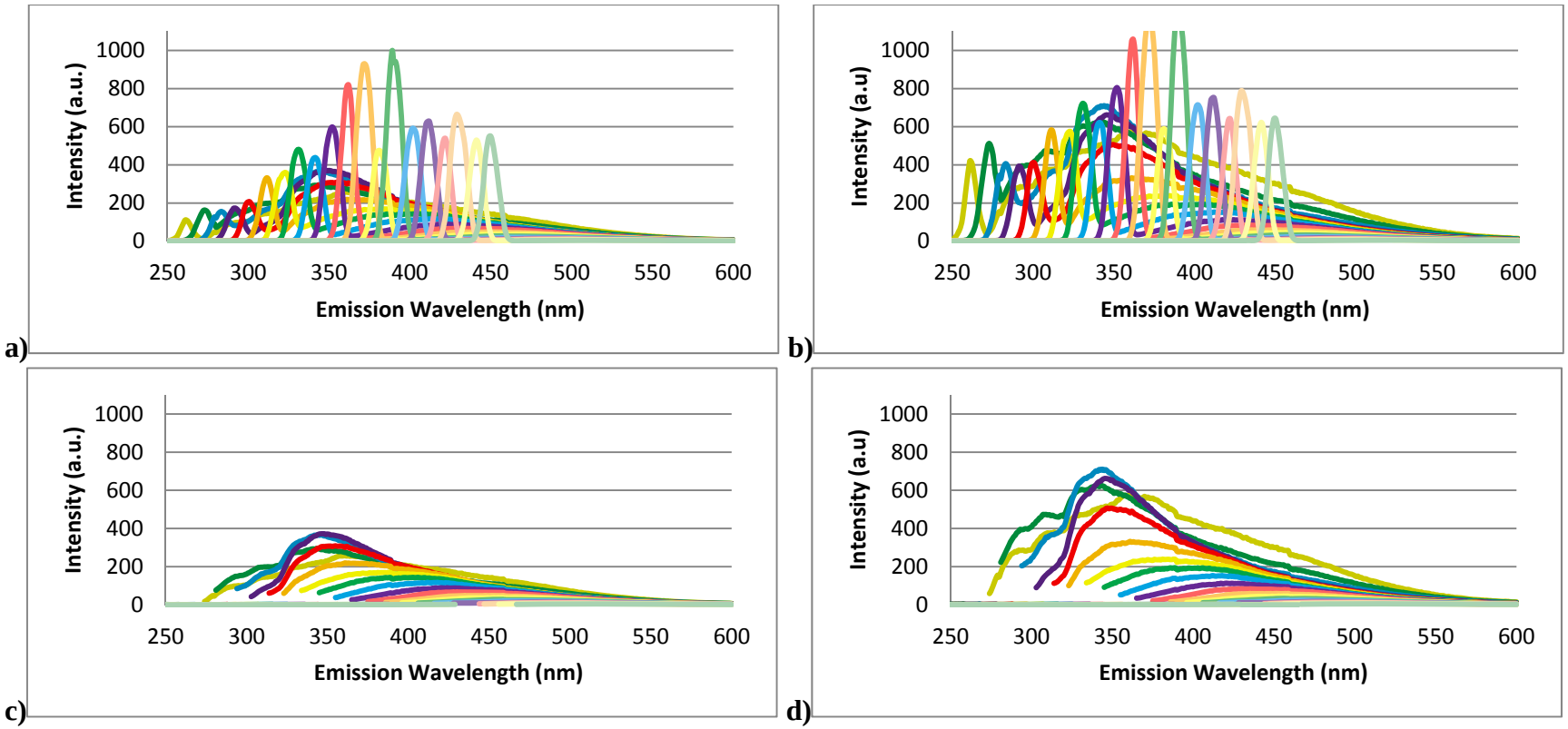

Figure F11: Albian process affected water filtered to .45µm and undiluted. A) Intensity values uncorrected for primary and secondary inner filtering effects with light scatter. B) Intensity values corrected for primary and secondary inner filtering effects with light scatter. C) Intensity values uncorrected for primary and secondary inner filtering effects without light scatter. D) Intensity values corrected for primary and secondary inner filtering effects without light scatter.

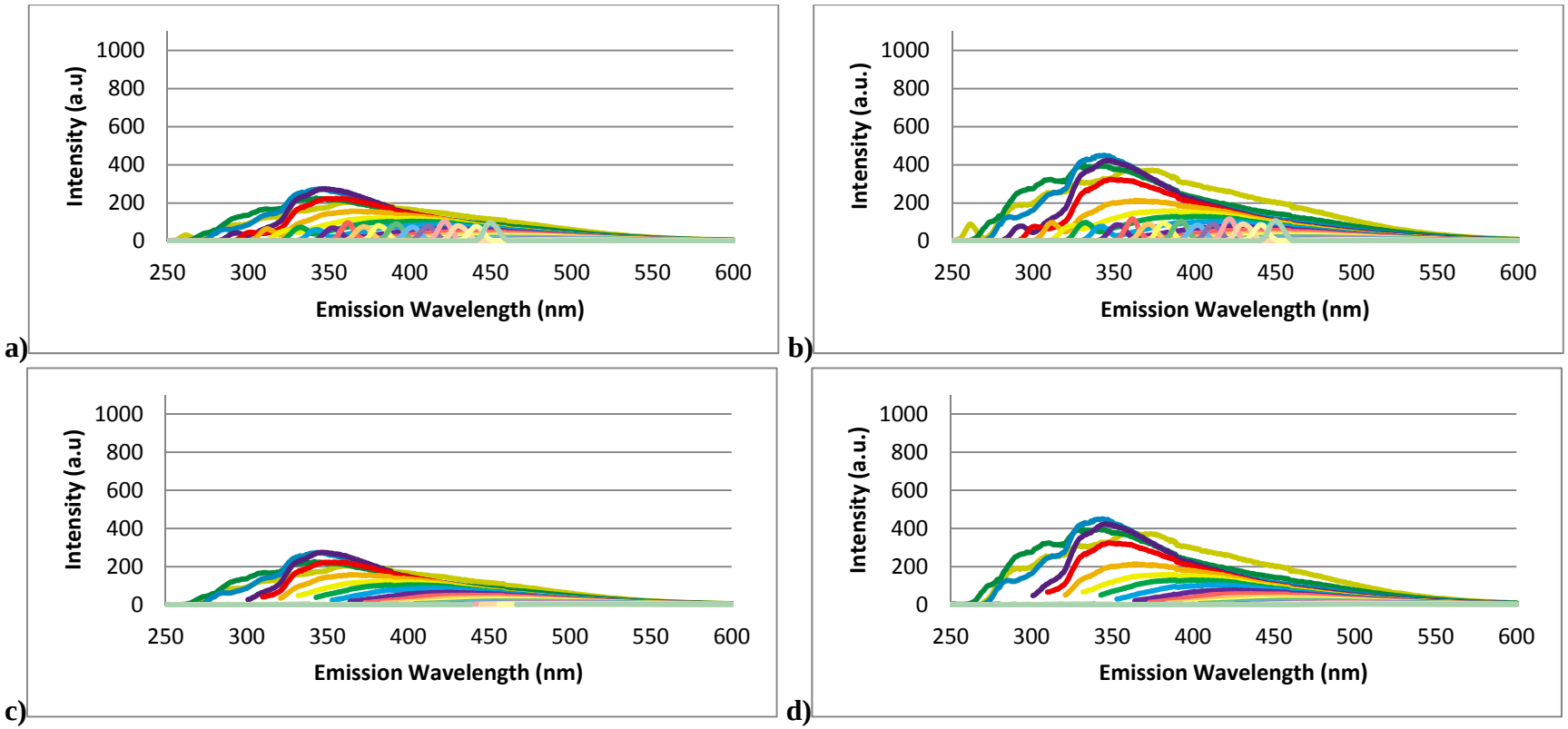

Figure F12: Albian process affected water filtered to .45µm and diluted to 75% with deionized water. A) Intensity values uncorrected for primary and secondary inner filtering effects with light scatter. B) Intensity values corrected for primary and secondary inner filtering effects with light scatter. C) Intensity values uncorrected for primary and secondary inner filtering effects without light scatter. D) Intensity values corrected for primary and secondary inner filtering effects without light scatter.

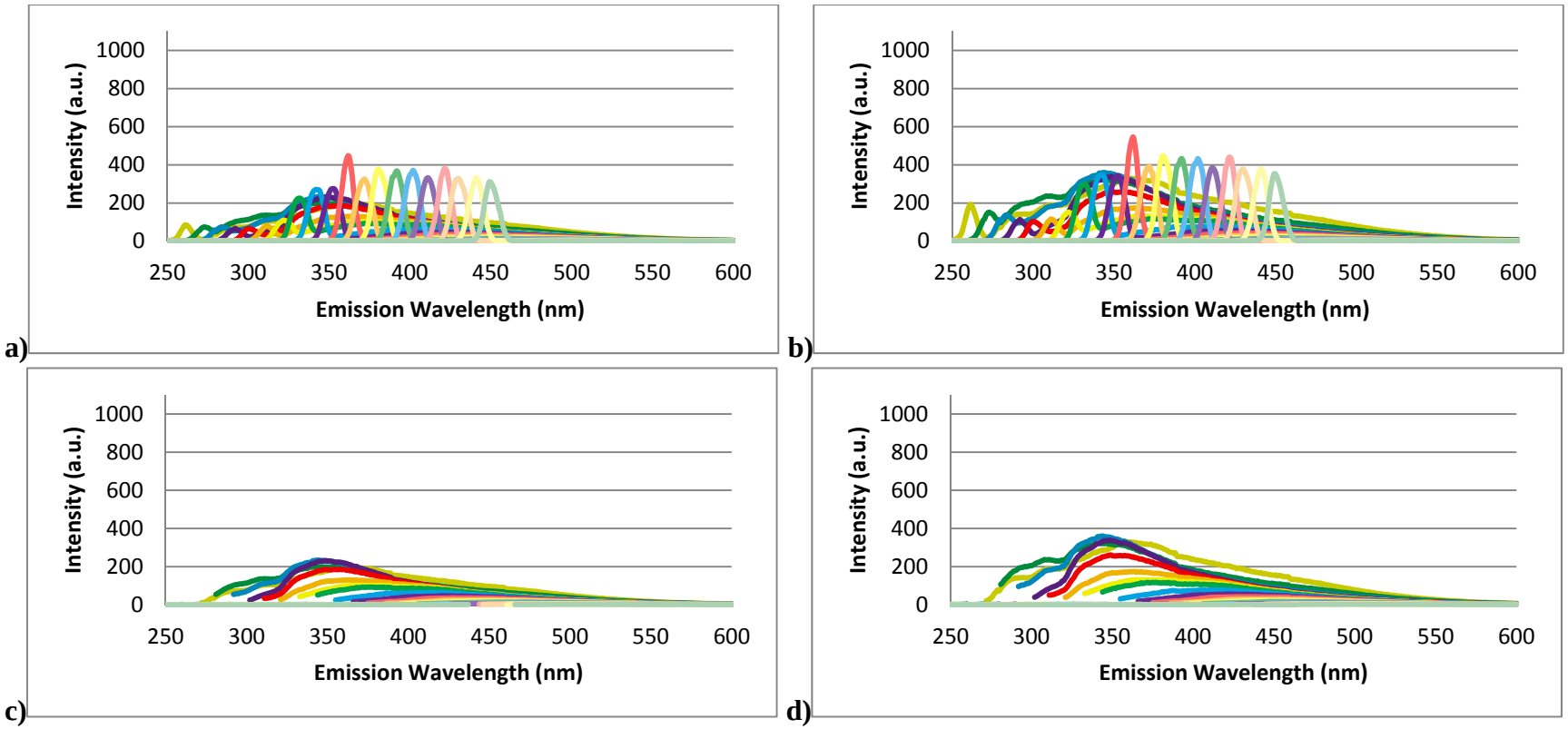

Figure F13: Albian process affected water filtered to .45µm and diluted to 50% with deionized water. A) Intensity values uncorrected for primary and secondary inner filtering effects with light scatter. B) Intensity values corrected for primary and secondary inner filtering effects with light scatter. C) Intensity values uncorrected for primary and secondary inner filtering effects without light scatter. D) Intensity values corrected for primary and secondary inner filtering effects without light scatter.

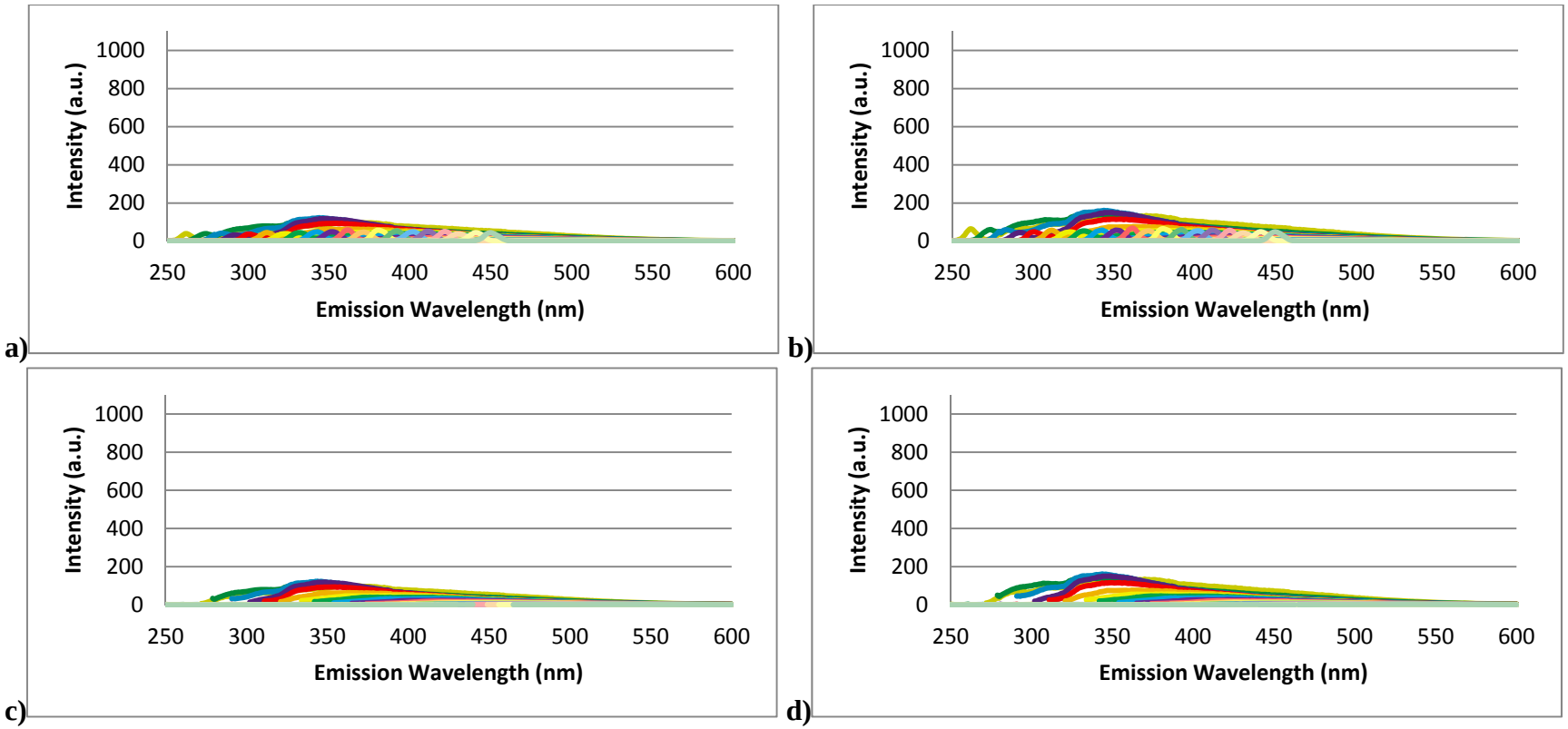

Figure F14: Albian process affected water filtered to .45µm and diluted to 25% with deionized water. A) Intensity values uncorrected for primary and secondary inner filtering effects with light scatter. B) Intensity values corrected for primary and secondary inner filtering effects with light scatter. C) Intensity values uncorrected for primary and secondary inner filtering effects without light scatter. D) Intensity values corrected for primary and secondary inner filtering effects without light scatter.

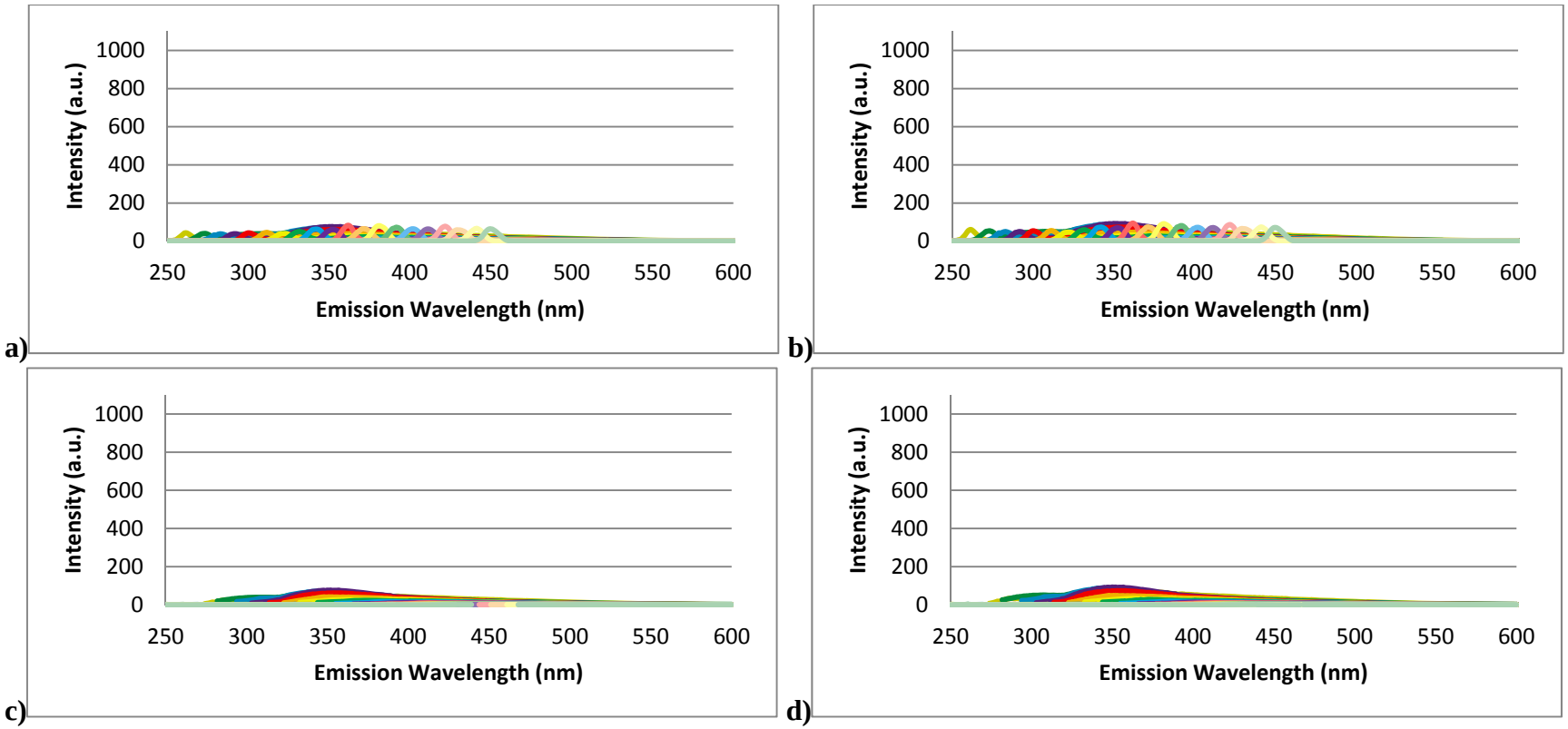

Figure F15: Albian process affected water filtered to .45µm and diluted to 10% with deionized water. A) Intensity values uncorrected for primary and secondary inner filtering effects with light scatter. B) Intensity values corrected for primary and secondary inner filtering effects with light scatter. C) Intensity values uncorrected for primary and secondary inner filtering effects without light scatter. D) Intensity values corrected for primary and secondary inner filtering effects without light scatter.

APPENDIX G: Process-Affected Water Filtered to 0.2µm

Process-affected water was filtered to.2µm in order to determine the effect of filtration on fluorescence signals for samples obtained from three oil sands operations. The second filtration step did not have any effect on the signals, however the amount of light scatter was reduced.

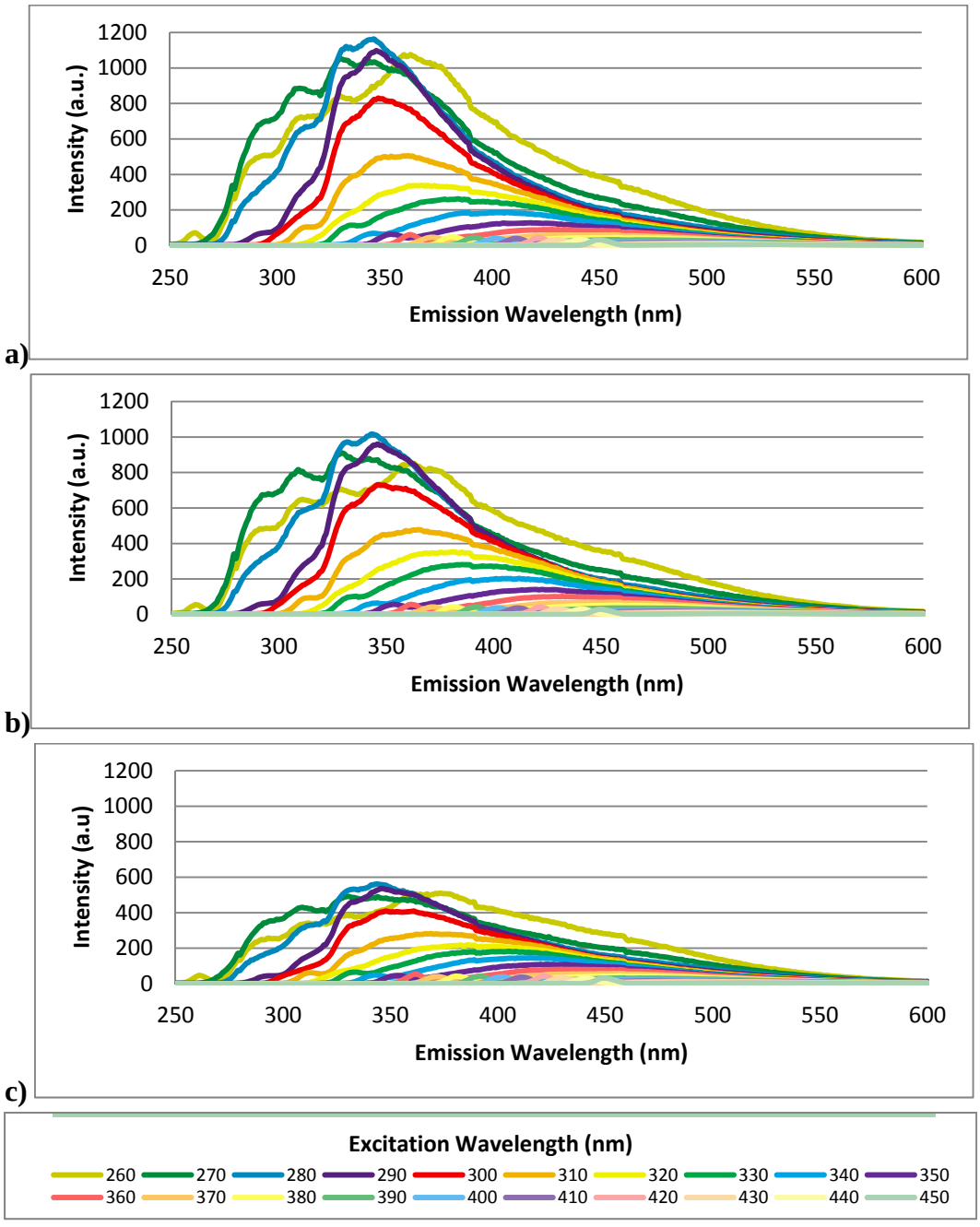

Figure G1: Emission spectra for undiluted process-affected water filtered to 0.2µm for excitation wavelengths 260 to 450 nm a) Syncrude b) Suncor c) Albian

APPENDIX H: Sigma Aldrich Naphthenic Acids

A stock solution of Sigma Aldrich naphthenic acids was prepared with methanol for a concentration of 200 mg/L. A dilution series was then prepared and all samples were fluoresced to observed the resulting fluorescence signal. Figures H1-H6 depicts the fluorescence scans of the commercial naphthenic acids prior and after to correction for absorbance, without the light scatter removed.

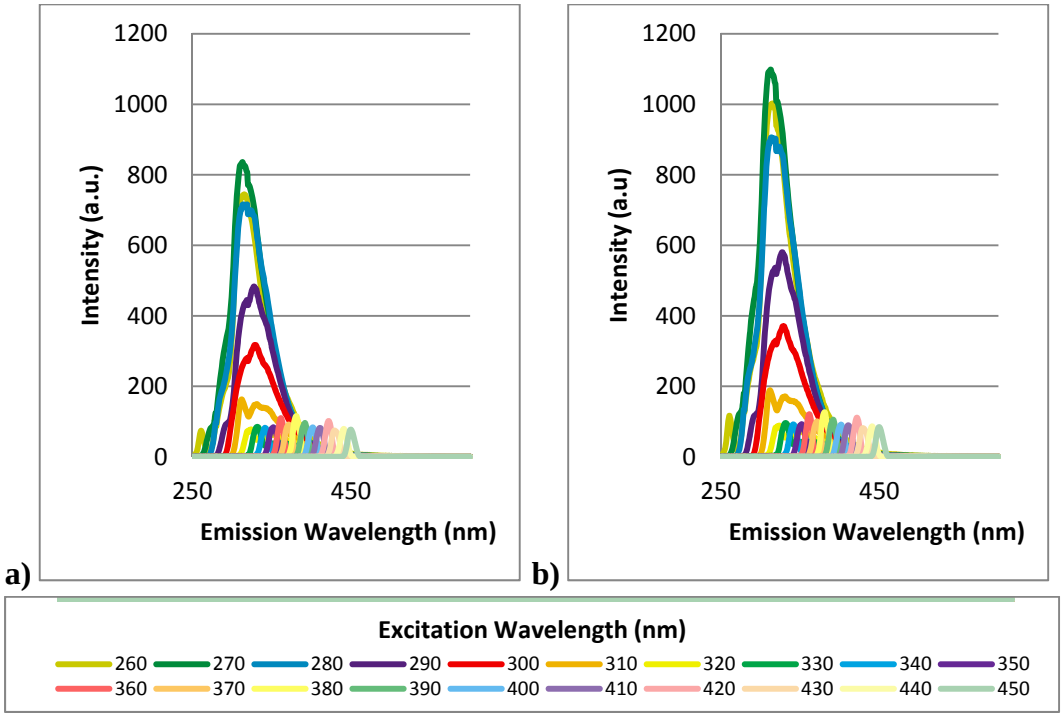

Figure H1: Stock solution of Sigma Aldrich naphthenic acids in methanol at a concentration of 200 mg/L a) Intensity values uncorrected for primary and secondary inner filtering effects b) Intensity values corrected for primary and secondary inner filtering effects.

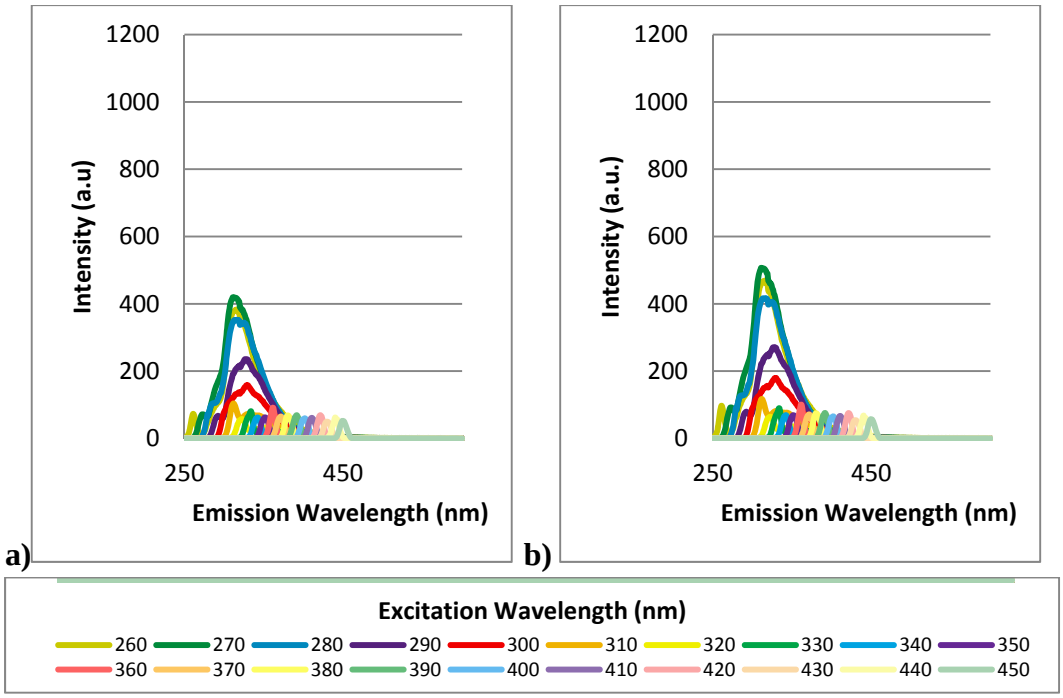

Figure H2: Sigma Aldrich naphthenic acids in methanol at a concentration of 100 mg/L a) Intensity values uncorrected for primary and secondary inner filtering b) Intensity values corrected for primary and secondary inner filtering effects.

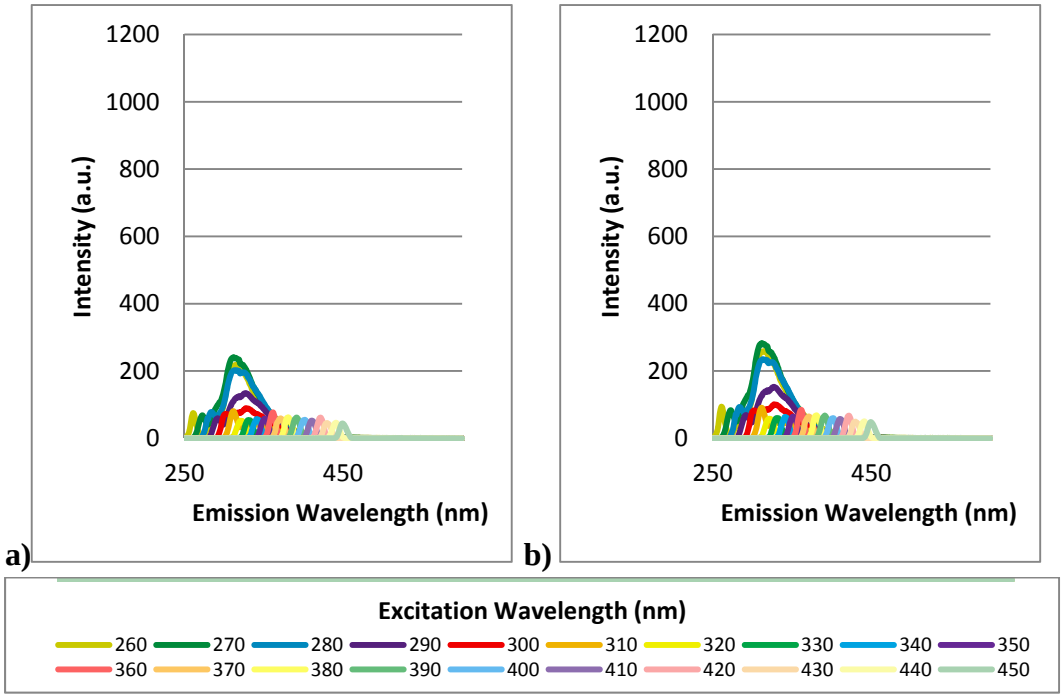

Figure H3: Sigma Aldrich naphthenic acids in methanol at a concentration of 50 mg/L a) Intensity values uncorrected for primary and secondary inner filtering effects b) Intensity values corrected for primary and secondary inner filtering effects.

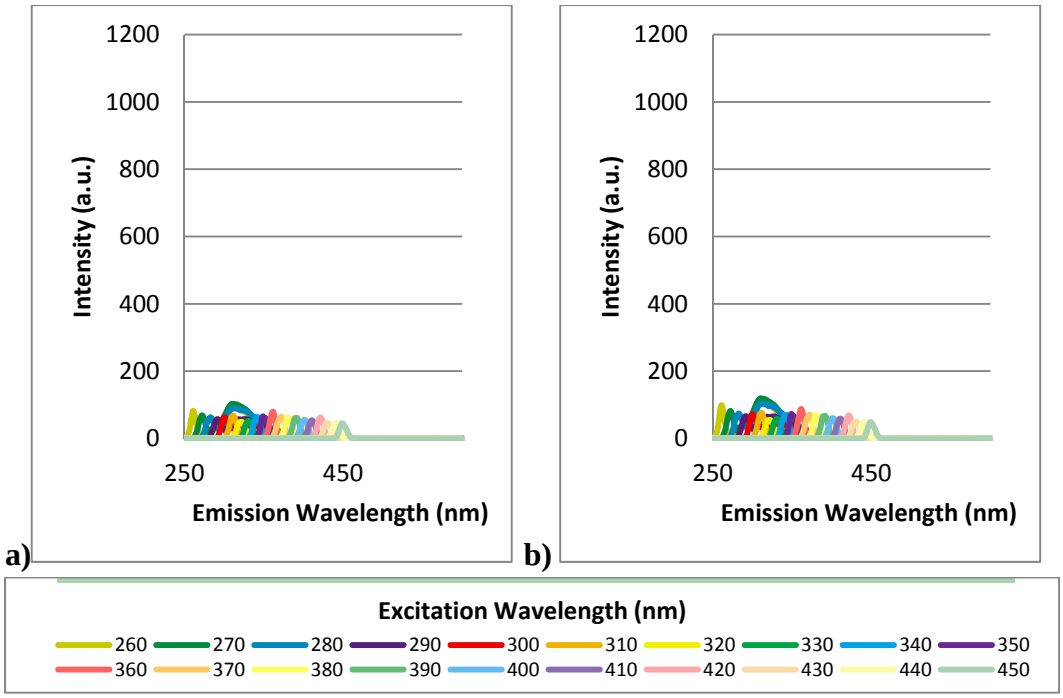

Figure H4: Sigma Aldrich naphthenic acids in methanol at a concentration of 20 mg/L a) Intensity values uncorrected for primary and secondary inner filtering effects b) Intensity values corrected for primary and secondary inner filtering effects.

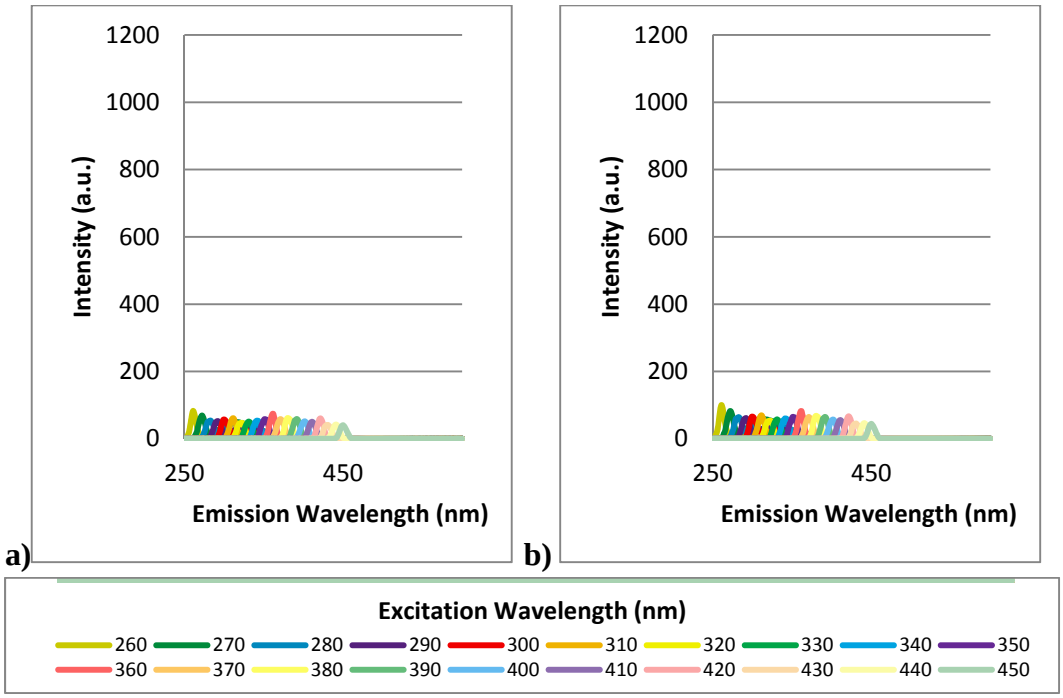

Figure H5: Sigma Aldrich naphthenic acids in methanol at a concentration of 10 mg/L a) Intensity values uncorrected for primary and secondary inner filtering effects b) Intensity values corrected for primary and secondary inner filtering effects.

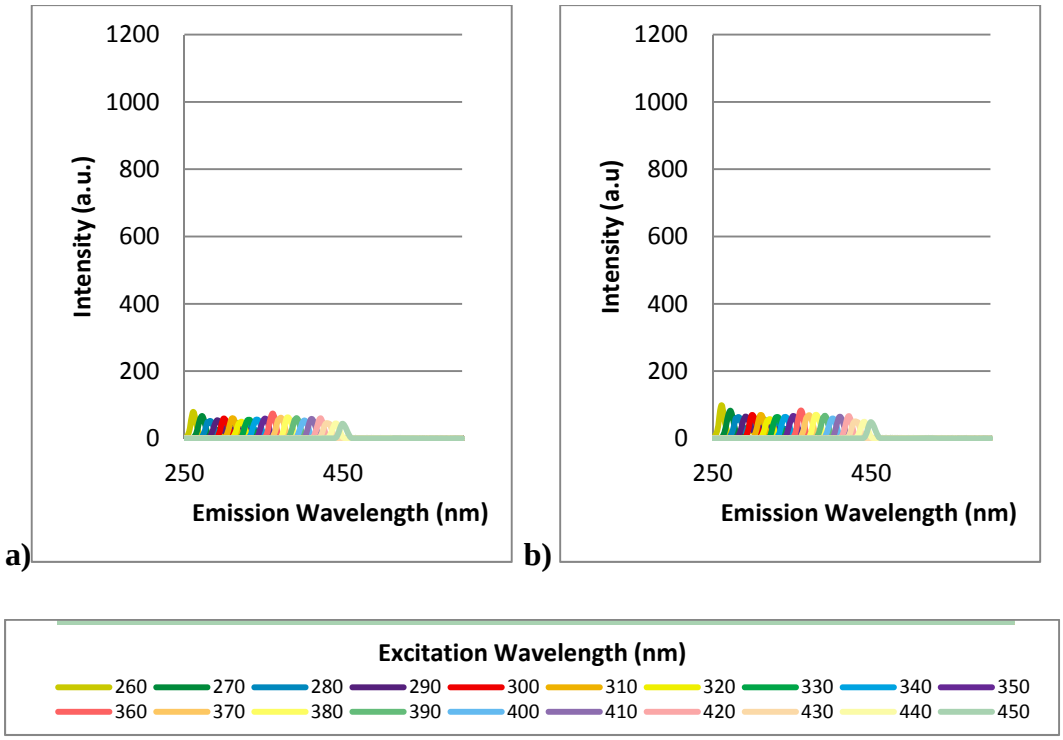

Figure H6: Sigma Aldrich naphthenic acids in methanol at a concentration of 5 mg/L a) Intensity values uncorrected for primary and secondary inner filtering effects b) Intensity values corrected for primary and secondary inner filtering effects.

APPENDIX I: FTIR Dilution Series

Process affected water samples were obtained from three companies: Syncrude, Suncor and Albian. A five sample dilution series of the process-affected water was prepared for each sample at 100%, 75%, 50%, 25% and 10% dilutions. Dilutions were prepared with deionized water for a total of 500mL each. The mass of each sample was additionally recorded for FTIR analysis. The initial pH was recorded for each sample, as well as the required pH levels for extraction. The recorded values are shown in Table I1.

Table I1: Recorded pH levels and mass of process affected water for FTIR dilution series

	Initial pH	Base pH	Acid pH	Mass of Container (g)	Mass of Container + Sample (g)	Mass of Sample (g)
Syncrude						
100	8.46	11.82	2.02	170.31	663.37	493.06
75	8.90	11.71	2.08	166.42	659.96	493.54
50	8.75	11.51	2.00	166.90	663.91	497.01
25	8.95	11.89	2.07	171.45	668.51	497.06
10	8.84	11.49	1.99	170.51	661.00	490.49
Suncor						
100	7.82	11.76	2.08	166.15	660.29	494.14
75	8.28	11.78	2.02	166.48	661.96	495.48
50	7.75	11.83	2.04	170.32	663.91	493.59
25	8.41	11.63	1.91	167.56	661.20	493.64
10	7.91	11.55	2.08	166.77	660.07	493.30
Albian						
100	8.88	11.68	2.01	166.56	660.11	493.55
75	8.09	11.60	2.03	168.50	663.80	495.30
50	8.71	11.90	2.02	166.70	660.00	493.30
25	8.00	11.79	2.06	166.52	658.56	492.04
10	8.76	11.69	1.98	172.03	665.33	493.30

Following the extraction procedure outlined in Appendix A, samples were evaporated to dryness. For this analysis neither the base nor neutral components were necessary, only the acid components were retained. For FTIR analysis the dried extract is then concentrated with fresh dichloromethane. Selecting the same parameters as outlined for the calibration curve, each sample was run three times in the spectrometer and an average was determined. Heights were recorded at 1743cm^{-1} and 1706cm^{-1}. The recorded heights and final average is shown in Table I2.

Table I2: Peak Heights of the Analyzed Spectrum

	1743 cm^{-1}	1706 cm^{-1}	Total Height	Average Height
Syncrude				
100	0.31368	0.27990	0.59358	
	0.31433	0.27253	0.58686	
	0.31554	0.26847	0.58401	0.58815
75	0.31644	0.28750	0.60394	
	0.31968	0.28074	0.60042	
	0.32127	0.27753	0.59880	0.60105
50	0.26587	0.21683	0.48270	
	0.26777	0.21132	0.47909	
	0.26904	0.20828	0.47732	0.47970
25	0.15610	0.09602	0.25212	
	0.15584	0.09274	0.24858	
	0.15650	0.09145	0.24795	0.24955
10	0.06259	0.02728	0.08988	
	0.06232	0.02624	0.08856	
	0.06311	0.02636	0.08947	0.08930
Suncor				
100	0.23408	0.17629	0.41037	
	0.23542	0.16862	0.40404	
	0.23640	0.16639	0.40279	0.40573
75	0.28000	0.22908	0.50908	
	0.28110	0.22337	0.50447	
	0.28323	0.22062	0.50385	0.50580
50	0.20664	0.14482	0.35146	
	0.20772	0.13839	0.34611	
	0.20868	0.13698	0.34566	0.34774
25	0.09826	0.04831	0.14658	
	0.09779	0.04576	0.14355	
	0.09828	0.04484	0.14312	0.14442
10	0.03711	0.01454	0.05165	
	0.03687	0.01364	0.05051	
	0.03712	0.01359	0.05071	0.05096
Albian				
100	0.15000	0.09186	0.24186	
	0.14980	0.08776	0.23756	
	0.15035	0.08610	0.23645	0.23862
75	0.15097	0.09324	0.24421	
	0.15117	0.08929	0.24046	
	0.15161	0.08726	0.23887	0.24118
50	0.06383	0.02794	0.09177	
	0.06368	0.02622	0.08990	
	0.06414	0.02573	0.08987	0.09051
25	0.04527	0.01912	0.06439	
	0.04471	0.01763	0.06234	
	0.04534	0.01799	0.06333	0.06335
10	0.03389	0.01587	0.04976	
	0.03317	0.01416	0.04732	
	0.03314	0.01392	0.04707	0.04805

Using the average total peak height the concentrated sample concentration is determined using the calibration curve. The original sample concentration is then determined using formula C1 and the recorded values for each sample are shown in Table I3.

$$Concentration = \frac{(Concentrated\ Concentration)(Mass\ of\ DCM\ added)}{(Mass\ of\ Original\ Water\ Sample)} \quad \text{(C1)}$$

Table I3: Sample Concentrations of Dilution Series by FTIR

	Concentrated Sample Concentration (mg/L)	Mass of DCM Added (g)	Mass of Sample (g)	Original Sample Concentration (mg/L)
Syncrude				
100	835.7857	39.57	493.06	67.08
75	854.2190	28.94	493.54	50.09
50	680.8619	24.38	497.01	33.40
25	352.0714	22.65	497.06	16.04
10	123.1452	23.50	490.49	5.90
Suncor				
100	575.1905	38.33	494.14	44.62
75	718.1429	23.99	495.48	34.77
50	492.3476	23.99	493.59	23.93
25	201.8800	29.13	493.64	11.91
10	68.3662	23.31	493.30	3.23
Albian				
100	336.4614	30.56	493.55	20.83
75	340.1152	20.39	495.30	14.00
50	124.8776	34.23	493.30	8.67
25	86.0762	25.74	492.04	4.50
10	64.2143	18.60	493.30	2.42

The concentrated sample concentration is determined from the calibration equation from the calibration curve. The original sample concentration is then determined by using ratios of the original sample's water mass and the amount of DCM added to the dried extract. The following calculations are an example using the undiluted Syncrude sample, 100.

$$Calibration\ Equation: y = 0.0007x + 0.0031$$

$$Rearrange: x = \frac{y - 0.0031}{0.0007}$$

$$Concentrated\ Concentration: x = \frac{0.58815 - 0.0031}{0.0007} = 835.79\ {}^{mg}/_{L}$$

$$Original\ Sample\ Concentration:$$

$$C = \frac{(Concentrated\ Concentration)(Mass\ of\ CH_2Cl_2)}{Mass\ of\ Water\ Sample}$$

$$Original\ Sample\ Concentration: C = \frac{\left(835.79\ {}^{mg}/_{L}\right)(39.57g)}{439.06\ g} = 67.08\ {}^{mg}/_{L}$$